Dissertation

submitted to the

Combined Faculties for the Natural Sciences and for Mathematics
of the Ruperto-Carola University of Heidelberg, Germany

for the degree of
Doctor of Natural Sciences

presented by

Dipl. Biol. Anna Katharina Krembel
born in Speyer (Germany)

oral examination:
5th March 2014

Adaptation and
methylation kinetics
in *Escherichia coli* chemotaxis

Referees: Prof. Dr. Victor Sourjik

                                                Prof. Dr. Matthias Mayer

Für meine Familie

Acknowledgement

I want to thank all people who helped me during my PhD time:

Zusammenfassung

Die Bindung periplasmatischer Liganden an Chemorezeptoren von *Escherichia coli* führt zur Weiterleitung eines Signals bis zu den Flagellenmotoren, welche, je nach Art des Liganden, die Schwimmrichtung der Zelle verändern. Die gerichtete Bewegung hin zu Nährstoffen oder weg von Giftstoffen wird Chemotaxis genannt. Eine wichtige Eigenschaft des Chemotaxis-Systems, um sich in komplexen Nährstoffgradienten zurechtzufinden, ist die Adaptation, welche durch die Methylierung spezifischer Glutamat-Reste im cytoplasmatischen Teil der Chemorezeptoren erfolgt. Der Aspartat-Chemorezeptor Tar besitzt vier solcher Methylierungsstellen, wobei noch nicht geklärt ist, warum mehr als eine Stelle notwendig ist und ob möglicherweise eine bestimmte Methylierungsabfolge besteht.

In der vorliegenden Arbeit wurde die Effizienz der Chemotaxis sowie die Präzision der Adaptation für Zellen bestimmt, die ausschließlich den Chemorezeptor Tar mit unterschiedlicher Anzahl mutierter Methylierungsstellen exprimierten. Zu diesem Zweck wurden Tar-Chemorezeptoren konstruiert, die alle Kombinationen aus Alanin- und Glutamat-Resten an den vier Methylierungsstellen besaßen, um bestimmte Stellen für die Methylierung zu blockieren. Diese Tar-Mutanten wurden auf ihre chemotaktischen Fähigkeiten in Weich-Agar-Platten untersucht. Außerdem wurden die Adaptationskinetiken der Tar-Mutanten mittels *in vivo* FRET-Mikroskopie bestimmt. Mittels massenspektrometrischer Analyse konnte sowohl die Kinetik als auch die Reihenfolge der Methylierung an einzelnen Methylierungsstellen des Wildtyp Tar Rezeptors während der Adaptation analysiert werden. Es stellte sich heraus, daß sich die Methylierungsraten der einzelnen Stellen unterscheiden. Am schnellsten wird Methylierungsstelle 2 methyliert, gefolgt von den Stellen 1 und 3. Stelle 4 wird am langsamsten methyliert. Demethylierung findet zuerst an Methylierungsstelle 3 statt, gefolgt von den Stellen 2 und 1. Außerdem stellten wir fest, daß die unterschiedlichen Methylierungsstellen für verschiedene Eigenschaften von Chemotaxis und Adaptation verantwortlich sind. Methylierungsstelle 1 trägt hauptsächlich zur Adaptationspräzision und zur Methylierungsrate bei, Stelle 2 ist sowohl wichtig für die Methylierungs- als auch für die Demethylierungsrate. Stelle 3 ist verantwortlich für die Demethylierungsrate und für die Chemotaxis, während Stelle 4 hauptsächlich zur Methylierungsrate beiträgt.

Zusammenfassend ermöglichen die Ergebnisse dieser Arbeit neue Aufschlüsse über die molekularen Vorgänge während der Adaptation von *E. coli* und das komplexe Zusammenspiel der verschiedenen Methylierungsstellen bei der Regulation von chemotaktischen Bewegungen.

Abstract

Transmembrane chemoreceptors of *Escherichia coli* bind periplasmic ligands and transduce the signal to the flagella motors, thereby adjusting the swimming behaviour of the cell according to the chemical nature of the ligand. Cell movement, directed either towards nutrients or away from toxic compounds, is known as chemotaxis. An important property of the chemotaxis signalling pathway essential for navigation in complex gradients of nutrients is adaptation, mediated by methylation of specific glutamate residues in the chemoreceptors cytoplasmic domain. The aspartate chemoreceptor Tar possesses four such sites, but it is still unclear why several sites of methylation are needed and if a certain hierarchy among these sites exists.

In this study, we systematically and quantitatively characterized the efficiency of chemotaxis and the precision of adaptation for cells expressing Tar mutated at one or more modification sites as the only chemoreceptor. Therefore, we constructed Tar chemoreceptors with all possible combinations of alanine substitutions at the methylation sites to specifically render them non-methylatable. These Tar mutants were then tested for their ability to mediate chemotaxis on soft agar plates. Furthermore, adaptation kinetics of Tar mutants were analyzed by *in vivo* FRET microscopy and wild-type Tar was investigated by mass spectrometrical analysis, which allows to follow the order and kinetics of methylation at individual modification sites during the adaptation process. We found that the receptor methylation rate following addition of attractant differs for the individual methylation sites with methylation site 2 being fastest, followed by sites 1 and 3, and site 4 having the slowest rate of methylation. Demethylation upon removal of attractant occurs first at methylation site 3, followed by sites 2 and 1. Furthermore, we discovered that specific methylation sites are responsible for different features of chemotaxis and adaptation. Methylation site 1 mainly contributes to the adaptation precision and the methylation rate, whereas methylation site 2 is important for the methylation rate as well as for the demethylation rate. Methylation site 3 is responsible for the chemotaxis and the demethylation rate and methylation site 4 mainly contributes to the methylation rate.

In summary, the results of the present study provide new insights into the molecular details of the adaptation process in *E. coli* chemotaxis and the subtle interplay of individual methylation sites in the regulation of chemotactic behavior.

Contents

III. Results & Discussion 47

Part I.

Introduction

1 | Introduction

1.1. Bacterial motility and chemotaxis

Bacteria have developed different mechanisms of motility, including gliding, twitching and flagella-driven swimming. Motility enables bacteria to actively change their location and to find the most optimal conditions for their survival. Flagella are long helical filaments composed of the protein flagellin, which emerge out of the cell membrane. Many bacteria are flagellated and various arrangements of flagella exist, from one polar flagellum over several flagella on one or two poles to many peritrichous flagella, distributed uniformly over the whole cell surface. In contrast to eukaryotic flagella, prokaryotic flagella do not deflect but are rotating. Each flagellum is propelled by a membrane-based motor which mainly uses proton motive force, but also sodium ion potential over the membrane is known as energy source of some bacteria [1, 2, 3]. Flagella-driven movement is regulated by changing flagella rotation direction. Also many other directed movements, referred to as taxis, are known in prokaryotes, for example phototaxis towards light, aerotaxis towards oxygen, thermotaxis towards certain temperatures and magnetotaxis towards a magnetic pole.

1.1.1. Biased random walk

The enterobacterium *Escherichia coli* (*E. coli*) and other flagellated bacteria exhibit a random walk in uniform surroundings. Cells change their swimming direction frequently by tumbling and reorientation. The four to six peritrichous flagella rotate in counterclockwise direction and form a collective bundle that propels the cell forward, resulting in smooth swimming motion. Tumbling occurs every one to two seconds due to at least one flagellum changing its rotational direction to clockwise and thereby dispersing the bundle. Tumbling lasts for only one-tenth of a second and is followed by a random directional reorientation of the cell and another swimming phase [4, 5, 6]. As the angle of reorientation increases, the more flagella of the cell rotate in clockwise direction during tumbling [7]. Bacteria swim with a

high velocity of approximately 20 μm per second, covering an area several times larger than their cell length.

Presence of an attractant gradient changes the swimming pattern of the bacterial cells. Phases of smooth swimming towards the gradient source are extended and tumbling occurs at a lower frequency. Flagella rotation is biased in counterclockwise direction and thus, net swimming is directed towards the gradient source (Fig.1.1). This is called biased random walk [8]. Accordingly, presence of repellent is thought to cause a higher tumbling frequency by mainly clockwise flagella rotation. In this way, cells can escape from harmful environments. This directed swimming behaviour is called chemotaxis [9].
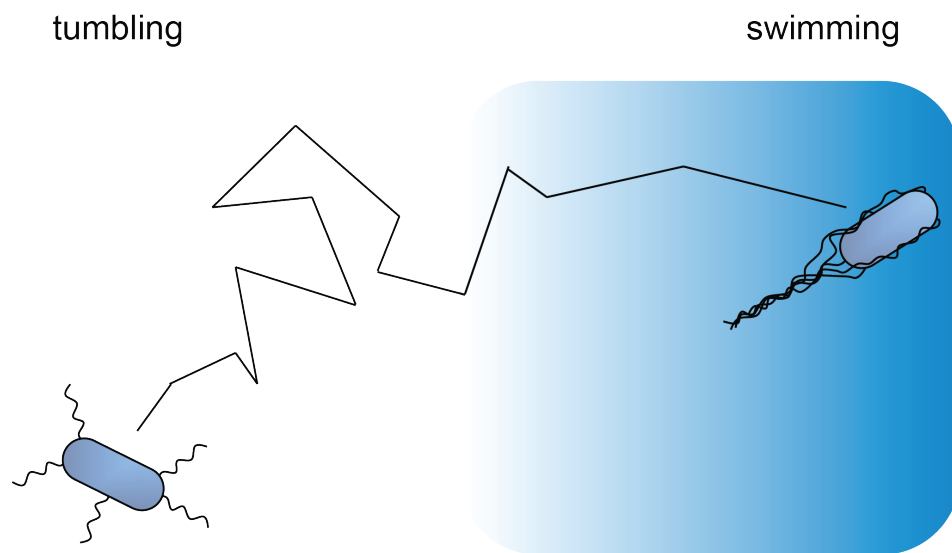
Figure 1.1.: Biased random walk of *E. coli*. Scheme of *E. coli* cell swimming behaviour in an attractant gradient (blue). Before encountering the gradient, the cells perform random walk (left). When attractant is sensed, cells perform biased random walk (right).

In contrast to eukaryotic cells, bacteria detect changing environments by temporal instead of spatial comparisons of their surrounding medium. The limiting factor is their small size which does not allow them to sense differences in concentration along their axis. Bacteria possess a short-term memory which enables them to make such temporal comparisons. It is based on differential protein modification governed by an adaptation system comprising methyltransferase CheR and methylesterase CheB.

1.1.2. Signalling pathway

Bacteria do not posses compartments or a nucleus, thus their signal transduction pathways are fundamentally different to eukaryotic ones. Furthermore, they have to adapt to numerous fast changes in their environment. Because the nutritional supply is often not constant, bacteria need to save energy wherever possible. Therefore, they adapt their lifestyle to the conditions in which they are currently existing by scanning their present surroundings as detailed as possible. For this purpose, bacteria essentially use two-component systems with an extracellular or periplasmic sensor and a cytoplasmic response regulator to transduce signals from outside and translate it into cytoplasmic reactions to cope best with current conditions. Two-component systems typically consist of a membrane-bound sensor kinase and a cytoplasmic response regulator [10, 11, 12]. They are not only found in prokaryotes, but also in a wide variety of eukaryotes. External signals are sensed by the extracellular or periplasmic domain of the sensor kinase and stimulate its autophosphorylation activity of a specific histidine residue. Subsequently, the kinase transfers the phosphate group to a conserved aspartate residue of the response regulator. Phosphorylated response regulators mainly serve as transcription factors that alter cellular processes, for example metabolism, osmotic balance, and antibiotic resistance [13].

In *E. coli* chemotaxis, a basic two-component system comprising the histidine kinase CheA, which is usually dimerized, and its response regulator CheY is present in the cytoplasm. In contrast to classical two-component systems, chemotaxis signalling system also involves other components. Attractants or repellents are sensed in the periplasm by membrane-spanning chemoreceptors with distinct ligand specificities [14]. Chemoreceptors bind to the kinase CheA via the adaptor protein CheW in the cytoplasm. The response regulator CheY interacts with a specific phosphatase, CheZ.

In case no attractant is bound to the chemoreceptors, they transduce a signal to the kinase CheA and stimulate its autophosphorylation. The phosphate group is then transferred to the response regulator. CheY phosphorylation occurs at the conserved residue Asp57 which alters CheYs conformation reducing its affinity for CheA [15]. CheY-P travels to the flagella motor where it has an increased affinity for the motor switch FliM [16]. The binding of CheY-P induces a change from counterclockwise (CCW) to clockwise (CW) flagellar rotation and therefore tumbling of the cell increases [17, 18, 19]. Binding of an attractant to the chemoreceptor disrupts the autophosphorylation activity of the kinase CheA, less CheY-P is formed and bound by the flagellar motor switch FliM and thus, the flagella rotates mainly in counterclockwise (CCW) direction which leads to longer straight runs of the cell. CheZ

reduces the overall concentration of CheY-P in the cell and ensures an only temporal binding of CheY-P to the flagelly motors (Fig.1.2). CheZ localizes to CheA and thus, both enzymes that modify CheY are at the same location [20]. This localization has the advantage that gradients in CheY-P distribution in the cytoplasm are avoided [21]. On the genomic level, most chemotaxis genes are organized in two operons, *mocha* and *meche* [22, 23]. Adaptation to attractant is achieved by reversible methylation of specific glutamate residues in the cytoplasmic part of the chemoreceptors by the methyltransferase CheR and the methylesterase CheB [24, 25, 26, 27, 28], at which methylation increases the chemoreceptors activity. Hence, chemoreceptors are also called methyl-accepting chemotaxis proteins (MCPs). Methylation enables the cells to counteract the binding of an attractant and therefore allows them to respond even to small changes in attractant concentrations over a wide concentration range. Thus, bacteria can establish a short-term-memory by comparing the attractant concentrations at consecutive time points and find the best conditions [29].
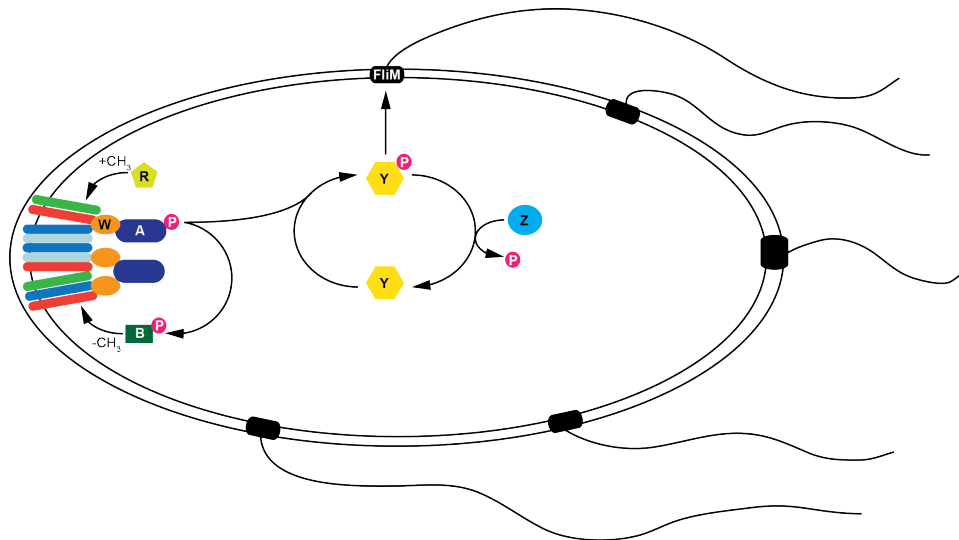
Figure 1.2.: Chemotaxis signalling pathway. Scheme of *E. coli* cell displaying all chemotaxis components. Polar or lateral mixed chemoreceptor clusters bind ligands and transduce this signal via the adaptor protein CheW to the kinase CheA, which is autophosphorylated and in turn transduces the phosphate group to the response regulator CheY. CheY-P binds to the flagellar motor switch FliM and induces CW rotation of the flagella and thereby tumbling of the cell. CheZ dephosphorylates CheY-P. CheR and CheB are methylating and demethylating specific residues of the chemoreceptors to mediate adaptation. CheB can also be phosphorylated by CheA and thereby increase its activity by a factor of 100.

Methylesterase CheB also serves as deamidating enzyme for specific glutamine residues of chemoreceptors to make them accessible for CheR mediated methylation. Moreover, CheB serves as alternative response regulator of kinase CheA. Phosphorylated CheB has a hundred-fold increased activity [30]. Nevertheless, phosphorylation of CheB has been shown to play a minor role in receptor methylation as CheR and CheB affinity is the crucial factor for receptor activation. CheR has a high affinity for inactive and a low affinity for active chemoreceptors. CheB has a low affinity for inactive and a high affinity for active receptors. Attractants sensed by *E. coli* are mostly nutrients, such as amino acids, sugars and dipeptides. Amino acids can bind directly to the chemoreceptors whereas sugars and dipeptides are first bound by periplasmic binding proteins [31]. Also non-metabolizable attractants exist, such as α-methyl-D,L-aspartate (MeAsp), a structural analog of L-aspartate or α-aminoisobutyrate, a structural analog of L-serine. Their use is commonly exploited for investigating chemotaxis signalling pathway. Repellents are usually toxic for the cell, e.g. divalent metal ions Ni^{2+} and Co^{2+}. Recently, pH taxis has been shown to place *E. coli* cells at an optimum and repelling them by both too high and too low pH values [32]. Also taxis towards temperature, oxygen and osmolarity have been shown to position cells at an optimum with repellent effects of extreme conditions [33, 34]. *E. coli* serves as a paradigm for bacterial chemotaxis as it displays the minimum chemotaxis protein setting a chemotactic bacterium needs to possess. Besides, diverse variations are known with additional chemotaxis proteins, alternative response regulators and methyltransferases [35].

1.1.3. Chemoreceptors

The *E. coli* chemoreceptors have been well characterized. Five different chemoreceptor types exist, four of which have a periplasmic domain with which they are sensing stimuli. The receptor proteins have a molecular weight of approximately 60 kDa each. Tar senses aspartate and maltose, Tsr serine, Trg sugars like ribose or galactose and Tap senses dipeptides, e.g. Pro-Leu. Also other specific attractants and repellents are known for these receptors, binding directly or via periplasmic binding proteins [14]. The fifth receptor Aer mediates aerotaxis. It possesses two transmembrane helices but lacks a periplasmic domain [36]. Furthermore it does not possess methylation sites for sensory adaptation [37]. Aer has an N-terminal PAS domain which binds FAD and therefore serves as a sensor for the redox state of the cell. Changes of the electron acceptor state are transduced to kinase CheA and changes its activity [38, 39, 40]. All four periplasmic sensing receptors are composed of a mostly helical structure which is segmented into a periplasmic and a cytoplasmic part (Fig.1.3).

The cytoplasmic portion is highly conserved among the receptors whereas the periplasmic part displays great differences as it forms the binding site for several specific ligands. Two transmembrane helices (TM1 and TM2) span the inner membrane and are followed in the cytoplasm by a HAMP domain which stands for histidine kinases, adenylate cyclases, methyl accepting chemotaxis proteins and several phosphatases [41]. HAMP domains are known to convert extracellular or periplasmic signals to an intracellular signal output [42, 43]. In a single chemoreceptor, the HAMP domain is organized in two parallel α helices. The remaining C-terminal receptor part consists of two antiparallel helices forming a coiled coil. These contain the methylation sites, depending on the receptor type four to six are present [44, 45, 46].
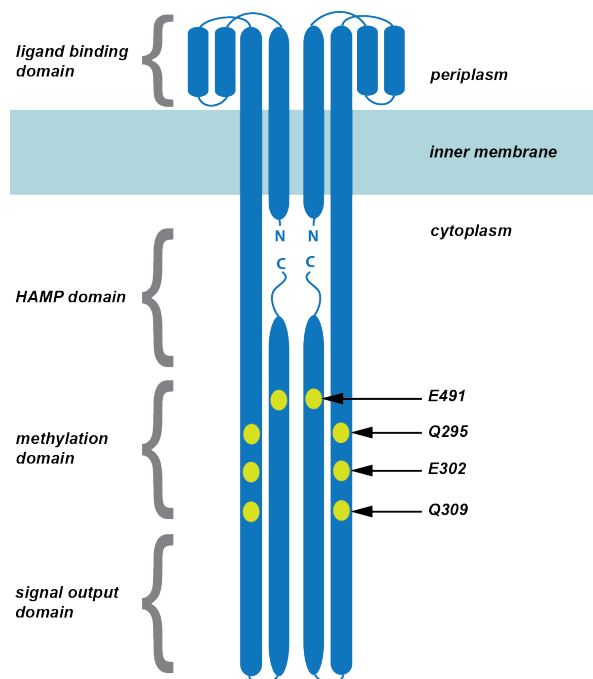
Figure 1.3.: Tar chemoreceptor dimer. (A) Scheme of *E. coli* Tar chemoreceptor dimer. The two periplasmic domains form two ligand binding sites. Transmembrane helices transduce the signal of ligand binding to the HAMP domain which converts the signal. The cytoplasmic tip contacts adaptor protein CheW and kinase CheA and thus transduces the signal output. The C-terminal pentapeptide tethers methyltransferase CheR and methylesterase CheB to the receptor. These enzymes methylate and demethylate specific sites and thereby mediate adaptation. Methylation sites of Tar are Q295, E302, Q309 and E491.

For aspartate chemoreceptor Tar, which is the primary subject of this work, four methylation sites are known, two glutamine (Q) and two glutamate (E) residues. These are particularly

Q295, E302, Q309 and E491, referred to as QEQE or site 1 through 4. All of these sites show slight variations of a consensus sequence: E-**E**-X-X-A-T/S where X stands for any amino acid [45] and the second glutamate is the site of modification. Methylation sites 1 to 3 are found on one helix, with seven amino acids distance between each of them. Three methylation sites are spaced at seven amino acids distance, which is called a heptad repeat, and thus face the same side of the helix because one turn of an α-helix spans over approximately 3.6 amino acids [47, 45]. Methylation site 4 resides on the antiparallel helix, but in a close spatial proximity to the other sites (Fig.1.3). Glutamine residues Q295 and Q309 are deamidated by CheB to glutamates before methyl esters of these residues can be formed [48].

On the very distal tip of the chemoreceptor, adaptor protein CheW and kinase CheA are bound, and therefore this site is supposed to transduce the signal output. Tar carries a specific pentapeptide at its C-terminus, NWETF, which tethers both methyltransferase CheR and methylesterase/deamidase CheB to the chemoreceptors [49, 50, 51]. Besides Tar, only Tsr receptors also contain that peptide. Thus, Tar and Tsr are considered major receptors. The remaining minor chemoreceptors do not possess such an enzyme tethering site and are dependent on CheR and CheB bound to neighboring major receptors. Major receptors are furthermore expressed at a higher level of several thousands per cell, whereas only several hundred copies of minor receptors are expressed in one cell [52].

1.1.4. Chemoreceptor organization and signal processing

The smallest functional unit is a chemoreceptor homodimer, moreover chemoreceptors have been supposed to form mixed trimers of homodimers [53, 54, 55, 56]. A further clustering occurs by binding of adaptor protein CheW and kinase CheA to the chemoreceptor tips. Together, these molecules form the core signaling units of chemotaxis and depend on each other to facilitate cluster formation [57, 58]. Sensory complexes are mainly found at the poles, but also at the cell sides, anticipating future division sides. However, it is not known yet how exactly these proteins interact with each other to form clusters. The formation of clusters is severely reduced when CheA and CheW are not present in the cell [59]. In a recent study though, smaller and less dense clusters are observed in cells lacking both CheW and CheA [60]. Apparently, binding of CheA and CheW to chemoreceptor trimers of dimers strongly enhances the stability of clusters but is not required. *In vitro* studies show that the cluster density influences the activity of the bound kinase CheA and the receptor methylation activity [61]. Binding of CheW is shown to change the arrangement of Tsr dimers and thereby increasing access to the methylation sites [62]. Influence of covalent receptor modification

is mediated only in receptor complexes with CheA and CheW [63]. High receptor density is attended by increased kinase activity and low methylation rates whereas low receptor densitiy is accompanied by decreased kinase activity and high methylation rates [64]. Clusters of chemoreceptors, CheW and CheA gradually recruit other chemotaxis proteins. CheY and CheB localize to the complexes as they are both cognate response regulators and compete for a binding site in the regulatory region of kinase CheA. CheB is besides also recruited to the sensory cluster by tethering to the N-terminal pentapeptide NWETF of major chemoreceptors, as well as CheR. Phosphatase CheZ localizes to a truncated form of kinase CheA, CheA$_s$ (short), which lacks 97 amino acids at the N-terminus of the protein [65, 66].

Receptors in trimers of dimers show interactions among each other, and binding of a single ligand molecule to one receptor induces changes in the other receptors within the trimer. The signal can even be transduced to neighbouring trimers of dimers and thus in a wide field of the whole receptor cluster [67, 68]. Diverse stimuli can be simultaneously sensed by a heterogenic receptor array, information is integrated and leads to a collaborative signal output, positioning cells at an optimum location in the gradient [69]. A unique feature thereby is the wide dynamic range of attractant concentrations upon which receptors can generate a specific output. Here, even tiny changes in concentration can be discriminated. Thus, the relation between signal input and signal output is not linear, a weak stimulus needs to be amplified to generate a perceptible signal output. It is postulated that signal amplification occurs at two consecutive levels. First amplification takes place at the kinase level and is further enhanced at the level of CheY-P binding to the flagellar motor switch FliM, which consists of approximately 30 cooperative subunits [3, 16, 70, 71]. Theoretical models have been developed of how signal integration and amplification can be reproduced [72, 73, 66, 74, 75]. The two-state-model of ternary complexes postulates that receptors coupled to CheW and CheA are either free and active (*on* state) or ligand-bound and inactive (*off* state), independent of other chemoreceptors in the cluster (Fig.1.4A) [76]. Activities of receptors and CheA are interdependent. An active receptor activates the kinase, whereas the inactivation of a receptor is also transduced to CheA and leads to its inactivation. The activity of a receptor is usually determined by its ligand occupancy and its methylation level. Thus, in mixed chemoreceptor clusters, allosteric cooperative effects between chemoreceptors and in their interaction with kinase CheA occur [77, 78, 68, 79]. Cooperativity between chemoreceptors is considered in the Monod-Wyman-Changeux (MWC) model, which can be seen as a further development of the two-state model [80, 74]. Signalling teams within a receptor cluster cooperatively change their state from *on* to *off* upon binding of a critical ligand amount (Fig.1.4B). The Ising model considers the whole cluster as one signalling team, where chemoreceptors changing

10

their activity state can only influence their directly neighboring receptors [81]. Depending on how strong receptors are coupled, the activity change of one receptor gets transduced over several other receptors in a distance dependent manner. This model was originally postulated for ferromagnetic fields and adapted to chemotaxis clusters (Fig.1.4C).
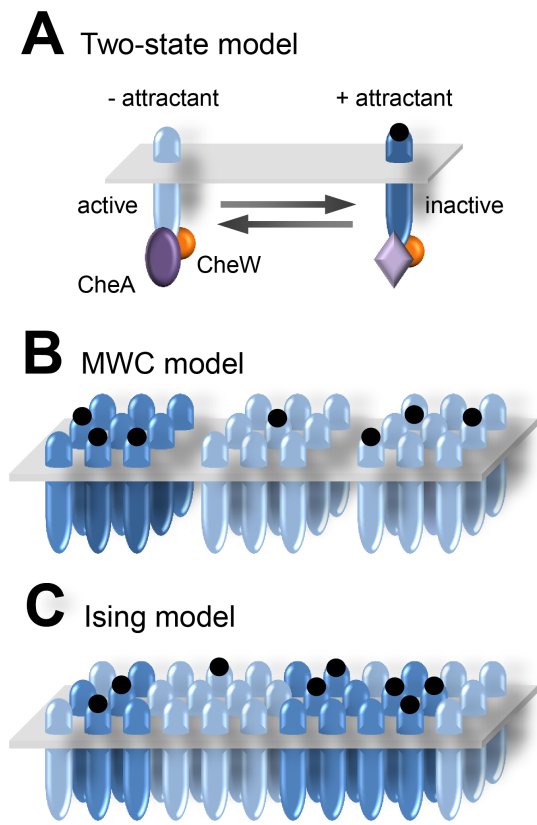
Figure 1.4.: Receptor signalling models. (A) Two-state model. Receptors coupled to CheA and CheW switch between active and inactive states, depending on bound ligands and receptor methylation. **(B)** MWC model. The Monod-Wyman-Changeux model proposes cooperative interactions between receptor subgroups, the signalling teams. These teams collectively change between *on* and *off* state depending on the ligand occupancy and methylation state of their individuals. **(C)** Ising model. The whole receptor cluster is considered to be a signalling team. Receptor coupling only reaches to neighboring receptors and influences their activity state. [Figure adapted from the PhD thesis of David Kentner.]

1.1.5. Adaptation system

The adaptation system enables cells to navigate in gradients of attractant. By measuring the attractant concentration at two consecutive time points, the direction of the gradient can be identified because of the differences in receptor methylation, and subsequently, cells can follow the gradient up to its source [82]. Cells are also able to move away from repellent gradients. Increase in methylation lets the cells follow their path, as it causes longer swimming phases and reduction of tumbling frequency. Still, tumbling needs to be performed by the cells to ensure that they are moving in the right direction. It was found that cells swimming up a gradient even regulate their reorientation angle after tumbling [7, 83, 84]. In order not to lose track of the gradient source too much, the angle is smaller than in cells performing random walk in the absence of a gradient. This implies that fewer flagella switch their rotational direction from counterclockwise to clockwise in a gradient than in an environment without attractant. To ensure that a gradient is perceived by the cells, it needs to be steep enough to cause an increase in chemoreceptor methylation at two consecutive time points. The adaptation system also ensures a robust adaptation towards uniform stimulus concentrations. The molecular basis of adaptation is the methylation of specific glutamates on the cytoplasmic helices of the receptors. Varying numbers of methylation sites are found in different chemoreceptor types. Tsr and Trg receptors each possess five, and Tar has four methylation sites, two of which are expressed as glutamines for all three receptors [45, 44, 46, 85]. The methylesterase CheB deamidates the two glutamines of each newly synthesized chemoreceptor. Thus, only glutamates are now available for methylation. First it was thought that specific sites only get methylated in the presence and others only in the absence of attractant [86]. Later it was found that all sites were methylated when cells get stimulated with attractant [87]. Still, the significance of having several methylation sites has not been allocated yet. Also the existence of different numbers of methylation sites in different chemoreceptor types needs to be elucidated.

As minor receptors Trg and Tap do not possess the C-terminal pentapeptide NWETF which tethers CheR and CheB to the chemoreceptors, they are dependent on major receptors Tar and Tsr which are providing adaptational assistance within chemoreceptor clusters [49, 50]. Tethering to the C-terminal pentapeptide sequence of one major chemoreceptor and the flexibility of the adjacent region allows the adaptation enzymes to jump between the methylation sites of different chemoreceptor dimers to modify them [88]. One molecule of either CheR or CheB that is tethered to the pentapeptide of a major receptor can catalyze methyltransfer or methylesterification on the adaptation domains of several neighboring chemoreceptors,

including both major and minor receptor dimers [89, 90]. This adaptational assistance is consequential under consideration of the chemoreceptor dimer-to-enzyme ratio, which has been determined as one CheR molecule for every 60 chemoreceptor dimers and one CheB molecule for every 40 chemoreceptor dimers [52]. Also *trans* methylation of chemoreceptors has been observed [91].

The aspartate chemoreceptor Tar is steadily methylated by CheR and CheB at equal rates, even in uniform surroundings without gradients of attractants or repellents. This causes a stable steady-state methylation level [76].

The methyltransferase CheR consists of an N-terminal helical regulatory domain and a C-teminal α/β catalytic domain that is responsible for chemoreceptor methylation (Fig.1.5) [92]. Its activity is not regulated by covalent modification, but CheR has a higher affinity for inactive chemoreceptors than for active ones [76]. CheR is tethered to the major chemoreceptors C-terminal pentapeptide NWETF by aligning it to a threestranded antiparallel β-sheet that is inserted into the catalytic domain. This domain contributes mainly to bind the methyl donor S-adenosylmethionine [93].

The methylesterase CheB is an alternative response regulator of kinase CheA, consisting of two domains joined by a linker sequence. The N-terminal helical regulatory domain can be phosphorylated and thereby exposes the C-terminal α/β catalytic domain and enhances its activity about 100-fold (Fig.1.6). The tethering site of CheB to the major chemoreceptors C-terminal pentapeptide NWETF is located at a sequence spanning from the C-terminal regulatory domain to the linker [94]. Besides, CheB regulatory region and linker contact CheA for phosphate transfer by binding to P2 fragment of CheA [95]. Thus, CheB localizes to chemoreceptor clusters by two different interaction mechanisms, on one hand by tethering to major chemoreceptors pentapeptide and on the other hand by binding to CheA for phosphate exchange purposes. Concluding, although their structures display similarities, the binding properties of CheR and CheB to NWETF are different.

In steady state conditions, methylation and demethylation are balanced and the average methylation level of one chemoreceptor is 0.5 methyl groups [87]. Binding of an attractant to the ligand binding site at the interface of the chemoreceptor dimer leads to an inactivation of the chemoreceptors and to a severe reduction of the autophosphorylation activity of the receptor-bound kinase CheA coming along with a decreased phosphorylation rate of response regulator CheY. Less CheY-P binds to the flagellar motor switch and thus flagellar rotation is biased to CCW which corresponds to longer straight runs of the bacterial cell [96].
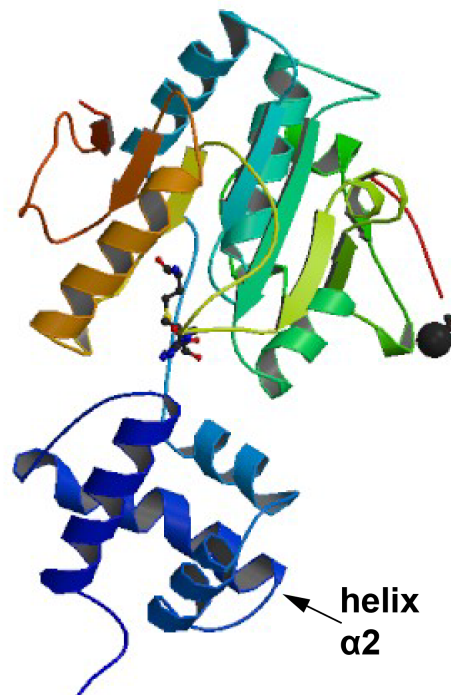
Figure 1.5.: Structure of methyltransferase CheR. CheR regulatory domain at the N-terminus (lower part) binds to the chemoreceptors pentapeptide NWETF and the catalytic domain at the C-terminus (upper part) transfers the methyl group to the methylation sites. PDB ID 1bc5 [93]. Shown is also the bound methyl donor S-adenosylmethionine and the N-terminal helix $\alpha 2$, indicated by the arrow.

The molecular mechanism is thought to be a piston-like movement of the transmembrane helix TM2 towards the cytoplasm and rectangular to the membrane [97, 96, 98, 99, 100]. It is not yet understood how this change in conformation might disrupt the signal transduction from the chemoreceptor to the kinase CheA. This process takes place very quickly. At the same time, adaptation via methylation mediated by CheR and CheB is initiated and renders the abruptly inactivated chemoreceptors slowly back to their active state again. This effect runs at a lower rate. For long time, it was thought that methylation of the chemoreceptors increases upon binding of ligand because CheB phosphorylation dramatically decreases due to reduced phosphotransfer from CheA. The unphosphorylated CheB has a significantly lower activity. In such a case, methylation would increase because CheR is still methylating the specific sites, which are then not efficiently demethylated anymore. But studies with a CheB
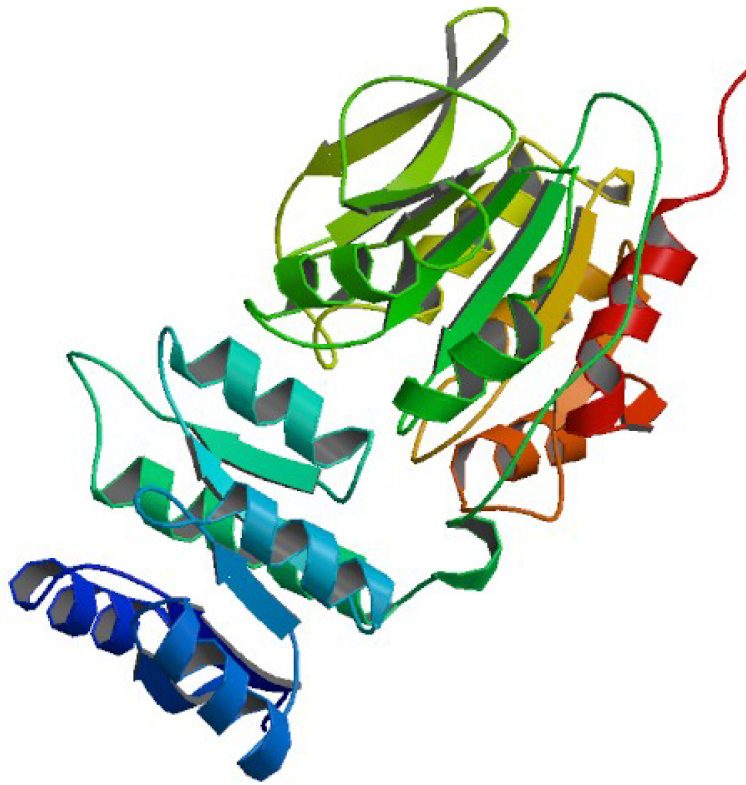
Figure 1.6.: Structure of methylesterase CheB. CheB regulatory domain with the phosphory-
lation site at the N-terminus (lower part) and catalytic domain at the C-terminus (upper part).
PDB ID 1a2o [92]

mutant that cannot be phosphorylated at all have shown, that adaptation can still take place.
Later it was found that the affinity of CheR and CheB for chemoreceptors depends on the
chemoreceptors activity. Phosphorylation of CheB reinforces the demethylation activity, but is
not necessary to initiate it. The methyltransferase CheR which catalyzes this modification has
an elevated affinity to inactive chemoreceptors (*off* state), the affinity of the counteracting
methylesterase CheB is highest for active chemoreceptors (*on* state) [76]. Thus, methylation
rises and demethylation falls when attractants are newly bound compared to steady-state
conditions.

High chemoreceptor methylation leads to a conformational change which is opposite to
the one induced by ligand binding and leads to receptor activation again. On average, two
methylation sites are occupied in that state [87]. It has been stated that the reactivation of a
chemoreceptor by methylation occurs through a neutralization of the four negatively charged
glutamate residues to neutral methyl-glutamates which induces the conformational change

of the receiver [101]. Thus, the activity of chemoreceptors can be restored again, although attractant is still present. In stable attractant concentrations, cells can search for regions with even more nutrients. As adaptation is a slow process, its outcome can be seen only with a delay compared to chemoreceptor inactivation upon attractant binding to chemoreceptors. When attractant is removed, chemoreceptors immediately are hyperactivated because of the summation of two effects: The activation by methylation and the activation by attractant removal from the ligand binding sites of the receptors. After this "overshoot" in activity, CheB demethylates the active receptor at a high rate, therefore the overall methylation level is decreasing until the steady-state conditions are restored again.

The methylation kinetics of the Tar receptor have been determined by Terwilliger and colleagues. Growth and stimulation of cells was performed in the presence of ^{3}H-tagged methionine, leading to an increased incorporation of radioactive methyl groups upon addition of attractant. Proteolytic digestion of Tar receptors resulted in four short peptides containing the separated methylation sites, which were analyzed for their radioactive methyl esters. A model was created where CheR and CheB are assumed to have rates proportional to the amounts of their substrates, unmethylated and methylated glutamate residues, respectively. Further, the time from addition of 1 mM aspartate until the completion of adaptation is estimated to be 3.5 minutes [102].

Methylation and demethylation rate constant were investigated experimentally and calculated by the model. Demethylation rate constant was determined, before aspartate addition and after adaptation to 1 mM aspartate. Both rates are essentially the same. Site 3 demethylation rate is highest, site 1 and 2 rates are less than half of the rate of site 3, and the turnover of methyl groups at site 4 is lowest with 30% of site 3 rate.

Also rate constants for methylation were determined before and after the addition of 1 mM aspartate at various time points for each site. Methylation level of all sites increased during adaptation. The rate constant for site 3 is the highest followed by site 2 with approximately two thirds of the rate of site 3. Site 1 displays one tenth and site 4 one fiftieth of site 3 methylation rate.

Terwilliger and colleagues found that high homologies between the consensus sequence, E-**E**-X-X-A-T/S and the sequences encompassing the methylation sites correlate with high methylation rates at the respective sites. Sequences encompassing site 2 and 3 have higher homologies to the consensus sequence. The sequence of site 2 possesses serine and site 3 possesses threonine as last residue. Thus, four residues are in agreement with the consensus for both sites. Site 1 sequence is E-**E**-X-X-S-A and site 4 sequence is Q-**E**-X-X-A-A, hence

only two amino acid residues are identical to the consensus. Recognition of methylation sites by CheR depends on the agreement of the respective site with the consensus sequence [87]. The interaction of Tar chemoreceptor and CheR was further investigated by mutagenesis of several glutamate residues at the methylation sites to aspartate residues. Substitution of site 2 or 3 led to a severe decrease of methylation at sites a heptad -or two helix turns- N-terminal to the aspartate residue, hence at site 1 or 2, respectively. One model is that CheR contacts the methylation site that undergoes modification in addition to contacting the site a heptad C-terminal on the same face of the helix. Aspartate substituted sites maintain the contact with CheR. As aspartate residues have a smaller size than glutamate residues, the overall geometry of the CheR-receptor complex is changed and the CheR active site cannot be properly positioned to methylate the respective glutamate [103].

This hypothesis was further investigated by substituting methylation sites with different amino acid residues, uncharged or negatively charged. Residues a heptad C-terminal of site 3 and 4 were also mutated. Methylation was severely reduced when the residue a heptad C-terminal was negatively charged, whereas neutral residues did not have an effect on methylation. These results suggested that the negatively charged residues a heptad C-terminal to a respective methylation site interact with positively charged residues of CheR and thereby disturb the geometry of the complex (Fig.1.7B). A neutral residue did not affect the CheR-receptor interactions (Fig.1.7C) [104].

A more recent study based on the crystal structure of CheR assumed a binding between the positively charged residues in the N-terminal domain of CheR and the negatively charged region of methylation in the chemoreceptor. Mutating positively charged arginine and lysine residues in the α2 helix of the N-terminal domain to neutral alanines reduced the methyl-transferase activity significantly. [105].

Cross-linking studies of the Tar methylation region and CheR revealed that the α2 helix in the N-terminal domain of CheR exhibits interaction with the chemoreceptor methylation region. Substitution of R53 with an alanine residue in CheR completely abolishes its methyltrans-ferase activity [106]. Perez and colleagues revealed that CheR α2 helix has a highly positively charged surface by calculating its electrostatic potential. Based on previous findings, they proposed an interaction between this region of CheR and the negatively charged methyla-tion region of the chemoreceptors. Exchanging one of the four positively charged residues (one lysine and three arginines) with alanines in the positively charged helix α2 of CheR resulted in four single site mutants, which were probed with wild-type Tar-enriched mem-branes. Particularly mutant protein R53A displayed significantly reduced methyltransferase activity with only 4% of the wild-type activity. This finding leads to the conclusion that R53
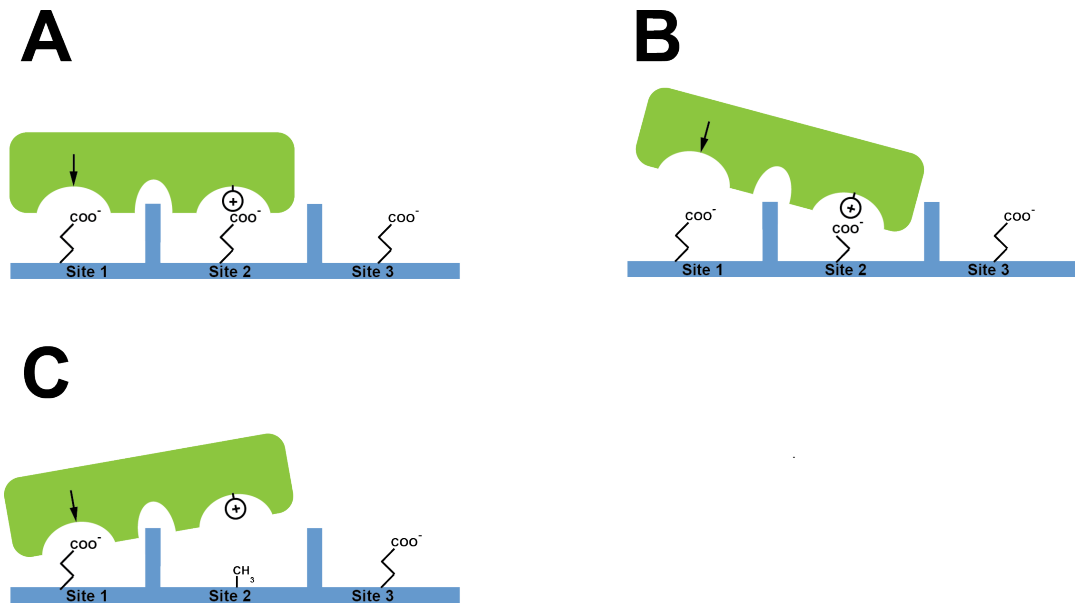
Figure 1.7.: Interaction models of the methyltransferase with the chemoreceptor wild-type or mutants. Methyltransferase CheR (green) exhibits the active site (arrow) and the potential additional contact interface, indicated by a positive charge (+). Only a portion of the chemoreceptor is shown, including the first three methylation sites (blue). Vertical rectangle represent Ala-Ser/Thr residues of the consensus sequence in between the sites of methylation and at the same helix face. Representative depiction of methylation site 1 interaction with the active site of CheR. **(A)** Wild-type chemoreceptor with three glutamates at the methylation sites. **(B)** Mutated chemoreceptor with an aspartate residue at methylation site 2. Geometry of the CheR- chemoreceptor complex and positioning of the enzyme active site to methylation site 1 is impaired. **(C)** Mutated chemoreceptor with an alanine residue at methylation site 3. Geometry of the CheR-chemoreceptor complex is slightly impaired but the alanine substitution at site 2 does not disturb the positioning of the active site to methylation site 1. Figure adapted from [104].

must be involved in the transfer of methyl groups, either by methylating sites directly or in correctly positioning them towards the active site of CheR. Two other sites, K46 and R59, might interact with the chemoreceptor at sites distant N- or C-terminal from the methylation sites. Residue K46 was identified when probing a respective CheR mutant with Tar having a glutamine at methylation site 3, that is in $\Delta cheB$ strain. Methylation at site 2 was severely reduced, hence supposing an interaction between K46 of CheR and a site seven amino acid residues C-terminal to the methylation site of the chemoreceptor. The same was true for methylation site 1 when site 2 was substituted with a glutamine residue. Residue R59 was found to play a role in site 4 methylation. Mutation R59A was not able to methylate site 4 at all. Here, the region N-terminal to site 4 seems to contribute to the CheR-chemoreceptor

interaction. A respective model where the chemoreceptor methylation region and the $\alpha2$ helix of CheR are oriented approximately antiparallel to each other was proposed (Fig.1.8).
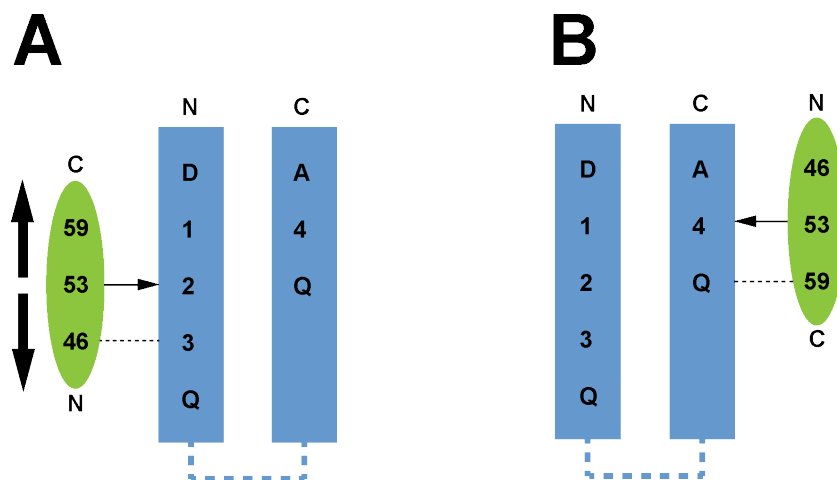
Figure 1.8.: Interaction models of CheR helix $\alpha2$ with the chemoreceptor methylation region. The blue oval represents helix $\alpha2$ of CheR with numbers indicating the positively charged amino acid residues. The two helices of the chemoreceptor are shown in green and display the four methylation sites (numbered 1 to 4) and the residues seven amino acids N- or C-terminal the them (one-letter code). **(A)** Interaction of CheR with methylation site 2 being subjected to methylation by the active site R53 (horizontal arrow). CheR residue K46 is thought to interact with the glutamate residue at methylation site 3, a heptad C-terminal to the site of methylation (black dotted line). Methylation of site 1 or site 3 can be achieved by movement of CheR in N- or C-terminal direction (vertical arrows). **(B)** An antiparallel orientation of CheR to the second cytoplasmic helix of the chemoreceptor is maintained. Methylation of site 4 is probably also mediated by CheR active site R53 (arrow), but stabilized by R59 (black dotted line). Figure adapted from [105].

The positively charged residues of CheR $\alpha2$ helix might serve to correctly position and orient the site of methylation through ionic interactions with the negatively charged glutamates, thereby stabilizing the CheR-chemoreceptor complex and allowing CheR to recognize specific sites of methylation [105].

1.2. Aims of this work

The chemotaxis system of *E. coli* is one of the best studied signal transduction pathways in prokaryotes. Still, adaptation in chemotaxis is not fully understood. It is well-established that the *E. coli* aspartate chemoreceptor Tar has four methylation sites in its cytoplasmic portion which are responsible for adaptation. After the discovery of these sites, it was thought, that some of them are methylated only when attractant is present and others only in the absence of attractant [86]. Later it was found that all sites are methylated upon stimulation [87]. It is not known why there are exactly four methylation sites, not more or less, and how these sites contribute to the adaptation process.

For a better understanding of the adaptation kinetics, mutants of the Tar receptor with only certain methylation sites available were constructed. The native amino acid residues at the methylation sites, glutamines and glutamates, were substituted with alanine residues, which cannot be modified by methylation. Glutamate residues at specific methylations sites and at specific quantities are then the only accessible sites for methylation by CheR. Measurement of the adaptation *in vivo* was done by a FRET set up that allowed us to follow the signalling pathway activity upon attractant addition [107]. The pathway activity was tested by stimulating the cells with defined concentrations of the non-metabolizable Tar ligand α-D,L-methylaspartate (MeAsp). The adaptation could be quantified from the received adaptation profiles for important mutant Tar receptors regarding the precision and rate. Also chemotactic behaviour and ability to activate kinase CheA were determined for cells expressing only one alanine-substituted chemoreceptor type.

Another objective of this project were the methylation kinetics of wild-type Tar chemoreceptor, which was determined by mass spectrometry. Thereby, a time course of receptor stimulation should shed light on which methylation sites are modified at which rate. Respective peptides containing the modified or unmodified methylation sites were analysed in the mass spectrometer. The exact positions of methylation could be determined over time by using targeted peptide fragmentation. This data combined with the results of our adaptation analysis presents an entire picture of receptor methylation.

Part II.

Materials & Methods

2 | Materials

Media and plates

Luria broth (LB) medium	10 g Bacto tryptone 5 g Bacto yeast extract 5 g NaCl addition of ddH$_2$O to a total volume of 1 l and adjust to pH 7.
LB plates	3% Agar added to LB medium
Tryptone broth (TB) medium	10 g Bacto tryptone 5 g NaCl addition of ddH$_2$O to a total volume of 1 l and adjust to pH 7.
5×M9 salt stock solution .	64 g Na$_2$HPO$_4$×7H$_2$O 15 g KH$_2$PO$_4$ 2.5 g NaCl 5g NH$_4$Cl

	addition of ddH$_2$O to a total volume of 1 l and autoclaving.
M9 minimal medium	200 ml M9 salt stock solution 2 ml 1M MgSO$_4$ 0.4% carbon source (glucose or glycerol) 1 M CaCl$_2$ 200 μl Thiamine (50 mg/ml) 8 ml amino acid mix (5 mg/ml L-threonine, L-methionine, L-histidine, L-leucine) addition of ddH$_2$O to a total volume of 1 l and autoclaving.
5×Minimal A salt stock solution	52.5 g K$_2$HPO$_4$ 22.5 g KH$_2$PO$_4$ 5g (NH$_4$)$_2$SO$_4$ 2.5 g Na-Citrate×2H$_2$O addition of ddH$_2$O to a total volume of 1 l and autoclaving.
Minimal A medium *soft-agar plates*	20 ml Minimal A salt stock solution 1 ml 20% glycerol 100 μl 1M MgSO$_4$ 5 mg/ml amino acid mix 50 mg/ml thiamine 0.25 % agar addition of ddH$_2$O to a total volume of 100 ml.

Buffers and solutions

Agarose gel electrophoresis

TAE buffer	242 g Tris base
	57.1 g Glacial acetic acid
	100 ml 0.5 M EDTA (pH 8)
	addition of ddH$_2$O to a total volume of 1 l.
6× DNA gel loading buffer	30 % (v/v) Glycerol
	0.25 % (w/v) Bromophenol blue
	0.25 % (w/v) Xylene cyanol
1 kb plus DNA ladder	20 μl DNA ladder stock
	40 μl 10x DNA gel loading buffer
	180 μl ddH$_2$O

SDS PAGE

3× SDS Laemmli buffer	6 % SDS
	30 % Glycerol
	15 % β-mercaptoethanol
	0.006 % Bromphenol blue
	0.25 M Tris
10× SDS gel running buffer	144.2 g Glycine
	30.3 g Tris
	10 g SDS

	addition of ddH$_2$O to a total volume of 1 l.
8 % SDS resolving gel	23.2 ml ddH$_2$O
	13.4 ml 30 % Acrylamide mix
	12.5 ml 1.5 M Tris (pH 8.8)
	500 μl 10 % SDS
	500 μl 10 % APS
	50 μl TEMED
5 % SDS stacking gel	5.5 mL ddH$_2$O
	1.3 ml 30 % Acrylamide mix
	1.0 ml 1.5 M Tris (pH 6.8)
	80 μl 10 % SDS
	80 μl 10 % APS
	8 μl TEMED

Immunoblot

Immunoblot transfer buffer	2.9 g Glycine
	5.8 g Tris
	3.8 g SDS
	200 ml Methanol
	addition of ddH$_2$O to a total volume of 1 l.
1× TBS buffer	150 mM NaCl
	10 mM Tris

	addition of ddH$_2$O to a total volume of 1 l.
1× TBST buffer	150 mM NaCl
	10 mM Tris
	0.05% Tween 20
	addition of ddH$_2$O to a total volume of 1 l.

Coomassie staining

Coomassie staining solution	400 ml Methanol
	100 ml Acetic acid
	1 g Coomassie R250
	addition of ddH$_2$O to a total volume of 1 l.
Coomassie destaining solution	400 ml Ethanol
	100 ml Acetic Acid
	addition of ddH$_2$O to a total volume of 1 l.

Others

Tethering buffer	100 ml 0.1 M KPO$_4$
	200 μl 0.5 M EDTA
	13.4 ml 5 M NaCl
	100 μl 10 M Methionine
	100 μl 10 M Lactic acid
	addition of ddH$_2$O to a total volume of 1 l and adjust to pH 7.

Antibiotics

Ampicillin	100 mg/ml in ddH$_2$O
Chloramphenicol	34 mg/ml in 70 % ethanol

Inducers

Isopropyl-β-D-thiogalactopyranosid (IPTG)	0.1 M in ddH$_2$O
Na-Salicylate	1 mM in ddH$_2$O

Reaction kits

QIAprep Spin Miniprep Kit	Qiagen, Hilden
QIAquick Gel Extraction Kit	Qiagen, Hilden

Ni-NTA Spin Kit	Qiagen, Hilden

Antibodies

Primary antibody

Rabbit primary polyclonal anti-Tar antibody	Charles Rivers Laboratories

Secondary antibody

Goat anti-rabbit IRDyeTM 800 IgG	Rockland

Enzymes

DNA polymerases

KAPA Hifi DNA polymerase	Peqlab, Erlangen
Pwo Superyield DNA polymerase	Roche

Restriction enzymes

BamHI	New England Biolabs
DpnI	Thermo Fisher
KpnI	New England Biolabs
PstI	New England Biolabs

Software

DNA Strider 1.3	Commissariat a l'Energie Atomique, France
Illustrator CS5	Adobe Systems, USA
KaleidaGraph 4.03	Synergy Software, USA
LabView 7.1	National Instruments, USA
Lasergene	DNASTAR, USA
LaTeX	http://www.latex-project.org/
GPMAW	Lighthouse Data, Denmark
Scaffold viewer	Proteome Software, USA
XCalibur Qual Browser	Thermo Fisher, USA

Chemicals

Chemical	Manufacturer
α-methyl-DL-aspartic acid (MeAsp)	Sigma-Aldrich, München
Acetic acid	Merck, Darmstadt
Agar	Applichem, Darmstadt
Agarose	Invitrogen, Karlsruhe
Amoniumpersulfate	Roth, Karlsruhe
Ampicillin	Applichem, Darmstadt
β-mercaptoethanol	Applichem, Darmstadt
Bacto tryptone	Difco, Hamburg
Bacto yeast extract	Difco, Hamburg
Bromphenol blue	Applichem, Darmstadt
Calciumchloride	Roth, Karlsruhe
Chloramphenicol	Applichem, Darmstadt

Continued on next page

Chemical	Manufacturer
Coomassie R250	Applichem, Darmstadt
di-Ammonium sulphate	Roth, Karlsruhe
di-Potassium hydrophosphate	Roth, Karlsruhe
di-Sodium hydrophosphate	Roth, Karlsruhe
DNA 1kB plus Marker ($1\mu g/\mu l$)	Invitrogen, Karlsruhe
dNTPs	Thermo Fisher, Schwerte
EDTA	Merck, Darmstadt
Ethanol	Applichem, Darmstadt
Ethidiumbromide	Applichem, Darmstadt
Glycerol	Roth, Karlsruhe
Glycine	Applichem, Darmstadt
IPTG	Roth, Karlsruhe
Isopropanol	J.T. Baker, Deventer
Kanamycin sulphate	Applichem, Darmstadt
Lactic acid	Sigma-Aldrich, München
L-histidine	Sigma-Aldrich, München
L-leucine	Sigma-Aldrich, München
L-methionine	Sigma-Aldrich, München
L-threonine	Sigma-Aldrich, München
L-serine	Sigma-Aldrich, München
Magnesium chloride	Merck, Karlsruhe
Magnesium sulfate	Merck, Darmstadt
Methanol	J.T. Baker, Griesheim
Midori Green	Biozym, Hessisch Oldendorf
Methionine	Sigma-Aldrich, München
Milk powder, non fat	Applichem, Darmstadt
Na-Salicylate	Sigma-Aldrich, München
Nitrocellulose Hybond-ECL, 0.45 μm	GE Healthcare, München
PageRuler Prestained Protein Ladder	Thermo Fisher, Schwerte
Poly-L-lysine	Sigma-Aldrich, München
Potassium chloride	Applichem, Darmstadt

Chemical	Manufacturer
Potassium hydrophosphate	Grüssing, Filsum
Potassium phosphate	Riedel de Haen, Seelze
Rotiphorese Gel 30 (Acrylamide mix)	Roth, Karlsruhe
SDS (Sodium dodecylsulfate)	Applichem, Darmstadt
Sodium citrate	Applichem, Darmstadt
Sodium chloride	Applichem, Darmstadt
Sodium hydroxide	Applichem, Darmstadt
TEMED	Applichem, Darmstadt
Thiamine hydrochloride	Sigma-Aldrich, München
Tris	Roth, Karlsruhe
Tween 20	Roth, Karlsruhe
Whatman paper	Whatman GmbH, Dassel
Xylene cyanol	Applichem, Darmstadt

3 | Methods

3.1. Molecular biology

Mutagenesis PCR

PCR reactions to generate plasmids encoding Tar chemoreceptor methylation site mutants were performed with KAPA Hifi DNA polymerase in a T professional thermocycler (Biometra). Primers encoding the specific base exchanges are listed in tab.3.1. Whole plasmid amplification products were digested for one hour at $37\,^{\circ}\mathrm{C}$ with DpnI to get rid of the template plasmid.

Table 3.1.: Primers for Tar mutagenesis
Mutated triplet sequences are underlined.

Primer	sequence 5'→3'	target
AK4_for	act gcc gcc agc atg gag <u>gcg</u> ctc acc gcg aca gtg	tar^{EEAE}
AK4_rev	cac tgt cgc ggt gag <u>cgc</u> ctc cat gct cgg cgg agt	tar^{EEAE}
AK5_for	ca tcg ctg gtg cag <u>gca</u> tca gct gcc gcc	tar^{EEEA}
AK5_rev	ggc ggc agc tga <u>tgc</u> ctg cac cag cga tg	tar^{EEEA}
AK6_for	cgt act gaa <u>gcg</u> cag gca tcc gcg ctg	tar^{AEEE}, tar^{AEEA}
AK6_rev	cag cgc gga tgc ctg <u>cgc</u> ttc agt acg	tar^{AEEE}, tar^{AEEA}

Continued on next page

Table 3.1.: Primers for Tar mutagenesis

Mutated triplet sequences are underlined.

Primer	sequence 5'→3'	target
AK7_for	tcc gcg ctg gaa <u>gca</u> act gcc gcc agc	tar^{EAEE}, tar^{EAEA}
AK7_rev	gct ggc ggc agt <u>tgc</u> ttc cag cgc gga	tar^{EAEE}, tar^{EAEA}
AK10_for	act gaa <u>gcg</u> cag gca tcc gcg ctg gaa <u>gca</u> act	tar^{AAEE}, tar^{AAAE}, tar^{AAEA}
AK10_rev	agt <u>tgc</u> ttc cag cgc gga tgc ctg <u>cgc</u> ttc agt	tar^{AAEE}, tar^{AAAE}, tar^{AAEA}
AK11_for	gaa <u>gcg</u> cag gca tcc gcg ctg gaa gaa act gcc gcc agc atg gag <u>gcg</u> ctc	tar^{AEAE}, tar^{AEAA}
AK11_rev	gag <u>cgc</u> ctc cat gct ggc ggc agt ttc ttc cag cgc gga tgc ctg <u>cgc</u> ttc	tar^{AEAE}, tar^{AEAA}

Restriction digestion

Plasmids and purified PCR products were digested with two appropriate restriction enzymes in their respective buffer at $37\,^\circ$C C for one to three hours. Restricted nucleic acids were purified using PCR purification or gel extraction kit.

Ligation

Restricted plasmid and insert were connected by adding ligase. Ligation reaction was performed for one hour at room temperature.

Preparation of competent cells

A 5 ml culture of LB was inoculated with cells and grown at $37\,^\circ$C over night. 3 ml of this culture were diluted into 300 ml fresh LB and grown until an optical density at 600 nm (OD_{600}) of 0.5 to 0.7. All subsequent steps were performed on ice or at $4\,^\circ$C, respectively. Cells are harvested by spinning them for 5 minutes at 4000 rpm, pellets are resuspended in ice cold 0.1 M $MgCl_2$ and incubated on ice for 30 minutes. Following, cells are centrifuged again for 5 minutes at 3000 rpm, pellet was resuspended in ice cold $CaCl_2$ and centrifugation was repeated. Cell pellet was resuspended in 0.1 M $CaCl_2$+18% gylcerol, aliquoted and frozen at $-80\,^\circ$C.

Transformation

For transformation, 0.5-1 μl of plasmid DNA or 5-10μl of ligation product and 30-50 μl of thawed competent cells were mixed and incubated on ice for 15 min. After applying a heat shock at $42\,^\circ$C for 1 minute, cells were stored on ice again for 5 min. Subsequently, 1 ml LB medium was added and cells were shaken at 600 rpm and $37\,^\circ$C for one hour. After spinning the cells for 3 mintes at 8000 rpm, the supernatant was reduced to 100 μl, the pellet was resuspended and plated on LB agar plates with respective antibiotics. Plates were incubated at $37\,^\circ$C over night.

Preparation of glycerol stocks

A 5 ml LB culture with respective antibiotics was inoculated with a single colony from the transformation LB agar plate and grown over night at $30\,^\circ$C on a rotator. Cells were centrifuged for 5 minutes at 4000 rpm, the cell pellet was resuspended in 1 ml LB+20%

glycerol and pipetted into cryotubes. These were then prechilled on ice for at least one hour before moving them to $-80\,^{\circ}\mathrm{C}$ where they can be stored for long term.

3.2. Cell cultivation

Strains

All strains used in this work are listed in tab.3.2.

Table 3.2.: Strains

Strain	relevant genotype	reference
VS181	RP437 Δ(cheY cheZ) Δ(tsr tar tap trg aer)	[Sourjik04]
VS274(=VH1)	RP437 Δ(cheR cheB cheY cheZ) Δ(tsr tar tap trg aer)	[Endres08]
UU1250(=VS188)	Δ(tsr tar tap trg aer)	J. S. Parkinson, Utah
SN1	LJ110 Δ(cheY cheZ)	S. Neumann
SN25	Δtar Δ(cheY cheZ)	S. Neumann
SN119	Δtsr Δ(cheY cheZ)	S. Neumann
MG1655	wild type	[Guyer81]
RP437(=HCB33)	wild type	[Parkinson82]
W3110	wild type	[Bachman72]

Plasmids

All plasmids used or generated in this work are listed in tab.3.3.

Table 3.3.: Plasmids

Plasmid	relevant genotype	induction	reference
pAK1	tar$^{\text{AEEE}}$, pKG110 derivative	2 μM Sal	This work
pAK2	tar$^{\text{EAEE}}$, pKG110 derivative	2 μM Sal	This work
pAK3	tar$^{\text{EEAE}}$, pKG110 derivative	2 μM Sal	This work
pAK4	tar$^{\text{EEEA}}$, pKG110 derivative	2 μM Sal	This work
pAK5	tar$^{\text{AAEE}}$, pKG110 derivative	2 μM Sal	This work
pAK6	tar$^{\text{AEAE}}$, pKG110 derivative	2 μM Sal	This work
pAK7	tar$^{\text{AEEA}}$, pKG110 derivative	2 μM Sal	This work
pAK8	tar$^{\text{EAAE}}$, pKG110 derivative	2 μM Sal	This work
pAK9	tar$^{\text{EAEA}}$, pKG110 derivative	2 μM Sal	This work
pAK10	tar$^{\text{EEAA}}$, pKG110 derivative	2 μM Sal	This work
pAK11	tar$^{\text{AAAE}}$, pKG110 derivative	2 μM Sal	This work
pAK12	tar$^{\text{AAEA}}$, pKG110 derivative	2 μM Sal	This work
pAK13	tar$^{\text{AEAA}}$, pKG110 derivative	2 μM Sal	This work
pAK14	tar$^{\text{EAAA}}$, pKG110 derivative	2 μM Sal	This work
pAK15	tar$^{\text{EEEE}}$ with C-terminal 6xHis tag, pKG110 derivative	2 μM Sal	This work
pAK16	tar$^{\text{AEEE}}$ with C-terminal 6xHis tag, pKG110 derivative	2 μM Sal	This work
pAK17	tar$^{\text{EAEE}}$ with C-terminal 6xHis tag, pKG110 derivative	2 μM Sal	This work
pAK18	tar$^{\text{EEAE}}$ with C-terminal 6xHis tag, pKG110 derivative	2 μM Sal	This work
pAK19	tar$^{\text{EEEA}}$ with C-terminal 6xHis tag, pKG110 derivative	2 μM Sal	This work
pAK20	tar$^{\text{AAEE}}$ with C-terminal 6xHis tag, pKG110 derivative	2 μM Sal	This work
pAK21	tar$^{\text{AEAE}}$ with C-terminal 6xHis tag, pKG110 derivative	2 μM Sal	This work
pAK22	tar$^{\text{AEEA}}$ with C-terminal 6xHis tag,	2 μM Sal	This work

Continued on next page

Table 3.3.: Plasmids

Plasmid	relevant genotype	induction	reference
pAK23	tar^{EAAE} with C-terminal 6xHis tag, pKG110 derivative	2 μM Sal	This work
pAK24	tar^{EAEA} with C-terminal 6xHis tag, pKG110 derivative	2 μM Sal	This work
pAK25	tar^{EEAA} with C-terminal 6xHis tag, pKG110 derivative	2 μM Sal	This work
pAK26	tar^{AAAE} with C-terminal 6xHis tag, pKG110 derivative	2 μM Sal	This work
pAK27	tar^{AAEA} with C-terminal 6xHis tag, pKG110 derivative	2 μM Sal	This work
pAK28	tar^{AEAA} with C-terminal 6xHis tag, pKG110 derivative	2 μM Sal	This work
pAK29	tar^{EAAA} with C-terminal 6xHis tag, pKG110 derivative	2 μM Sal	This work
pKG110	Sal regulation (PnahG), pACYC ori, CmR	-	J. S. Parkinson, Utah
pVS88	cheY-eyfp cheZ-ecfp, pTrc99a derivative	50 μM IPTG	[Sourjik04]
pVS362	tsr^{EEEEE}, pBAD33 derivative	0.6 μM Sal	G. Schwarz
pVS472	tar^{AAAA}, pKG110 derivative	2 μM Sal	S. Hermann
pVS1086	tar^{EEEE}, pKG110 derivative	2 μM Sal	D. Kentner
pVS1110	cheY-eyfp cheZ-ecfp cheR	50 μM IPTG	D. Kentner

Cell preparation

A 10 ml culture of TB medium with respective antibiotics and inducers was inoculated with a small amount of the glycerol stock and grown over night (16 hours) at $30\,°C$ with 200 rpm shaking. A fresh 10 ml TB culture was inoculated with 500 μl of the preculture and grown at $34\,°C$ with 275 rpm shaking until an OD_{600} of 0.6 was reached. The cells were washed

twice with 10 ml tethering buffer an stored for at least 30 minutes at $4\,°\text{C}$ to minimize their metabolic activity.

TB Soft agar assay

To test the chemotactic spreading of the generated strains, a soft agar based swarming assay was performed. Therefore, a melted mixture of 100 ml TB and 0.25% agar with respective antibiotics and inducers was poured into a square petri dish. After solidifying, 2 μl of prepared cells were spotted onto the surface of the agar. Plates were incubated at $34\,°\text{C}$ for around 16 hours, a photo was taken afterwards with Nikon D5200 camera and evaluated using ImageJ software.

Soft agar MeAsp gradient assay

For further investigation of the chemotactic spreading, Minimal A Medium soft agar plates having an applied gradient of the stimulus MeAsp were used. Again, 0.25% agar was melted in 100 ml of Minimal A Medium and poured into a square petri dish with respective antibiotics and inducers. The MeAsp gradient was established after solidifying of the agar by pipetting 12×10 μl 0.1 M MeAsp solution in a vertical line onto the agar surface. Plates were stored at $4\,°\text{C}$ over night to establish a uniform MeAsp gradient before spotting prepared cells (2μl) onto them at varying distances to the stimulus source. Plates were then incubated at $34\,°\text{C}$ for around 48 hours and a photo was taken afterwards with Nikon D5200 camera and evaluated using ImageJ software.

3.3. Protein biochemistry

Tar methylation immunoblot

To test the influence of MeAsp stimulation on the methylation of the Tar chemoreceptor, cells were stimulated for different time periods and lysed by pipetting 100 μl of cell suspension in 50 μl of 3$\times$Laemmli buffer which was preheated to $95\,°\text{C}$ and boiling them for another 5 minutes. By doing so, not only lysis but also ongoing methylation is stopped immediately. Samples were loaded on an 8% SDS polyacrylamide gel with an extended length of around 40 cm and run for one hour at 150 V at room temperature to ensure a straight running front in the stacking gel. The main gel run was performed at $4\,°\text{C}$ over night (approximately 16 hours) at 250 V.

The SDS gel was cut in between the the 72 and 43 kDa bands of the Protein Marker (as the expected protein size is 60 kDa) and blotted onto a nitrocellulose membrane using a wet blot device (Biorad). Transfer was performed at 100 V for one hour at $4\,^{\circ}\mathrm{C}$. Uncovered binding sites of the membrane were blocked with milk protein by incubating it with 5% skim milk solution for 30 minutes. After washing 3×5 minutes with TBST, the membrane was incubated with a 1:5000 dilution of thepolyclonal rabbit α-Tar antibody containing 1% skim milk over night at $4\,^{\circ}\mathrm{C}$ on a shaker. Subsequently, cells were washed again 3×5 minutes with TBST and finally incubated with the secondary goat α-rabbit IRDye800 (1:5000 dilution) for 45 minutes. After washing 2×5 minutes with TBST and additional 5 minutes with TBS, the nitrocellulose membrane could be evaluated on an Odyssesy Imager (LI-COR). Thereby, the fluorophore coupled to the secondary antibody gets excited and emission is imaged.

Further analysis of Tar methylation immunoblot was done by plotting intensity profiles using ImageJ software. Profiles correspond to the receptor mobility on the SDS gel, with higher receptor mobility according to higher methylation. The profile of each sample was normalized to the integral intensity of all bands within the respective lane after subtracting the background.

3.4. Fluorescence microscopy

Fluorescent proteins have become a powerful tool to investigate intracellular mechanisms and the behaviour of whole organisms. A wide variety of fluorescent proteins with differing spectra have been developed being suitable for many purposes in biological applications *in vivo*, including control of gene expression, protein localization and monitoring of complete signalling pathways. Fluorescent proteins can be fused to many proteins of interest without affecting their function in the cell. In this work, we used two proteins, yellow fluorescent protein (YFP) and cyan fluorescent protein (CFP) which have different excitation and emission spectra. Interestingly, emission spectrum of CFP and excitation spectrum of YFP do overlap to a large extent as illustrated in Fig.3.1A.

If CFP gets excited with light of appropriate wave length, its emission light can in turn excite YFP which has to be in close proximity of at least 10 nm. This effect is called Fluorescence Resonance Energy Transfer (FRET). With this approach, the interaction of two proteins of interest can be determined by constructing fusion proteins and monitoring both YFP and CFP emission (Fig.3.1B).
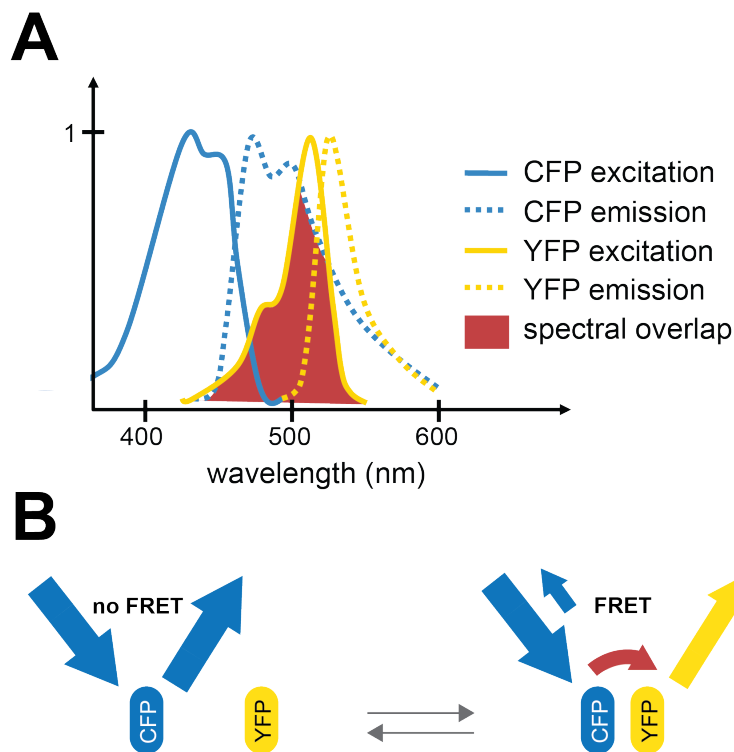
Figure 3.1.: FRET occurs due to spectra overlap of CFP and YFP. (A) Emission and excitation spectra of CFP and YFP with spectral overlap indicated.**(B)** FRET between YFP and CFP occurs only when both are in close proximity of less than 10 nm.

Stimulus-dependent FRET

Stimulus-dependent FRET has been described before to monitor the activity of the chemotaxis signalling pathway with the FRET reporter pair CheY-YFP/CheZ-CFP []. Briefly, when signals are transduced from chemoreceptors to flagella motors, CheY and CheZ are interacting. Upon stimulation, interaction is usually nearly fully aborted and only slowly rises again due to adaptation. The experimantal set-up including a Zeiss Axiovert 200 microscope is shown in Fig.3.2A.
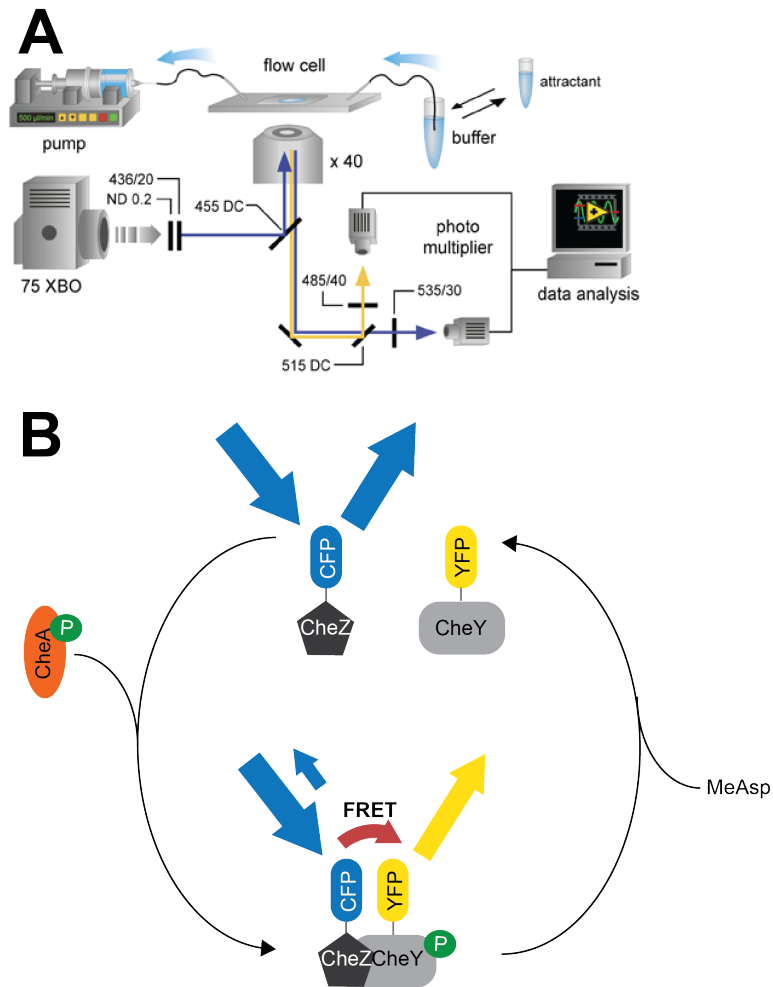
Figure 3.2.: Stimulus-dependent FRET of chemotaxis signalling pathway. (A) Microscope setup.**(B)** Stimulus-dependent FRET between CheY-YFP and CheZ-CFP influenced by presence or absence of stimulus (e.g. MeAsp).

Microscopy coverslips were prepared by incubating them for 20 minutes with poly-lysine and washing them before the attachment of 20 μl cell suspension. The complete coverslip is sealed onto a flow chamber which allows pumping of liquid over the cells by a syringe pump (Harvard Apparatus 22). A constant flow of 300 or 500 μl/min, depending on the type of measurement, was established and only stopped shortly when attractant solutions were added or removed. Emission of several hundreds of cells in focus was monitored and the YFP/CFP ratio changes were taken as representatives of the kinase CheA activity and therefore the chemotaxis signalling pathway activity (Fig.3.2B).

The change in the YFP/CFP ratio (R) after the addition of stimulus was calculated using the equation

$$FRET = \frac{\Delta R_{max} - \Delta R}{\frac{\Delta YFP}{\Delta CFP} + R_0 + \Delta R_{max} - \Delta R} \tag{3.1}$$

where ΔR was calculated for each stimulus concentration as the difference of the ratios before and right after stimulation. A saturating stimulus causes a maximum change in R, ΔR_{max}, at which the corresponding ratio is R_0 which reflects that there is no energy transfer. The constant ratio $\frac{\Delta YFP}{\Delta CFP}$ is microcope specific and was calculated to be 1.2 for the used Zeiss Axiovert 200.

The calculated FRET values in dose response measurements were fitted using a Hill equation

$$FRET(|L|) = m_1 \cdot \left(1 - \frac{m_0^{m_2}}{m_0^{m_2} + m_3^{m_2}}\right) \tag{3.2}$$

with m_0 as the ligand concentration, m_1 as the amplitude of response, m_2 being the Hill coefficient, m_3 as EC_{50}, the stimulus concentration that causes a half maximal response. The response amplitudes in the dynamic range measurements were defined as the difference in ratios right after the respective stimulations and of the adapted state of the previous stimulus concentration.

3.5. Mass spectrometry

Mass spectrometry is used for many biological tasks, including identification of proteins, analysis of protein conformation and detection of posttranslational modifications. A mass spectrometer consists of three parts: first there is an ion source that brings the molecules into the gas phase and ionizes them. The second part is a mass analyzer that separates the ions in space or time according to their mass-to-charge ratio (m/z), and finally, there is a detector that detects the separated ions.

Proteins of interest are digested with proteases to small peptides. Ionization of these peptides can be performed by electrospray ionization (ESI) by first dissolving them in an appropriate solvent. The solution is then injected through a needle to which a voltage is applied that highly positively charges the peptide solution and leads to droplet formation to increase the surface. Before entering the mass spectrometer, the droplets explode due to the electrostatic repulsion of the peptide ions which enter the gas phase. For the detection of posttranslational modifications in proteins, tandem mass spectrometry (MS/MS) is used, where two mass spectrometers are connected in series. The first one filters the detection of the peptide of interest according to its m/z ratio, the second mass spectrometer fragments the peptide by collision-induced dissociation (CID) and detects the m/z ratios of the resulting fragments, and the full amino acid sequence including the exact positions of posttranslational modifications can be determined by the distances between the fragment peaks. An upstream HPLC increases the separation of the peptide ions (LC-MS/MS).

Preparation of time series

Stimulation time series to study the methylation kinetics were prepared in two different ways. For the first method, 50 ml of TB with inducers and respective antibiotics were inoculated with 2.5 ml of overnight culture and grown at $34\,°C$ with 200 rpm shaking until they reached an OD_{600} of 0.6. Cells were washed twice, concentrated into 1 ml tethering buffer and shaken at room temperature for at least 30 minutes. Cells were then stimulated with 100 μM MeAsp for the respective time periods. Methylation reaction was stopped and cell were lysed by sonicating them on ice. Cell debris was removed by spinning the sample 15 minutes at 2000 rpm. The supernatant was centriguged again in an ultracentrifuge at $45000\times g$ (120000 rpm) for 30 minutes. The resulting pellet was then directly digested with trypsin as described in section 3.5.

The second method included a protein purification step on a Ni-NTA resin and was therefor

only used with receptors containing a C-terminal 6×His-tag. 50 ml of TB with inducers and respective antibiotics were inoculated with 2.5 ml of overnight culture and grown at $34\,^{\circ}C$ with 200 rpm shaking until they reached an OD_{600} of 0.6. Cells were washed twice, concentrated into 1 ml tethering buffer without EDTA and shaken at room temperature for at least 30 minutes. Cells were then stimulated with 100 μM MeAsp for the respective time periods. Methylation reaction was stopped by pipetting the cells into 10 ml ethanol which is supposed to denature all proteins. After spinning down, cell pellets were dried and resuspended into 8 M Urea containing buffer, prepared after the recipe from Qiagen Ni-NTA Spin kit, which finally lysed the cells.

Protein purification on Ni NTA columns

Purification of 6×His-tagged Tar was performed by using the denaturing protocol of the Qiagen Ni-NTA Spin kit according to the manufacturers instructions.

Coomassie staining

Samples with flow through, wash or elution fractions were tested by running them onto small 10% SDS polyacrylamide gels and staining these gels with Coomassie afterwards. Gels were covered with a 0.1% Commassie solution and heated for one minute in the microwave. Solution was discarded and gels were washed several times with ddH$_2$O to remove residual Coomassie dye. Gels were covered with destaining solution and heated for one minute in the microwave. Solution was removed and gels were incubated with fresh destaining solution on a shaker at room temperature over night. Photos were taken with Nikon D5200 camera.

Trypsin digestion by filter aided sample preparation (FASP)

Crude membrane fractions or Ni-NTA-purified elution fractions containing Tar chemoreceptors were digested with trypsin by using filter aided sample preparation (FASP) as described by [108]. Briefly, protein containing extracts kept on a filter with 30 kDa cut-off were first extensively washed and alkylated before they are digested with trypsin to peptides (see also http://www.biochem.mpg.de/226356/FASP).

Mass spectrometrical analysis

For further purification reasons, peptides were trapped on a C18 column, eluted with 90% acetonitrile at a flow rate of 15 μl/min and eluate was collected in a time window of 2

minutes. Acetonitrile was removed by SpeedVac. 25 μl of the resulting sample was analysed by a nanoHPLC system (Eksigent, Axel Semrau) coupled to an ESI LTQ Orbitrap mass spectrometer (Thermo Fisher). Sample was loaded on a C18 trapping column (Inertsil, LC Packings) with a flow rate of 10 μl/min 0.1% TFA. Peptides were eluted and separated on an analytical column (75 μm x 150mm) packed with Inertsil 3 μm C18 material (LC Packings) with a flow rate of 200 nl/min in a gradient of buffer A (0.1% formic acid) and buffer B (0.1% formic acid, acetonitrile): 0-6min: 3% B; 6-60min: 3-40% B; 60-65min: 60-90% B. One survey scan (res: 60000) was followed by 3 information dependent product ion scans in the Orbitrap (res: 7500). 2+, 3+ and 4+ charged ions were selected for fragmentation. In addition, the +2 and +3 ion of the unmodified, singly methylated and two times methylated peptide (m/z = 813.7; 818.4; 823.1; 1220.1; 1227.1; 1234.1) were continuously fragmented in a data independent mode. To get quantitative information, peak areas from the extracted ion chromatograms were used. Analysis of the raw data was performed by using QualBrowser of Xcalibur software (Thermo Fisher) and GPMAW (Lighthouse data, Denmark).

Part III.

Results & Discussion

4 | Results

4.1. Investigation of the adaptation kinetics in chemotaxis

Bacterial chemoreceptors contain in their cytoplasmic part several glutamate residues which are subject to methylation and thereby mediate adaptation of cells to persistent stimuli. Although this is well-known for a long time, the necessity of having more than one site remains unclear. In this study, we wanted to decipher the role of individual methylation sites for chemotaxis and adaptation. Therefore, we used the *E. coli* aspartate chemoreceptor which possesses four sites of methylation. The contribution of each individual methylation site to chemotaxis and adaptation was investigated by making specific sites unavailable for modification. Analysis of the altered adaptation in chemotaxis was done by rendering specific sites unavailable for modification. In wild-type Tar^{QEQE} receptors, the two glutamine residues are deamidated first to glutamates before they can be methylated. Hence, we consider Tar^{EEEE} as wild-type chemoreceptor in this study. However, substitution of methylation sites with glutamine residues in order to mimick methylation has the disadvantage that glutamines are deamidated to glutamates by CheB and receptors become wild-type Tar^{EEEE}. Thus, we used chemoreceptors with specific alanine substitutions, because these allowed us to investigate their properties in a CheRB^{+} background. Inducible plasmids encoding mutant Tar sequences were generated by site-directed mutagenesis using primers containing the respective triplet exchange(s).

A total of 16 Tar receptors were created with zero to four alanine substitutions at the methylation sites in all possible combinations (2^4), hereafter referred to as Tar mutants. Tar mutants were expressed in a receptorless strain together with the FRET reporter pair CheY-YFP and CheZ-CFP. Cells expressing the FRET reporter pair were used for all experiments to exclude variations between different strains.

## 4.1.1. Ability of Tar mutants to mediate chemotaxis on TB soft agar plates

The ability of alanine-substituted chemoreceptors to mediate chemotaxis was tested by a TB soft agar assay. In soft agar, cells can spread through the pores created by the polysaccharide network. In contrast to liquid medium, cells can get stuck in agar pores and need to change the swimming direction to free themselves. The control of flagellar rotation depended on the ability of the cells to compare spatiotemporal differences in concentration which in turn depended on chemoreceptor methylation. If this ability is impaired, cells can either display a swimming phenotype where they either get stuck in the agar pores because they fail to tumble and reorient, or cells display a tumbling phenotype with a high tumbling frequency and are thus hardly moving away from the inoculation site.

In addition, nutrients contained in the TB medium are taken up by the cells which gradually leads to the establishment of a local gradient of nutrients spanning from the inoculation site to outer areas. Cells can follow such a gradient by utilizing their adaptation system for making spatiotemporal comparisons in nutrient distribution. Thereby, differences in receptor methylation at two consecutive time points can be detected. Due to constant nutrient uptake by the cells, the nutrient gradient is permanently in flux. Both, the ability to change the rotational direction of the flagella and the sensing of the nutrient gradient are essential to move within TB soft agar.

Tar mutants did not have all sites available for methylation and could have an altered ability to make such spatiotemporal comparisons. Thus, their ability to spread on soft agar plates could deviate from wild-type behaviour. To quantify the differences between mutant and wild-type receptors, a strain expressing wild-type Tar^{EEEE} was used as a positive control on each plate. As negative control, cells expressing Tar^{AAAA} were used. These cells were adaptation-deficient and served as a reference for the amount of basal spreading on TB soft agar. Nevertheless, this mutant showed a moderate ring of cells which we considered as basal spreading, but it could not effectively follow the nutrient gradient because it was unable to make spatiotemporal comparisons. Representative TB soft agar plates of Tar mutants can be found in Fig.4.1.

The difference between basal and chemotaxis driven spreading was visualized by the diffuse borders of the cell ring of Tar^{AAAA} in contrast to very defined borders of the Tar^{EEEE} ring of cells (Fig.4.1). As the adaptation-deficient Tar^{AAAA} still had more than 60% of wild-type spreading ability (Fig.4.2), we consider cells displaying values close to that percentage and lower as spreading on a basal level and not driven by chemotaxis. The transition zone between
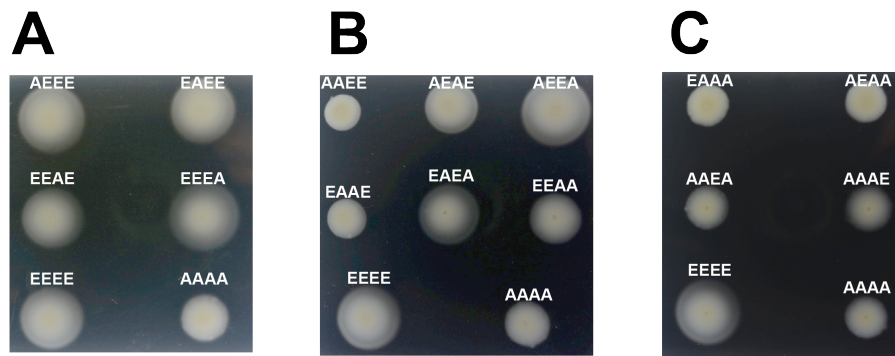
Figure 4.1.: TB soft agar chemotaxis assay. The assay was performed with Tar mutant receptors carrying one **(A)**, two **(B)**, or three **(C)** alanines at their methylation sites as indicated. The soft agar plates consist of TB medium and 0.25% agar. As inducers, 2 μM Sal and 50 μM IPTG were used. Plates were inoculated with 2 μl of over night cultures and incubated at $34\,^{\circ}\text{C}$ for 16 to 20 hours. As controls, cells expressing wild-type Tar$^{\text{EEEE}}$ and the adaptation-deficient Tar$^{\text{AAAA}}$ were spotted onto each soft agar plate.

basal and chemotactic spreading could not be determined definitely. Cells expressing receptors with three alanine substitutions were considered to spread only on a basal level due to their small ring diameters. The obvious differences in ring diameters in the 3×A receptor subset were probably caused by different flagellar bias towards either a swimming or a tumbling phenotype.

Most of the Tar mutants displayed a decreased ring diameter in comparison with the wild-type chemoreceptor Tar$^{\text{EEEE}}$, which was also illustrated in the quantitative evaluation of their spreading in Fig.4.2. Several Tar mutants with only one alanine substitution at the methylation sites (Fig.4.1A) displayed diameters that were comparable to wild-type. In particular, Tar$^{\text{EEEA}}$ and Tar$^{\text{AEEE}}$ spreading was similar to the wild-type. Following, Tar$^{\text{EEAE}}$ and Tar$^{\text{EAEE}}$ showed noticeable, but slightly less spreading than the wild-type. This indicated the low importance of methylation site 4 for chemotactic sensing of gradients, followed by site 1, site 3 and site 2, which were consequently more important for mediating chemotaxis, as the blocking of these sites for methylation showed the strongest effects.

Also several receptors carrying two alanine substitutions at their methylation sites (Fig.4.1B and Fig.4.2) showed only basal spreading on soft agar plates. Tar$^{\text{AAEE}}$ displayed even smaller rings of cells than the negative control Tar$^{\text{AAAA}}$. This receptor mutant probably affected the flagella bias even more than the negative control. Chemotaxis driven spreading was clearly observed for Tar$^{\text{AEEA}}$ and Tar$^{\text{EAEA}}$, with more than 90% and more than 85% of the wild-type level, respectively. Tar$^{\text{AEEA}}$ combines the two least affected mutants of the 1×A
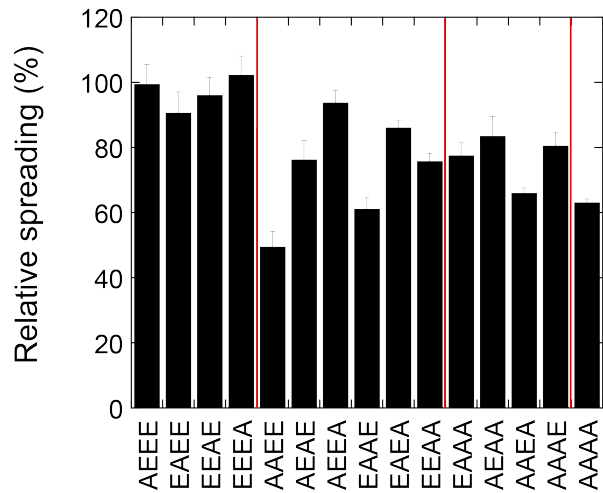
Figure 4.2.: Relative spreading determined from TB soft agar assay. The spreading was determined by measuring the cell ring diameters and calculating the ratio of the respective Tar chemoreceptor in comparison to the positive control, Tar^{EEEE} which is defined as 100%. Error bars represent the standard error of the mean (SEM) of four independent experiments.

receptor set, Tar^{AEEE} and Tar^{EEEA}. Also Tar^{EAEA} combines the least affected 1×A mutant Tar^{EEEA} with the stronger affected mutant Tar^{EAEE}. These receptors were able to perform spatiotemporal comparisons to some extent due to their remaining available methylation sites and thus could sense the nutrient gradient. Other combinations of 2×A substitutions failed to mediate chemotaxis on soft agar plates.

4.1.2. Ability of Tar mutants to sense attractant gradients

In the previous analysis, cells were gradually creating a nutrient gradient on TB soft agar plates by themselves, which was changing permanently over time. In order to investigate if the chemotactic spreading of the mutants in a self-created gradient is similar to spreading in an artificial gradient, we tested spreading of Tar mutants in a defined attractant gradient. Minimal A medium was used instead of rich medium such as TB medium to prepare the soft agar and to make sure that cells respond exclusively to the externally applied attractant α-D,L-Methylaspartate (MeAsp), which is a structural analog of aspartate that cannot not be metabolized. Furthermore, we tested the dependence of chemotactic spreading on the concentration range by inoculating cells at different distances from the gradient source. (Fig.4.3A). Gradient formation on soft agar plates was confirmed before by visualization with fluorescein (Yiling Yang, PhD thesis, data not shown). Attractant solution was spotted in 10 μl aliquots and 1 cm intervals onto the agar plates and gradient was allowed to form over

night. The shape of the gradient followed a Gaussian normal distribution. A summary of mean spreading towards or away from the gradient source can be found in Tab.4.1 for all receptors spotted at different distances. The chemotactic bias of cells expressing different chemoreceptors was calculated by the ratio of their spreading up (+) and down (-) the MeAsp gradient (Fig.4.3B), i.e. values above 1 indicate chemotaxis driven spreading towards the attractant source.

Wild-type Tar^{EEEE} showed strongest chemotactic bias compared to Tar mutants. Besides, best chemotaxis ability of this strain was observed at distances around 2 cm from MeAsp source. The MeAsp concentration at a distance of 2.5 cm was approximately 50 μM (Yiling Yang, PhD thesis). The negative control Tar^{AAAA} was spreading symmetrically up and down the gradient, resulting in a chemotactic bias of 1. Thus, this strain could not follow the attractant gradient.

The two mutants Tar^{EEEA} and Tar^{AEEE} showed the most efficient spreading towards the attractant among all mutants, with best chemotactic bias at a distance of 2 to 3 cm from the stimulus center, indicating that these strains responded better to a slightly lower MeAsp concentration range than the wild-type. As these two receptors were least affected in comparison to wild-type Tar, this confirmed the minor importance of site 4 and site 1 for the sensing of MeAsp.

Among receptors with one alanine replacement, also Tar^{EAEE} showed a significant chemotactic bias along the MeAsp gradient, but still not as efficient as the two above mentioned receptors. Tar^{EEAE} did not display a notable chemotactic bias towards the attractant gradient, suggesting a major role of site 3 for gradient sensing. Not all of the 2×A receptors showed a clear chemotactic bias towards the gradient. Tar^{AEEA} and Tar^{EAEA} were able to perform chemotaxis-driven spreading. Tar^{AEEA} showed strongest chemotaxis among this receptor set. This receptor combines alanine substitutions at site 1 and 4, the two substitutions with the weakest effects in the single alanine receptor set. Tar^{EAEA} contains alanine substitutions at site 2 and 4, two substitutions which also showed weak effects in the 1×A receptor set. Other combinations of two alanines and two glutamates did not display a relevant chemotactic bias. These receptors were more affected in their ability to perform chemotaxis than Tar^{AEEA} and Tar^{EAEA}. Also the receptor set with three alanine substitutions did not display any noticeable spreading up the gradient. The impairment of these receptors was apparently too high to respond to the MeAsp gradient in a significant way.
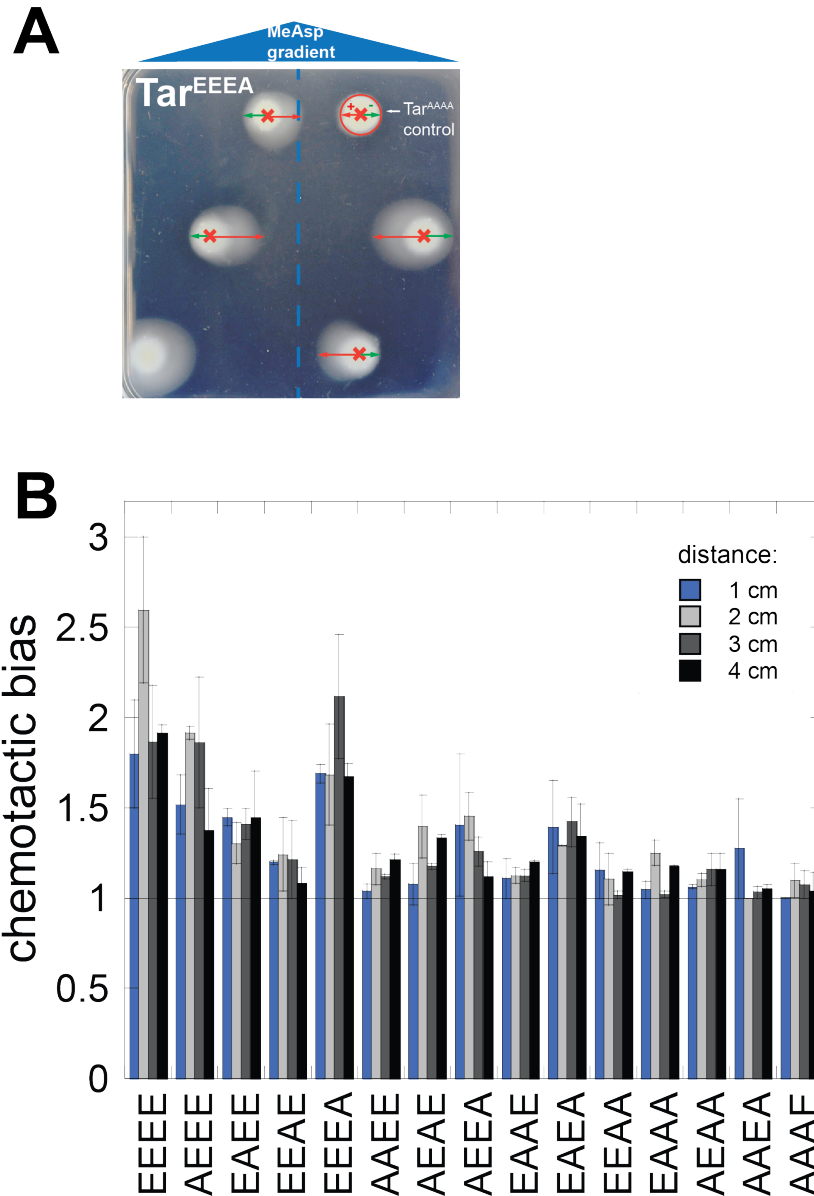
Figure 4.3.: Chemotaxis of Tar mutants in a MeAsp gradient on soft agar plates. (A) The soft agar plates consist of Minimal A medium and 0.25% agar. As inducers, 2 μM Sal and 50 μM IPTG were used. The MeAsp solution was spotted in a vertical line in the center of the plate, marked by the blue line, and gradient formed in 16 hours. Plates were inoculated with 2 μl of over night cultures and incubated at $34\,°$C for 48 hours. Cell suspension was spotted at different distances from the MeAsp source: 1 cm, 2 cm, 3 cm, 4 cm and 5 cm. Cells inoculated at a distance of 5 cm from the gradient source were spreading to the borders of the plate and could not be evaluated. Shown here is a representative example of cells expressing Tar[EEEA]. As controls, cells expressing the adaptation-deficient Tar[AAAA] were spotted onto each soft agar plate at a distance of 1.5 cm. **(B)** Diagram showing the chemotactic bias of Tar methylation site mutants towards MeAsp at different distances from its source. The bias was calculated by dividing the run distance of the cells towards the gradient source (+) by the run distance away from it (-). Chemotactic bias of Tar[AAAA] was approximately 1 (Tab.4.1). Error bars represent SEM of two independent experiments.

Table 4.1.: Spreading down (-) and up (+) the MeAsp gradient
Evaluated with ImageJ software

Distance	1 cm			2 cm			3 cm			4 cm		
Gradient	-	+	bias	-	+	bias	-	+	bias	-	+	bias
Receptor												
EEEE	31	54	1.8	27	70	2.6	38	71	1.86	43	81	1.91
AEEE	35	53	1.52	36	54	1.91	34	64	1.86	37	64	1.37
EAEE	29	42	1.45	32	42	1.3	37	51	1.41	33	48	1.44
EEAE	32	38	1.2	35	38	1.24	29	35	1.21	33	41	1.08
EEEA	29	49	1.69	32	60	1.68	30	66	2.12	42	65	1.67
AAEE	37	38	1.04	38	47	1.16	39	44	1.12	36	41	1.21
AEAE	38	41	1.08	33	41	1.4	33	38	1.18	27	39	1.33
AEEA	34	45	1.4	40	47	1.45	39	50	1.26	38	53	1.12
EAAE	29	33	1.11	31	36	1.12	33	37	1.13	29	33	1.2
EAEA	32	44	1.39	35	48	1.29	34	49	1.42	34	42	1.34
EEAA	33	38	1.15	34	35	1.11	36	37	1.02	33	39	1.15
EAAA	27	27	1	29	31	1.1	27	29	1.07	28	30	1.04
AEAA	24	32	1.28	29	30	1	29	30	1.03	33	34	1.05
AAEA	26	28	1.06	30	33	1.1	27	32	1.16	28	33	1.16
AAAE	31	32	1.04	30	38	1.25	30	31	1.02	29	35	1.18
AAAA	30	30	1	-	-	-	-	-	-	-	-	-

Summarizing the results from TB soft agar plates and MeAsp gradient soft agar plates, cells expressing Tar mutants with one alanine substitution were able to perform chemotaxis, though mostly to a lesser extent in comparison to wild-type receptors, depending on which site was alanine-substituted. Particularly, Tar^{AEEE} and Tar^{EEEA} showed best sensing of the gradient in both assays. Also cells expressing Tar^{EAEE} followed the attractant gradient, whereas Tar^{EEAE} hardly sensed the MeAsp gradient. However, Tar^{EEAE} showed spreading on TB soft agar plates, possibly because these cells could respond to the concentration range of the nutrient gradient. In contrast, Tar^{EEAE} failed to detect the MeAsp gradient. Chemotaxis of this mutant towards high attractant concentrations was worse than in the wild-type. From the $1\times$A receptors, we could also conclude the effect of individual methylation sites on chemotaxis in soft agar. For both assays, we observed that substitution of site 3 was associated with the strongest effect on chemotaxis among the $1\times$A receptor set. Therefore, site 3 has the highest impact on the performance of proper chemotaxis. Substitution of site 2 displayed the second highest effect on chemotaxis, thus this site has the second highest impact for performing proper chemotaxis similar to the wild-type. For both assays, substitution of site 1 or site 4 showed the weakest effects on chemotaxis in comparison with wild-type receptors. Hence, site 1 and site 4 have the lowest impact for proper chemotaxis.

Only several $2\times$A chemoreceptors were able to perform chemotaxis in both assays. A combination of the two least affected mutants Tar^{AEEE} and Tar^{EEEA} in the $2\times$A receptor set, Tar^{AEEA}, displayed best chemotaxis driven spreading and gradient sensing among $2\times$A chemoreceptors in both assays. Furthermore, Tar^{EAEA} was able to perform chemotaxis and to follow attractant gradients. It combines two less affected mutants of the $1\times$A receptors, Tar^{EEEA} and Tar^{EAEE}. Other combinations of two alanine substitutions and all $3\times$A chemoreceptors failed to perform proper chemotaxis and to sense attractant gradients, but only spread in an undirected manner. We conclude that these cells were not able to properly detect the concentration range of the attractant on both TB and MeAsp gradient plates due to their truncated adaptation system.

4.1.3. Dose response measurements of Tar mutants

We wanted to know how the activity and sensitivity of the mutant Tar chemoreceptors was influenced by the alanine substitutions in contrast to wild-type receptors. Therefore, we further characterized the nature of the mutant receptors by determining their specific EC_{50} values, which are the attractant concentrations that reduce the receptors activity by about one half. The activity of the chemoreceptors is directly coupled to the activity of the kinase CheA. The more active the receptor and the kinase were at steady state, the more attractant needed to bind in order to inactivate the receptor and the higher the EC_{50} value was.

With a stimulus-dependent FRET setup (Chapter 3), dose response measurements were carried out *in vivo*. Cells were expressing the FRET reporter pair CheY-YFP and CheZ-CFP. These two fusions to fluorescent proteins have been shown to monitor the chemotaxis signalling pathway activity *in vivo* [107]. Briefly, the response regulator CheY only interacts with its specific phosphatase CheZ when it is phosphorylated, which is the case when its phosphate donor, the kinase CheA, is active. Upon binding of an attractant to the chemoreceptor, CheA activity drops significantly and therefore only a reduced number of phosphorylated CheY molecules is present in the cell. Interaction of the two fluorescent fusion proteins monitors their interaction when exciting CFP and measuring the emission change of both CFP and YFP. The ratio of YFP and CFP emission is proportional to chemoreceptor and CheA activity.

Dose response curves were measured by first adapting the cells to buffer and then stimulating them with MeAsp concentrations increasing in approximately threefold steps and always changing back to buffer in between the different MeAsp solutions (Fig.4.4A). Data were evaluated in a kinase activity plot where no response to the stimulus was defined as full activity and response to a saturating stimulus was defined as no activity. Data points were fitted with eq.4.1 (Fig.4.4B) and the respective EC_{50} values were determined (Tab.4.2).

The calculated FRET values in dose response measurements were fitted using a Hill equation

$$FRET(|L|) = m_1 \cdot \left(1 - \frac{m_0^{m_2}}{m_0^{m_2} + m_3^{m_2}} \right) \tag{4.1}$$

with m_0 as the ligand concentration, m_1 as the amplitude of response, m_2 being the Hill coefficient, m_3 as EC_{50}, the stimulus concentration at the half maximal response.

The change in the YFP/CFP ratio (R) after the addition of stimulus was calculated using the equation

$$FRET = \frac{\Delta R_{max} - \Delta R}{\frac{\Delta YFP}{\Delta CFP} + R_0 + \Delta R_{max} - \Delta R} \tag{4.2}$$
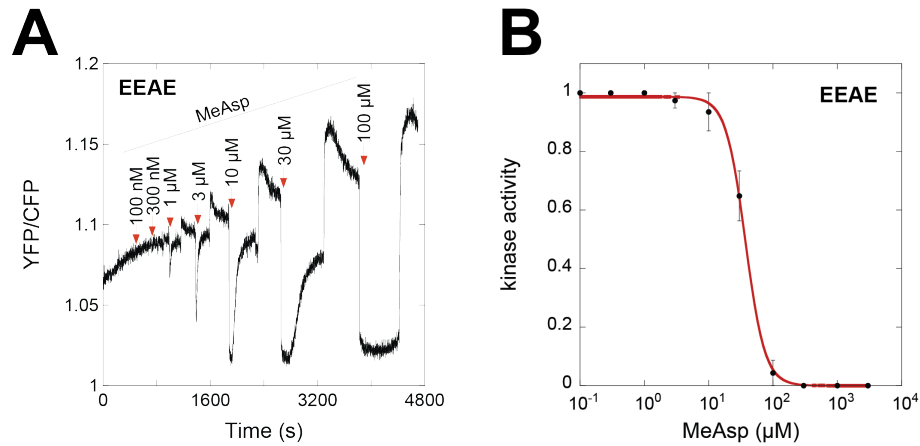
Figure 4.4.: Dose response measurement and calculation. **(A)** Representative stimulus-dependent FRET measurement of Tar^{EEAE}. **(B)** Calculated dose response from **(A)** fitted with formula 4.1. Kinase activity of 0.5 (y-axis) indicates the respective EC$_{50}$ concentration on the x-axis. Error bars represent the SEM of two independent experiments.

where ΔR was calculated for each stimulus concentration as the difference of the ratios before and right after stimulation. A saturating stimulus causes a maximum change in R, ΔR$_{max}$, at which the corresponding ratio is R$_0$ which reflects that there is no energy transfer. The constant ratio $\frac{\Delta YFP}{\Delta CFP}$ is microscope specific and was calculated to be 1.2 for the used Zeiss Axiovert 200.

Exemplary, also the absolute response amplitudes of cells expressing different receptors to saturating MeAsp concentrations were determined by means of the dose response measurements (Fig.4.5).

Table 4.2.: EC$_{50}$ values of Tar mutants [μM MeAsp]

Data for Q-substituted Tar receptors kindly provided by David Kentner. SEM of at least two experiments.

| Amino Acid (x) Strain / Receptor	Q ΔcheRB		A ΔcheRB		A CheRB$^+$	
	mean EC$_{50}$	$\pm$ SEM	mean EC$_{50}$	$\pm$ SEM	mean EC$_{50}$	$\pm$ SEM
EEEE	-	-	-	-	0.83	0.04
xEEE	-	-	-	-	0.59	0.13
ExEE	-	-	-	-	1.3	0.4
EExE	-	-	-	-	3	0.3
EEEx	-	-	-	-	0.64	0.12
xxEE	7.55	0.82	0.77	0.06	1.35	0.31
xExE	5.41	0.34	1.33	0.21	3.52	0.46
xEEx	4.43	0.24	-	-	0.94	0.06
ExxE	0.91	0.08	-	-	4	0.96
ExEx	1.2	0.16	-	-	1.33	0.16
EExx	1.61	0.05	53	4	53	3
Exxx	7.7	0.1	58	4	79	8
xExx	15	1.6	109	5	119	12
xxEx	16.8	1.4	43	2	59	11
xxxE	21.2	0.5	69	10	118	9
xxxx	39	2.1	385	61	303	75

EC_{50} values could not be measured for all Tar methylation site mutants in the adaptation-deficient $\Delta cheRB$ strain (Tab.4.2). The wild-type receptor Tar^{EEEE}, all receptors with one alanine substitution and three out of six receptors with two alanine substitutions were affected. We assume that the steady-state activity of these receptors was extremely low and could not be significantly lowered by the addition of the attractant MeAsp. In the presence of the adaptation enzymes CheR and CheB, we were able to measure dose response curves for all receptors. By methylation of specific amino acid residues and a subsequent conformational change, CheR increased the activity of the chemoreceptors. In the $CheRB^{+}$ strain, the receptor activity was increased compared to the $\Delta cheRB$ strain due to a certain steady-state receptor methylation so that binding of attractant induced a measurable drop in activity caused by an opposing change of conformation.

EC_{50} values were previously determined for Q-substituted Tar receptors in $\Delta cheRB$ strains to prevent CheB-mediated demaidation of glutamine residues (Fig.4.2, David Kentner, unpublished). A correlation to the EC_{50} values of A-substituted receptors in the $\Delta cheRB$ was observed only for the same number of substitutions. The more methylation sites were substituted with either alanine or glutamine residues, the higher was the respective EC_{50}. However, A- or Q-substitution of exactly the same methylation sites did not display a correlation, indicating that alanine and glutamine substitutions do not have similar effects on the receptor activity. Because EC_{50} values of all $2\times Q$ receptors could be determined in contrast to only three out of six $2\times A$ receptors, we suggest that glutamine residues activate the receptor to a higher extent than alanine residues.

With increasing numbers of alanine substitutions starting from the wild-type receptor Tar^{EEEE} to a fully alanine substituted receptor, steady-state activities of the receptors, and therefore also EC_{50} values increased. We also observed a positive correlation between the EC_{50} values and the response amplitudes to saturating stimuli in $CheRB^{+}$ strain (Fig4.5), as expected. The higher the steady state activity and the EC_{50} were, the bigger was the response amplitude.

Receptors with two alanine substitutions mostly showed low EC_{50} values from 1 to 4 μM, except for Tar^{EEAA} with 53 μM. Two alanine substitutions placed at methylation sites 3 and 4 increased the receptors steady state activity much more than any other $2\times A$ combination. Possibly, Tar^{EEAA} conformation was highly different in comparison to other $2\times A$ receptors. Tar^{EEAA} EC_{50} values were the same in both strains, indicating that receptors are methylated only at a low level, even in the presence of CheR and CheB. Also Tar^{AAEE} and Tar^{AEAE} steady state activity was rather high because we were able to determine EC_{50} values even in the absence of CheR and CheB. Thus, not only the quantity of alanine substitutions alone determined the receptor activity, but also at which positions the alanine residues were placed.
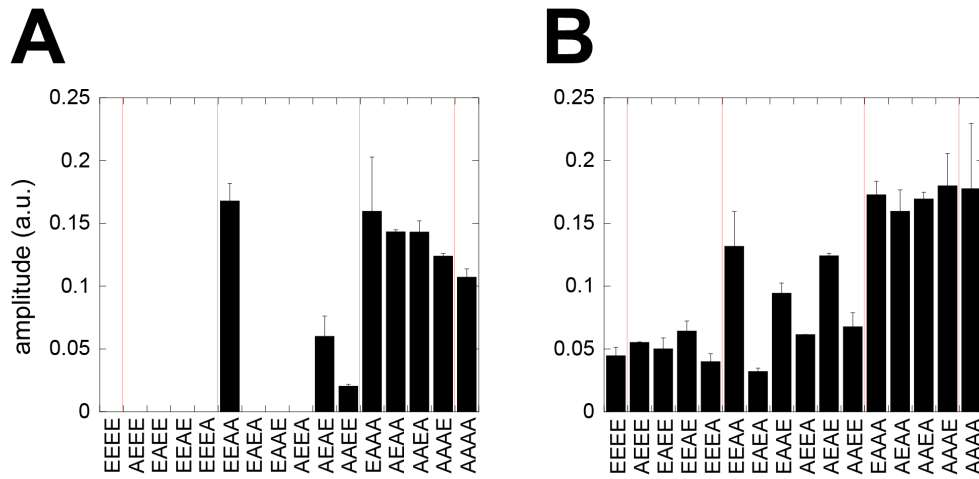
Figure 4.5.: Response amplitudes to a saturating stimulus. (A) $\Delta cheRB$ strain. **(B)** CheRB$^+$ strain.

Likewise, the receptor set with three alanine substitutions displayed a big spread of EC$_{50}$ values, depending on the position of the single glutamate. Tar^{AEAA} displayed the highest EC$_{50}$ value, followed by Tar^{AAAE}, Tar^{EAAA} and Tar^{AAEA} with the lowest EC$_{50}$. Generally, we observed slightly higher EC$_{50}$ values in the CheRB$^+$ than in the $\Delta cheRB$ strain. The expression of CheR and CheB enabled the cells to modify the fourth remaining methylation site and thereby shift the attractant concentrations to which they could respond. A range shifted to higher concentrations consequently caused higher EC$_{50}$ values. However, this activity increase was exceptionally high for Tar^{AAAE} with a rise of 70% when CheR and CheB were present. For other 3$\times$A receptors, the increases ranged from 10% (Tar^{AEAA}) to more than 30% (Tar^{EAAA} and Tar^{AAEA}). The EC$_{50}$ increase in the presence of CheR and CheB pointed to the level of conformational change that methylation on the solely available glutamate caused. Tar^{AAAA} EC$_{50}$ was the highest among all receptors in both strains.

Overall, the amplitudes of full responses confirmed the EC$_{50}$ values in CheRB$^+$ strain, i.e. chemoreceptors with high activity and thus high EC$_{50}$ also displayed higher amplitudes when responding to a saturating stimulus. Big differences in EC$_{50}$ within the 3$\times$A receptor set produced only minor changes in amplitudes (Fig.4.5B). In a $\Delta cheRB$ strain (Fig.4.5A), the response amplitudes of the three 2$\times$A receptors that could be measured were in perfect agreement with their respective EC$_{50}$ values, with higher maximal amplitudes for higher EC$_{50}$. However, the maximal amplitude of Tar^{EEAA} and the amplitudes of the 3$\times$A receptors were higher than the one of Tar^{AAAA} which however clearly displayed the highest EC$_{50}$. We

suppose that these difference occured due to an experimental error. A correlation of EC_{50} and chemotaxis on soft agar was observed to some extent. Lower EC_{50} values come along with higher chemotaxis, as observed mostly in wild-type, $1\times A$ and several $2\times A$ chemoreceptors. Especially the receptors Tar^{AEEA} and Tar^{EAEA}, which showed the only noticeable chemotaxis on soft agar among $2\times A$ receptors, also displayed lowest EC_{50} and thus lowest activity of all receptors with two alanine substitutions.

Tar mutants were also tested for their mobility on an SDS gel by immunoblotting with an α-Tar antibody (Fig.4.6). In an SDS-PAGE, the negatively charged sodium dodecylsulfate (SDS) binds in a linear fashion to the denatured protein. Recent studies suggest that proteins prepared for SDS-PAGE are not completely denatured but retain their conformation to a certain degree (John S. Parkinson, unpublished). Thus, also the remaining conformation could influence the mobility of Tar mutants on the SDS gel. Therefore, proteins migrate towards the anode of an electrical field with velocities inversely correlated with protein size. However, remaining charges of the native protein can influence the mobility on an SDS-PAGE. Positively charged amino acid residues bind more SDS than neutral ones, which in turn bind more SDS than negatively charged amino acid residues. For Tar protein, the neutralization of negatively charged glutamate residues at the methylation sites by methyl groups or replacement with Q or A residues enhances its mobility since more SDS can be bound to the neutral residues. The negative charge of the bound SDS has a stronger effect than the negatively charged glutamate residue. Each receptor modification state is represented by a separate band. As control, Tar proteins with a fixed number of Q residues were run on every SDS-PAGE. Strains expressing the following Tar receptors from their genome were used: Tar^{EEEE}, Tar^{QEEE}, Tar^{QEQE}, Tar^{QEQQ}, and Tar^{QQQQ}.
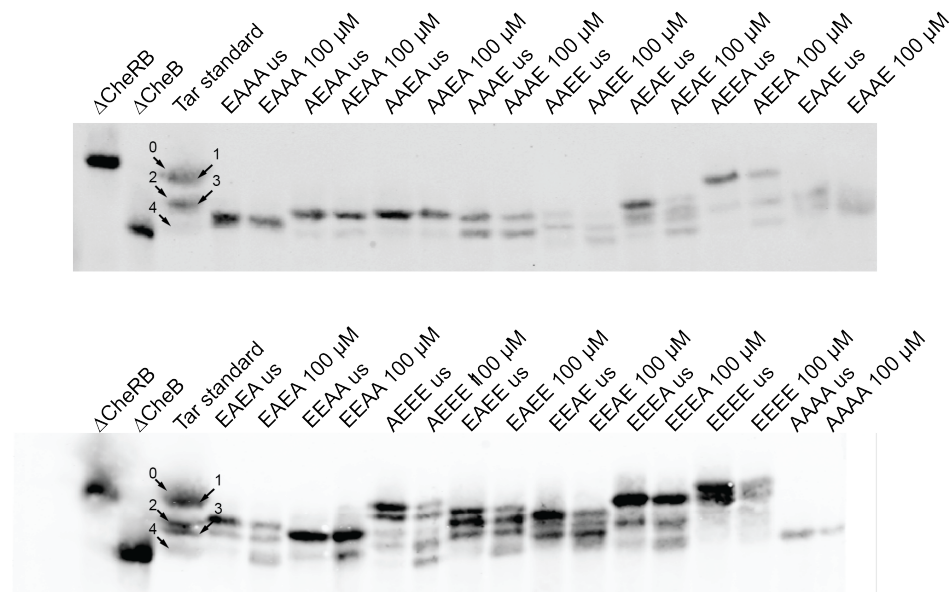
Figure 4.6.: Immunoblot of alanine-substituted Tar mutants before and after stimulation. Tar protein bands were obtained by immuno-blotting of SDS-PAGE with a Tar-specific antibody. Cells expressing Tar mutants were either unstimulated (us) or stimulated with 100 μM MeAsp for 20 minutes (100 μM). Cells were lysed by boiling samples in Laemmli buffer at $95\,°C$. Higher modified receptors showed an increased mobility on the gel. As controls, $\Delta cheRB$ and $\Delta cheB$ strains both expressing Tar^{EEEE} were used. As Tar standard, $\Delta cheRB$ strains expressing Tar with fixed numbers of Q residues (as indicated by arrows) were used.

The methylation-deficient receptor Tar^{AAAA} displayed only one low band, as it cannot be modified upon stimulation. For 3×A receptors, a maximum of two bands were visible only in Tar^{AAAE}. For this receptor, we also observed strongest increase in EC$_{50}$ when CheR and CheB were expressed. We suppose that these receptors existed in an unmodified state or with one methyl group. Stimulation did not evidently change the band pattern. An increased ability to be methylated correlated with low EC$_{50}$ and good chemotaxis on soft agar plates. Wild-type and 1×A receptors showed a higher number of protein bands which further increased and shifted downwards upon stimulation of these receptors. The upper bands of 1×A receptors were nearly as high as the upper band of wild-type Tar^{EEEE}. Moreover, the two 2×A receptors displaying remarkable chemotaxis on soft agar plates, Tar^{AEEA} and Tar^{EAEA}, displayed the strongest downward shift of protein bands after stimulation with 100 μM MeAsp on the immunoblot.

4.1.4. Determination of adaptation kinetics by stimulus-dependent FRET

To investigate the influence of Tar receptors substituted at a single site, the adaptation kinetics of 1×A receptors to persistent stimulation with the attractant MeAsp were determined by stimulus-dependent FRET in a CheRB$^+$ strain (VS181). The observed differences between adaptation kinetics of wild-type Tar^{EEEE} (Fig.4.7) and 1×A substituted Tar (Fig.4.8) enabled us to roughly estimate the effect of the substituted site on the performance of proper adaptation, marked by a high precision and kinetics similar to the wild-type. Impaired kinetics of a Tar mutant indicates a strong effect of the respective substituted methylation site on the recovery of CheA activity. Cells expressing the respective receptor as well as the FRET reporter pair were kept under a constant flow of buffer for 30 minutes to monitor the steady-state activity of the kinase CheA before the attractant was added for the same time. Upon stimulation, an almost instantaneous decrease of the YFP/CFP ratio indicates inactivation of the kinase. Recovery of the kinase activity by adaptation was determined by analyzing the slope of the adaptation curve.
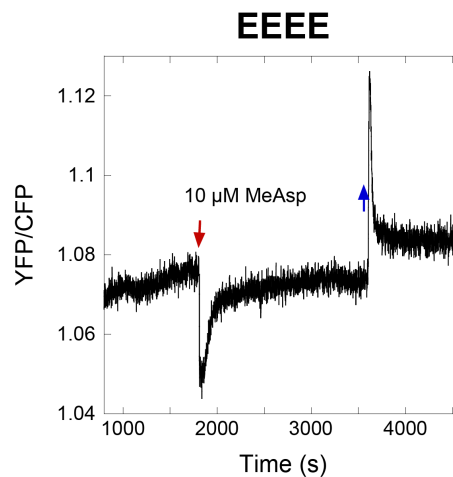
Figure 4.7.: Adaptation kinetics of wild-type chemoreceptor Tar^{EEEE}. Cells were induced with 2 μM Sal and 50 μM IPTG, respectively. A saturating MeAsp concentration of 10 μM was added for 30 minutes to stimulate an attractant response (red arrow). Blue arrow indicates removal of the attractant.
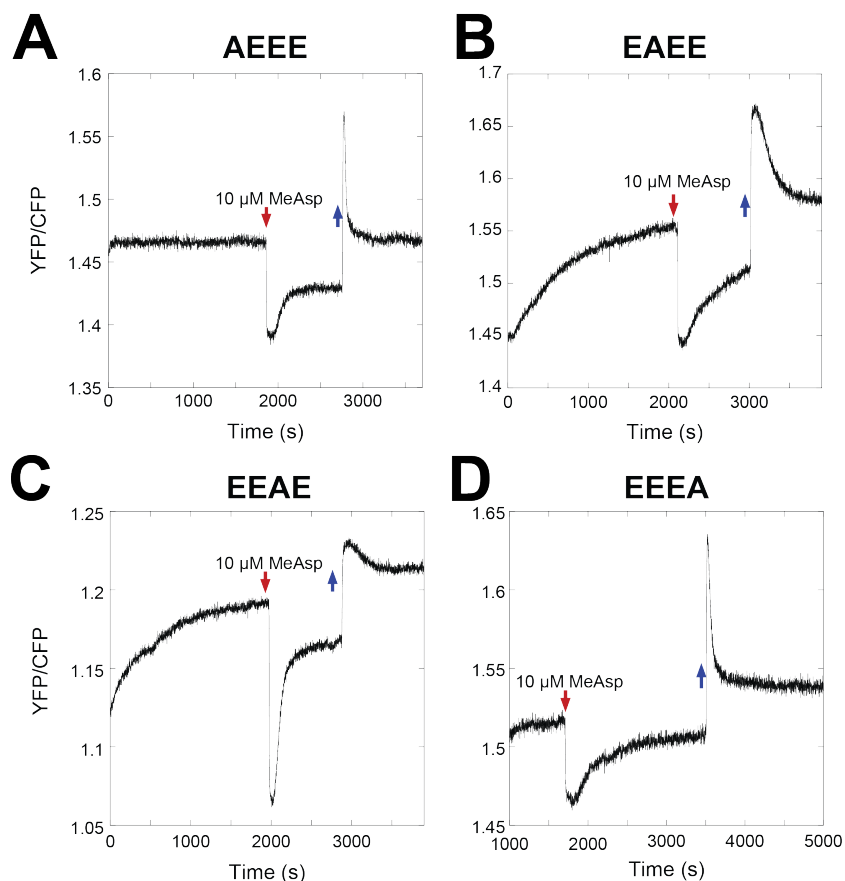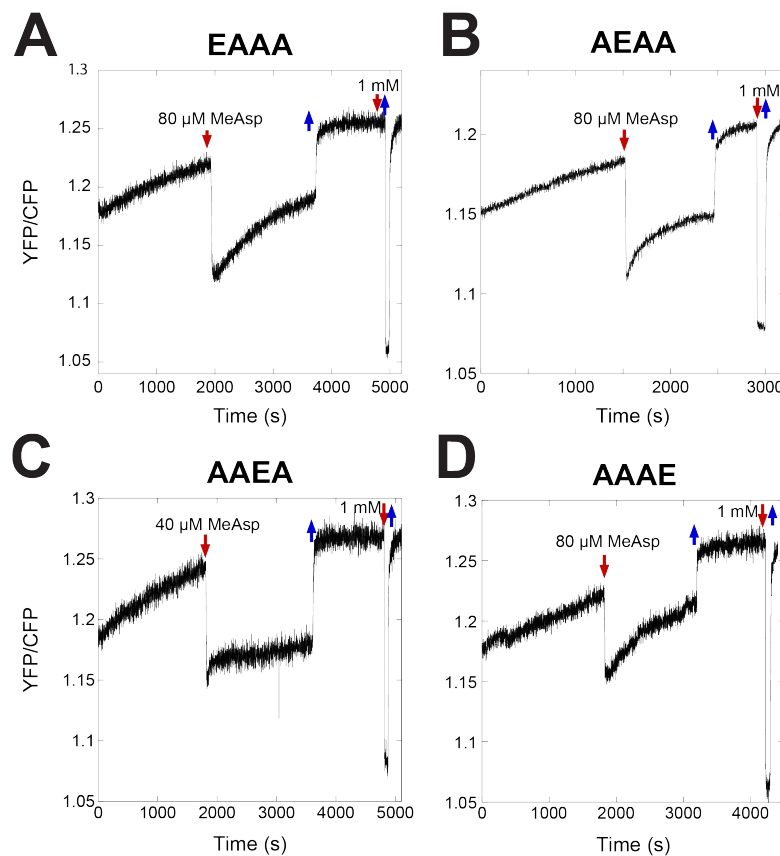
Figure 4.8.: Adaptation kinetics of Tar receptor mutants each carrying one alanine substitution at a single methylation site. (A) Tar^{AEEE} **(B)** Tar^{EAEE} **(C)** Tar^{EEAE} **(D)** Tar^{EEEA}. Cells were induced with 2 μM Sal and 50 μM IPTG, respectively. After 30 minutes, a saturating MeAsp concentration of 10 μM was added for another 30 minutes to stimulate an attractant response (red arrow). Blue arrow indicates removal of the attractant.

Adaptation kinetics appeared different depending on the position of the alanine substitution. For example, Tar^{EEAE} and Tar^{EEEA} adapted to a pathway activity similar to the prestimulation level whereas positioning of alanine at site 1 (Tar^{AEEE}) or 2 (Tar^{EAEE}) lowered this precision significantly. The rate of adaptation increased with the time needed for reactivation of the kinase being shorter for Tar^{EEAE} compared to other 1×A receptors. The slow kinetics of the response upon removal of attractant, especially in Tar^{EEAE} but also in Tar^{EAEE}, differed from wild-type Tar^{EEEE}, which showed a sharp peak upon attractant removal. Quantification of the removal peak (data not shown) revealed that the time required to return to the prestimulus level of activity was nearly ten times longer than for wild-type Tar, suggesting

that CheB-mediated demethylation is less efficient when site 2 or 3 are substituted with an alanine residue.

To obtain an even better understanding of the effect of individual methylation sites on adaptation, a complementary approach using chemoreceptors with three substituted methylation sites (3×A Tar) and a single methylatable glutamate was employed (Fig.4.9). As 3×A receptors do not adapt to saturating stimuli, a subsaturating concentration of MeAsp corresponding to the EC_{50} of the respective receptor was used for stimulation. At the end of each measurement, the full response of each chemoreceptor was visualized by the addition of a saturating stimulus (1 mM MeAsp).

Figure 4.9.: Adaptation kinetics of Tar receptor mutants each carrying alanines at three methylation sites. (A) Tar^{EAAA} **(B)** Tar^{AEAA} **(C)** Tar^{AAEA} **(D)** Tar^{AAAE}. Cells were induced with 2 μM Sal and 50 μM IPTG, respectively. After 30 minutes, a subsaturating MeAsp concentration, corresponding to the EC_{50} of the respective receptor, was added for another 30 minutes (red arrow). Blue arrow indicates removal of the attractant.

Adaptation varied in this receptor set depending on the position of the glutamate residue. Adaptation differed in precision as well as in the duration, e.g. Tar^{AAEA} showed an imprecise and fast adaptation as determined from the difference in steepness of the YFP/CFP ratio before and after addition of the attractant, whereas Tar^{AEAA} showed a more precise and slower adaptation. Both Tar^{EAAA} and Tar^{AAAE} showed the slowest and most precise adaptation among the 3×A receptors. Adaptation was most impaired for Tar^{AAEA} with exclusively methylation site 3 available.

Quantification of adaptation kinetics was done by considering three parameters: Precision of adaptation, adaptation halftime and adaptation rate. For determining adaptation precision, the ratio between the initial and the adapted response in presence of the stimulus was calculated (Fig.4.10A).
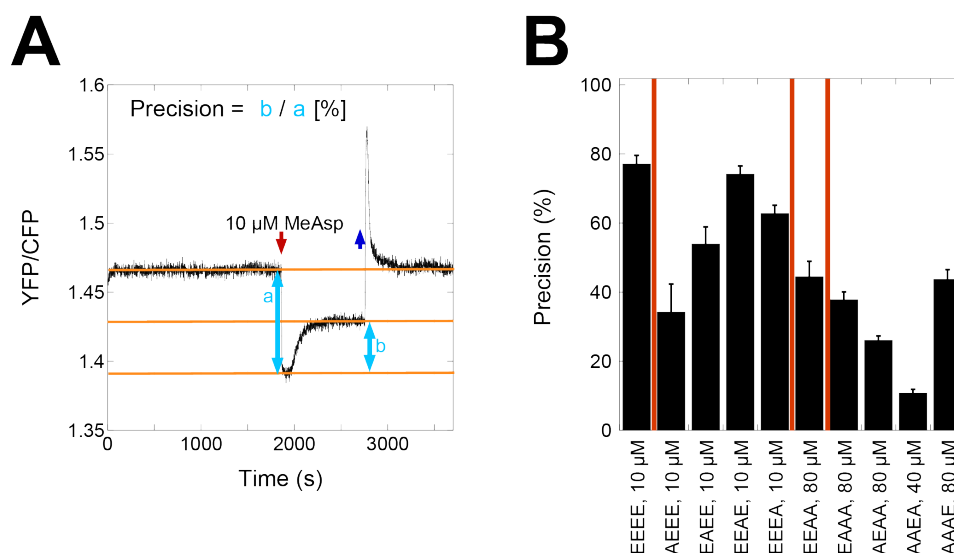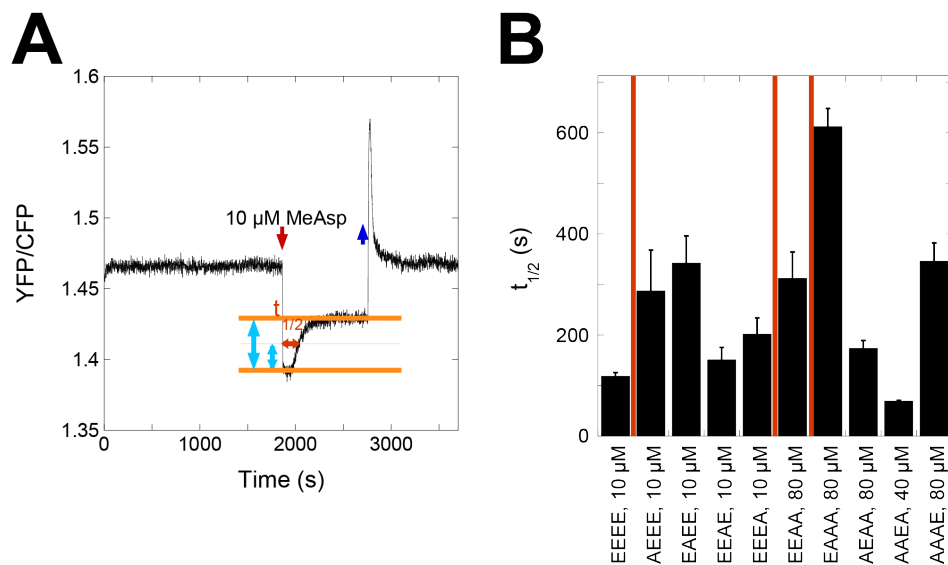

Figure 4.10.: Adaptation precision of Tar mutants. **(A)** Determination of the adaptation precision, defined as the percentage of recovery of kinase activity in presence of attractant. The precision was calculated by comparing the initial response to a stimulus to the adapted level of kinase activity. A full recovery depicts 100% precision. **(B)** Diagram of precision values for Tar mutants calculated from stimulus-dependent FRET measurements. Red vertical lines group the receptors according to their number of alanine substitutions. Error bars represent SEM of at least two experiments.

The highest precision was observed for the wild-type chemoreceptor Tar^{EEEE} (Fig.4.10B), reaching a value of nearly 80%. Precision similar to wild-type was also obtained for Tar^{EEAE}, followed in decreasing order by Tar^{EEEA}, Tar^{EAEE} and Tar^{AEEE} with approximately 30% preci-

sion. We assume that the higher the percentage of adaptation precision of a certain mutant was, the lower was the effect of the corresponding subtituted methylation site on the adaptation precision. These values were roughly reversely complemented by precision values of $3 \times A$ receptors. Tar^{AAEA} showed the least precise adaptation among this receptor set followed by Tar^{AEAA}, Tar^{EAAA} and Tar^{AAAE}.

Furthermore, the adaptation halftime was determined, defined as the time that the receptors need to adapt to half of the final level (Fig.4.11A).

Figure 4.11.: Adaptation halftime of Tar mutants. (A) Determination of adaptation halftime, defined as the time that the chemoreceptors adapted to half of the final level in presence of the ligand. First, the ratio of the initial response (lower thick orange line) and the adapted response (higher thick orange line) were determined. Half of the final response is indicated by the thin orange line. The adaptation halftime is indicated by the red double arrow on the thin orange line. **(B)** Diagram showing adaptation halftimes of Tar mutants calculated from stimulus-dependent FRET measurements. Red vertical lines group the receptors according to their number of alanine substitutions. Error bars represent SEM of at least two experiments.

As depicted in Fig.4.11B, a very short adaptation halftime was displayed by wild-type receptor Tar^{EEEE}. However, the adaptation halftime of Tar^{AAEA} was even shorter due to its extremely low adaptation precision which goes hand in hand with these low adaptation halftimes, in contrast to wild-type Tar^{EEEE} with a high adaptation precision. Longest adaptation halftimes were found for Tar^{EAAA} and Tar^{AAAE}, which were also the most precise mutants within the

$3\times A$ receptor set. Apart from that, distribution of adaptation halftime values was very wide within the upper and lower limits.

Also the initial rate of adaptation was determined from stimulus-dependent FRET measurements as shown in Fig.4.12A. The net linear increase of the YFP/CFP ratio after attractant stimulation, which reflects the rate of kinase activity recovery due to methylation-induced increase of receptor activity, was calculated by subtracting the slope of the YFP/CFP ratio before stimulation.

The by far highest adaptation rate was observed for Tar^{EEAE} and not, as expected, for the wild-type Tar^{EEEE} (Fig.4.12B). Regarding adaptation precision and halftime, Tar^{EEAE} showed the most similar behaviour to wild-type, whereas blocking site 3 for methylation strongly increased the adaptation rate in comparison to the wild-type. An alanine residue at methylation site 3 seems to increase the efficiency of CheR-mediated methylation leading to comparatively fast recovery of CheA activity. However, response amplitudes displayed big differences in size (Fig.4.12C). Thus, the adaptation rates were normalized to the amplitudes (Fig.4.12D). Indeed, the ratio of adaptation rate to amplitude was nearly the same for wild-type Tar^{EEEE} and Tar^{EEAE}. The second highest ratio was seen in Tar^{AAEE} and Tar^{EEAE} with approximately 70% of the wild-type ratio. Also Tar^{AEEE} and Tar^{EAEE} displayed rather high normalized rates. Remaining $2\times A$ and all $3\times A$ receptors showed only very low values, indicating slow relative adaptation rates.

We presumed that there might be a mutual dependence of all three parameters, precision, halftime and rate of adaptation. Especially, the knowledge of adaptation precision and halftime of a particular receptors should enable us to determine its adaptation rate because the rate describes the recovery of kinase CheA activity (represented by adaptation precision) over time (represented by adaptation halftime). The ratio of adaptation precision to halftime indeed reflected a similar distribution as shown for the normalized adaptation rate (Fig.4.12D and Fig.4.13A). Also the values for the adaptation rate before normalization (Fig.4.12B) showed the same pattern as the ratio of precision to halftime multiplied with the amplitude (Fig.4.13B). Hence, the ratio between precision and halftime is an alternative way to calculate the adaptation rate. Similar results obtained for the adaptation rate using two different approaches indicate a stable relation of the analysed signalling parameters and confirm the robustness of our data.
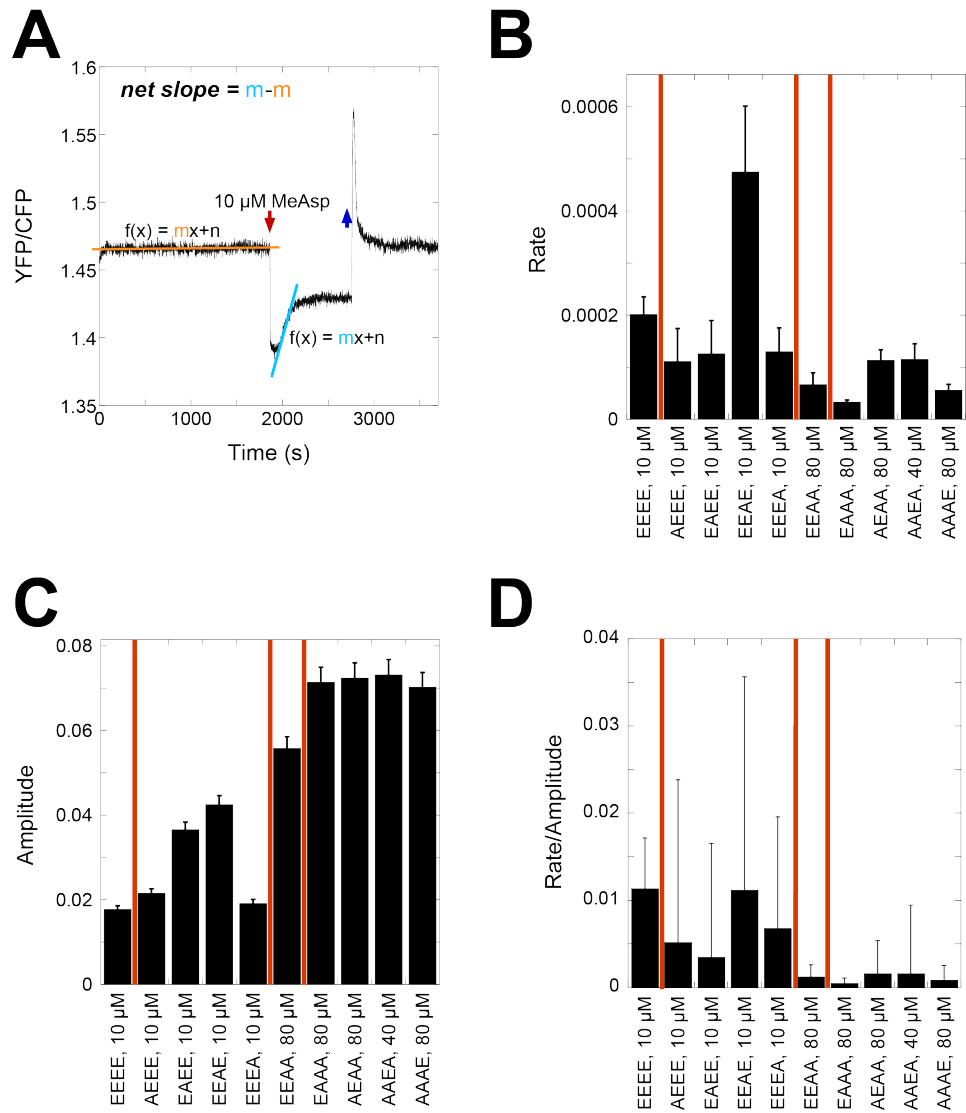
Figure 4.12.: Adaptation rate of Tar mutants. (A) Determination of adaptation rate from a stimulus-dependent FRET measurement. The adaptation rate was calculated by subtracting the slope of the YFP/CFP ratio before stimulation from the slope of the initial adaptation. **(B)** Diagram showing calculated adaptation rates of Tar mutants calculated from stimulus-dependent FRET measurements. **(C)** Diagram of the response amplitudes. **(D)** Diagram of adaptation rate divided by response amplitude. Red vertical lines group the receptors according to their number of alanine substitutions. Error bars represent SEM of at least two experiments.
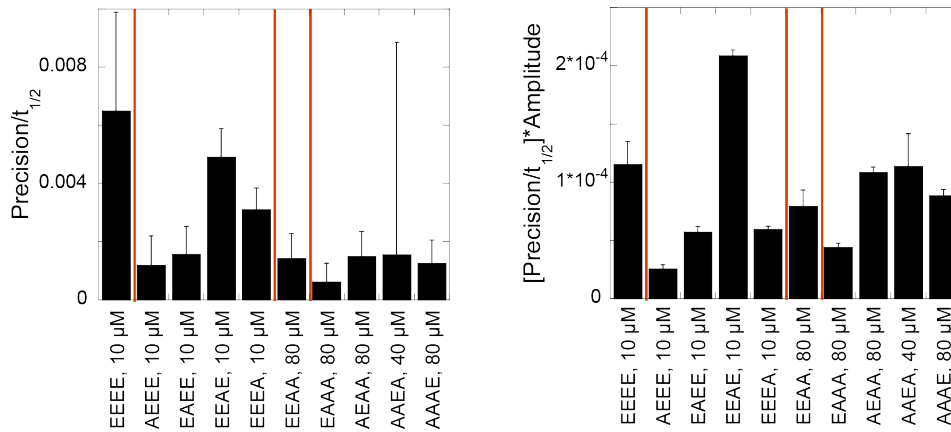
Figure 4.13.: Ratio of precision to halftime resembles adaptation rate distribution. (A)
The ratio of precision to halftime, obtained by division of the data in Fig.4.10B and Fig.4.11B,
displays a similar pattern as the adaptation rate normalized to the amplitude (Fig.4.12D). **(B)**
Values of the ratio precision to halftime in panel A were multiplied with the response amplitude
(Fig.4.12C). The values of (precision/halftime)*amplitude display a similar pattern as the values
of the unnormalized adaptation rate (Fig.4.12B).

Summing up chapter 4.1, methylation sites play different roles in *E. coli* chemotaxis to-
wards nutrients, chemoattractant gradient detection, chemoreceptor activity and adaptation
in chemotaxis. Tar mutants were only able to sense gradients of either nutrients or MeAsp
on soft agar plates when two or less methylation sites were substituted. However, several
$2 \times A$ receptors and all $3 \times A$ receptors failed to mediate chemotaxis towards attractant gradi-
ents. Their spreading behaviour was often similar to the adaptation-deficient negative control
Tar^{AAAA}. Strongest impairment of gradient sensing was observed for receptors with site 3
mutated, followed by receptors mutated at site 2 and 1, leading to the conclusion that site
3 is most crucial for gradient detection. Site 4 was found to be least important for detec-
ting attractant gradients. Also, gradients were detected slightly better by $1 \times A$ receptors in
comparison to wild-type Tar^{EEEE} at a higher distance to the source. This could either be
due to the shallower gradients or to a lower concentration range at that particular distance
(Fig.4.3).
EC$_{50}$ values were measured in $\Delta cheRB$ and CheRB$^+$ strains to determine the kinase stimu-
lating activity of Tar receptor mutants, with a high EC$_{50}$ corresponding to receptor activity
at steady-state in the absence of a stimulus. We found that receptors with one glutamate
at site 2 or site 4 were most active among all $3 \times A$ receptors. Thus, receptors with one of
these two sites available for methylation have a higher ability to perform adaptation similar
to wild-type than receptors with sites 1 or 3 available. Receptors with one glutamate residue

at site 1 displayed the second highest receptor activity and receptors having the glutamate residue at site 3 showed the lowest activity among receptors with only one methylation site available, indicating that site 3 is least crucial for adaptation. Expression of CheR and CheB strongly increased EC_{50} of several 3×A receptors in comparison to $\Delta cheRB$ strain. Especially Tar^{AAAE} had a much higher EC_{50} in the presence of CheR and CheB, indicating that the glutamate at site 4 was efficiently methylated by CheR. The glutamate in Tar^{EAAA} and Tar^{AAEA} was also, but less efficiently methylated. Only a very low increase in EC_{50} was seen for Tar^{AEAA} in presence of CheR and CheB suggesting that site 2 was hardly methylated in steady-state.

Detailed analysis of adaptation to a persistent stimulus regarding precision, halftime and rate revealed that specific methylation sites had different significances for the proper performance of adaptation. We found that the availability of site 1 and site 4 was most important for adaptation. Site 2 seems to be of minor importance and finally site 3 was least crucial for adaptation. In comparison to the impact of single methylation sites on sensing of gradients, the order of the sites significance was reversed for adaptation, indicating that the different methylation sites play different roles for chemotactic sensing and proper adaptation.

4.2. Investigation of the order of methylation during adaptation

Quantification of the adaptation kinetics of alanine substituted chemoreceptors broadened our understanding of the adaptation process, indicating that specific methylation sites had a greater influence on certain features of adaptation and chemotaxis. To investigate the adaptation of wild-type receptors in detail, we studied the differences in methylation of the individual sites in response to attractant stimulation. A connection between progressing adaptation and the respective methylated sites could elucidate the whole adaptation process. We approached this aim by using immunoblot and mass spectrometry to determine methylation levels of the Tar protein at specific time points after stimulation. With the latter method, exact positions of methylated amino acids could be identified, meaning that different peptide species having the same number of methyl groups, but at different positions, could be detected, distinguished with the help of peptide fragmentation and quantified, even though the mass of these peptides is the same.

### 4.2.1. Determination of methylation kinetics by immunoblot

Methylation kinetics were investigated by stimulating receptorless CheRB$^+$ cells expressing wild-type Tar^{EEEE} with 100 μM MeAsp for different time spans up to 20 minutes and analyzing Tar protein levels on an immunoblot. One sample was stimulated for 20 minutes, washed twice and afterwards incubated for another 20 minutes in attractant-free buffer. To allow the comparability of the immunoblot analysis with the mass spectrometrical measurements, samples were prepared in the same way for both assays. Cells were lysed and methylation was stopped by sonication and further purified by ultracentrifugation before they were boiled in Laemmli buffer at $95\,°\mathrm{C}$. Due to the time-consuming sonication procedure, less early time points could be prepared.

Receptor methylation increased with ongoing stimulation, reflected by the elevated mobility of these proteins on an SDS gel (Fig.4.14A and B). As described in Fig.4.6, each receptor modification state is represented by a separate band. Tar proteins with a fixed number of Q residues were run on every SDS-PAGE as a size standard.

For all experiments, we verified the stimulation-dependent response by immunoblot and stimulus-dependent FRET (Fig.4.14C) and we were thus able to unite these data with the

mass spectrometrical results. At each time point of stimulation, the adaptation state, the methylation level as well as the site of methylation should be resolved.
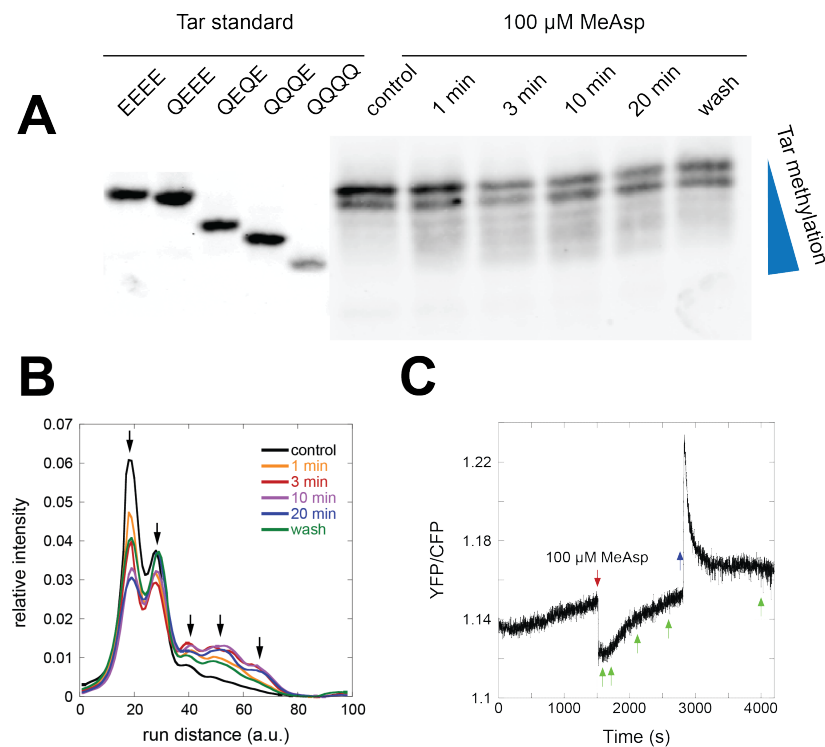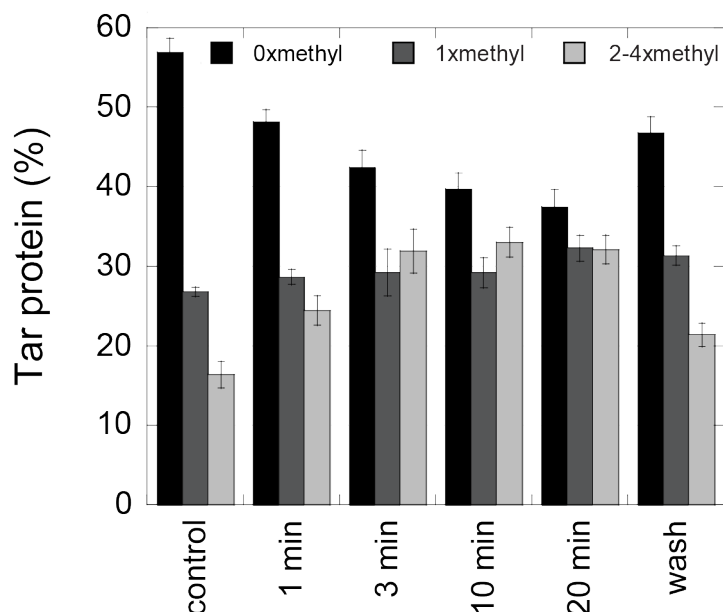

Figure 4.14.: Representative immunoblot of Tar methylation and stimulus-dependent FRET measurement of Tar adaptation upon stimulation with 100 μM MeAsp. (A) Cells expressing Tar^{EEEE} from plasmid pVS1086 were stimulated with 100 μM for the indicated time periods. The "wash" sample was stimulated for 20 minutes, attractant was removed and cells were incubated in attractant-free buffer for another 20 minutes. The reaction was stopped and cells were lysed by sonication, followed by ultracentrifugation and boiling of the samples in Laemmli buffer at $95\,^{\circ}$C. Tar methylation was gained by immunoblotting of SDS-PAGE with a Tar-specific antibody. Higher methylated receptors showed an increased mobility on the gel. Tar standard strains with fixed numbers of Q residues are shown in the first five lanes. **(B)** Intensity profile of immunoblot in **(A)**. The intensity profile was obtained using ImageJ. All values were normalized to the integrated density under the curve. Peaks representing the differently methylated receptors are indicated by arrows. **(C)** Stimulus-dependent FRET response of Tar^{EEEE} to stimulation with 100 μM MeAsp. Addition of the attractant is indicated by the red arrow, whereas the blue arrow indicates the removal of the attractant. Green arrows indicate the time points that were investigated by immunoblotting.

Unmethylated and once methylated Tar could clearly be distinguished on the immunoblot as well as in the immunoblot intensity profile (Fig.4.14A and B). Higher methylated bands converged and could not be analysed separately anymore. Quantification of immunoblot bands revealed the relative changes of unmethylated, once or higher methylated Tar protein over time after stimulation (Fig.4.15). A clear decrease of unmethylated Tar over time was observed. At the same time, once methylated Tar increased slightly whereas the amount of higher methylated Tar doubled within the first three minutes and did not significantly change anymore after 10 and 20 minutes. Apparently, methylation was nearly finished after 3 minutes which might be due to a lower affinity of the methyltransferase CheR to receptors with an increased activity at later time points. After 20 minutes of attractant stimulation and subsequent incubation in attractant-free buffer for the same time, less higher methylated and more unmethylated Tar protein was observed, although the pre-stimulus level was not completely reestablished (Fig.4.15, "wash"). Most probably, the elevated CheB-mediated demethylation of receptors after removal of the attractant was incomplete. Some residual traces of attractant might have led to a higher methylation level in buffer-washed cells.

In the stimulus-dependent FRET measurement of the Tar^{EEEE} response to 100 μM MeAsp (4.14C), green arrows indicate the same time points also analysed by SDS-PAGE. Surprisingly, the adaptation profile did not show a rising curve at the first time points of 1 and 3 minutes which would indicate a reactivation of receptors by methylation. In contrast, methylation levels increased strongly during this time span (Fig.4.15), which could be explained by the high affinity of CheR for inactive chemoreceptors. Immediately after the addition of attractant and inactivation of the chemoreceptors, CheR activity was maximal. The delayed activity regain of chemoreceptor and kinase CheA in the FRET measurement was caused by an elevated receptor methylation. CheR activity was decreased due to its lower affinity for active receptors. Knowledge of exact positions of the methyl groups could reveal the impact of each individual methylation site in adaptation.

Figure 4.15.: Quantification of Tar methylation from immunoblots after stimulation with 100 μM MeAsp. Quantification was done by integrating the area under the respective peak in Fig.4.14B. Error bars represent SEM of seven independent experiments.

4.2.2. Mass spectrometrical analysis of Tar methylation

To determine the exact positions of methylated sites during adaptation, cells expressing wild-type Tar^{EEEE} were stimulated with 100 μM MeAsp and subsequently lysed by sonication. The membrane fraction including Tar chemoreceptors was purified by ultracentrifugation and digested with the protease trypsine, which cleaves C-terminal to lysine and arginine residues. Methylation sites were distributed onto two peptides. One peptide contained methylation sites 1 to 3 (TE**E**QASALE**E**TAASME**E**LTATVK, sites of methylation are bold), the second peptide contained site 4 (VTQQNASLVQ**E**SAAAAAALEEQASR). Filters were applied in the tandem mass spectrometer for the expected peptide masses, leading to a fragmentation of only those peptides, which could verify their sequence and also the exact positions of methyl groups could be determined. Quantification was done by using the elution profiles of the respective peptide from the upstream HPLC (Chapter 3).

Unstimulated control cells already showed a certain methylation level which was in agreement with our preliminary immunoblot experiments and due to a constant low methylation and

demethylation of Tar by CheR and CheB in steady-state. Both peptides, TE**E**QASALE**E**T AASME**E**LTATVK and VTQQNASLVQ**E**SAAAAAALEEQASR were found unmethylated and with one methyl group.

Fragmentation of peptide TE**E**QASALE**E**TAASME**E**LTATVK in this measurement was not effective, probably due to high background noise of other peptides causing the peptide of interest to fall below the threshold for fragmentation, so that methylation levels of peptide TE**E**QASALE**E**TAASME**E**LTATVK were detected, but specific positions of the methyl groups could not be determined (Fig.4.16A). Before attractant stimulation, a total amount of about 30% of the peptides was methylated, wherefrom 5% with two methyl groups and the remaining part once methylated. After one minute of MeAsp stimulation, the overall methylation level increased by about 5%, distributed over once and twice methylated peptides. Stimulation over three minutes resulted in a total amount of 45% methylated peptide. Here, the twice methylated peptide doubled its pre-stimulus level from 5% to 10%. Longer stimulation over ten minutes did not further change the total amount of methylated peptide. Only small rearrangements occured in the twice methylated peptide fraction, becoming slightly more dominant in comparison to the once methylated peptide.
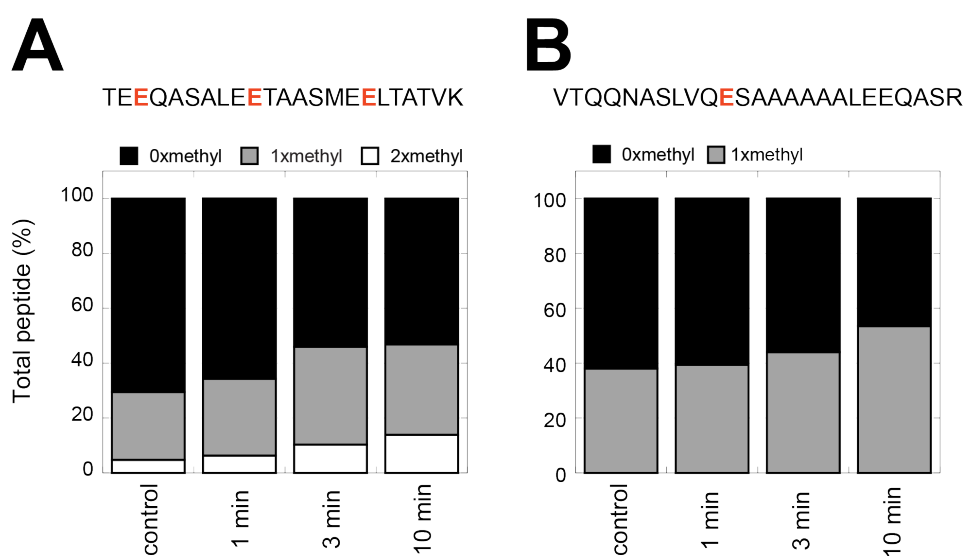
Figure 4.16.: Distribution of methylation upon stimulation of Tar^{EEEE} with 100 μM MeAsp. **(A)** Peptide TE$\underline{E}$QASALE$\underline{E}$TAASME$\underline{E}$LTATVK. **(B)** Peptide VTQQNASLVQ$\underline{E}$SAAAAAALEEQASR.

Upon stimulation with 100 μM MeAsp, peptide VTQQNASLVQ**E**SAAAAAALEEQASR, containing methylation site 4, slowly increased its already high methylation level from nearly 40%

before stimulation up to more than 50% , with the biggest change occuring inbetween 3 and 10 minutes (Fig.4.16B).

Experimental conditions were customized by applying constant fragmentation of peptide TEEQASALEETAASMEELTATVK, i.e. target peptides of the expected masses did not have to reach a certain threshold over the background to get fragmented, but they were fragmented automatically all the time. Also, longer stimulation durations were performed. In comparison with the previous assay (Fig.4.16), not only a 20 minute time point was conducted additionally, but also cells were washed twice after 20 minutes of stimulation to get rid of attractant traces and then incubated for another 20 minutes in attractant-free buffer. By doing so, restoration of conditions before stimulation could possibly be investigated. Peptide VTQQNASLVQESAAAAAALEEQASR could not be detected in this measurement, probably due to its low abundance, whereas peptide TEEQASALEETAASMEELTATVK was detected and the different positions of the methyl groups could be determined. When observing the methylation levels, slightly more than 20% were carrying one methyl group and the remaining portion of this peptide was unmethylated before stimulation (Fig.4.17A). Upon addition of 100 μM MeAsp, the overall methylation of peptide TEEQASALEETAASMEELTATVK increased to a maximum of more than 60% methylation after 3 minutes. This percentage was maintained over some time, because we still found the same levels in samples taken 10 and 20 minutes after starting the stimulation. After washing the cells from attractant and incubating them for 20 minutes into buffer, the overall methylation level decreased to slightly more than 40% indicating that demethylation was still in process as the prestimulus methylation level was not reached yet (Fig.4.17A).

By using constant peptide fragmentation, we could distinguish the specific methylation sites that were modified in peptide TEEQASALEETAASMEELTATVK (Fig.4.17 B and C). In peptides with only one methyl group, we found the position of this group either on site 1 or site 2. Interestingly, methylation site 3 was never modified solely. Upon stimulation, both site 1 and 2 got methylated to a higher extent (Fig.4.17 B). After recovery of the cells from attractant by washing, site 2 was mainly methylated while site 1 already returned to its prestimulus methylation level (Fig.4.17B). A representative fragmentation spectrum of a twice methylated peptide is shown in Fig.4.18.

The twice methylated peptide occured only after stimulation (Fig.4.17A). At the very onset, we found 20% twice methylated peptide with two different peptide species, site 3 in combination with either site 1 or site 2 modified. We assume that site 3 was the second site of these peptides, getting methylated only after site 1 or site 2, due to the data from singly methylated peptides, where we could not detect single methylation of site 3 (Fig.4.17C).

78
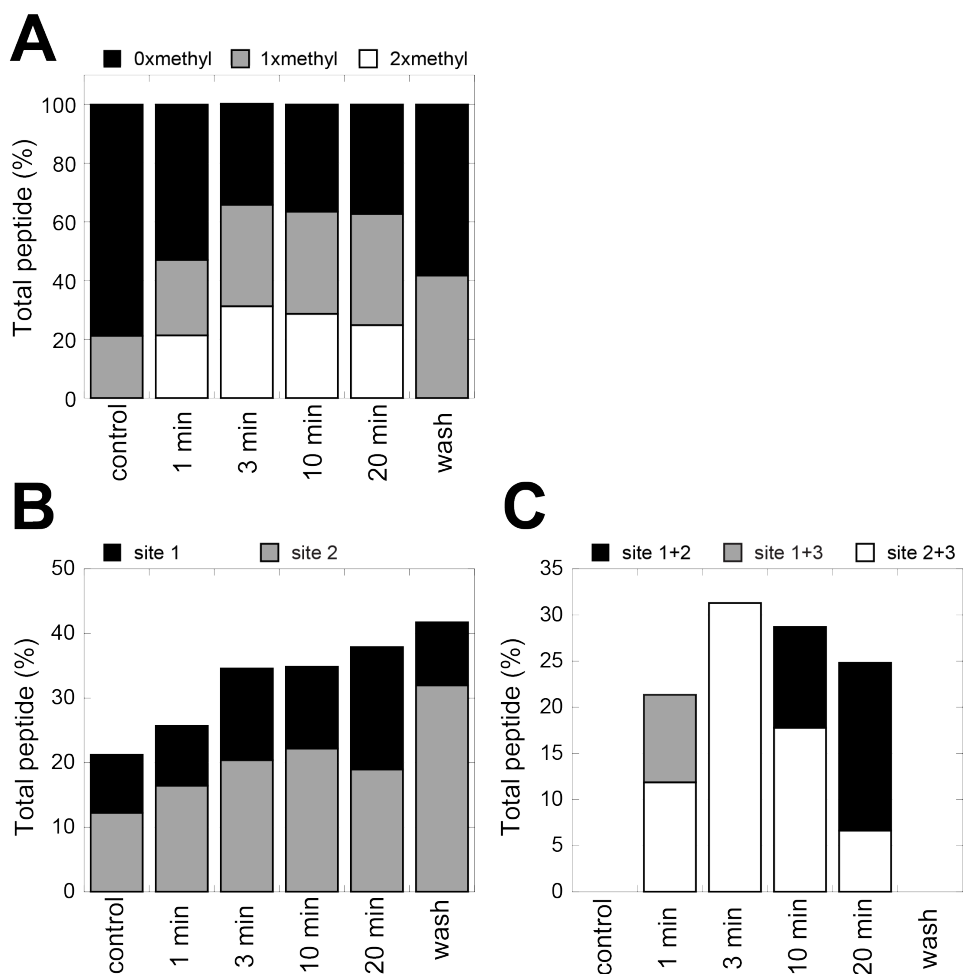
Figure 4.17.: Methyl groups at different sites in peptide TEEQASALEETAASMEELTATVK upon stimulation of Tar^{EEEE} with 100 μM MeAsp. (A) Overview of whole peptide amount. **(B)** Quantification and position analysis of peptides with one methyl group. **(C)** Quantification and position analysis of peptides with two methyl groups.

After 3 minutes, only twice methylated peptides with methyl groups on site 2 and 3 could be found, accounting for 30% of all peptides. This peptide species decreased to approximately 17% after 10 minutes and 7% after 20 minutes. Peptide with site 1 and 2 methylation occured with more than 10% after 10 minutes and prevailed with aprroximately 18% after 20 minutes. The overall abundance of twice methylated TEEQASALEETAASMEELTATVK reached from slightly more than 20% after 1 minute of stimulation to a peak of more than 30% after 3 minutes and decreased again to 28% and 25% after 10 and 20 minutes, respectively. Washing of stimulated cells and adapting them to attractant-free buffer completely

abolished twice methylated peptides. Peptide TE**E**QASALE**E**TAASME**E**LTATVK was never methylated at all three methylation sites at the same time.
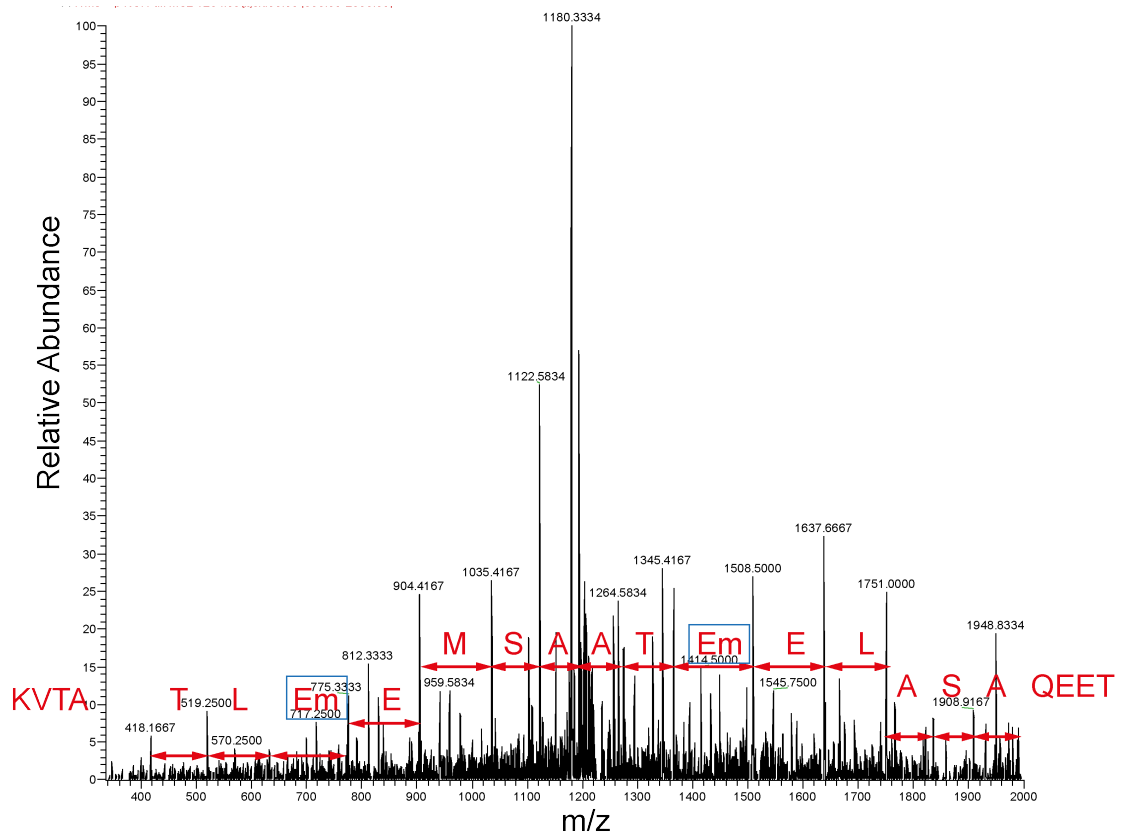

Figure 4.18.: MS/MS spectrum of y-ions derived from fragmentation of peptide TEEQASALEETAASMEELTATVK with two methyl groups. Relative abundance as a function of the mass to charge ratio (m/z). The peptide sequence is displayed from right to left, because the y-ions contain the C-terminus of the peptide. Methylated glutamates (Em) at site 2 (right) and 3 (left) are indicated by the blue boxes.

Concluding, methylation site 4 was methylated at a rather high percentage already before stimulation (Fig.4.16B). Also, its methylation slowly increased upon addition of attractant. Site 1 and 2 played a role during initial adaptation, because methylation of both sites increased in the first few minutes, of which site 2 methylation is faster and seemed to be the last being removed by demethylation (Fig.4.17A and B). Methylation site 3 got only modified when at least site 1 or site 2 were already methylated. Methylation of site 1 or 2 could serve as docking site for methyltransferase CheR to reach site 3 (Fig.4.17C).

Analysis of individual methylation sites in peptide TE**E**QASALE**E**TAASME**E**LTATVK revealed that strongest methylation increase upon stimulation occured at site 2, rising from

12% to approximately 50% after three minutes (Fig.4.19). This high level was maintained even after 10 minutes, but reduced again after 20 minutes to slightly more than 30%.
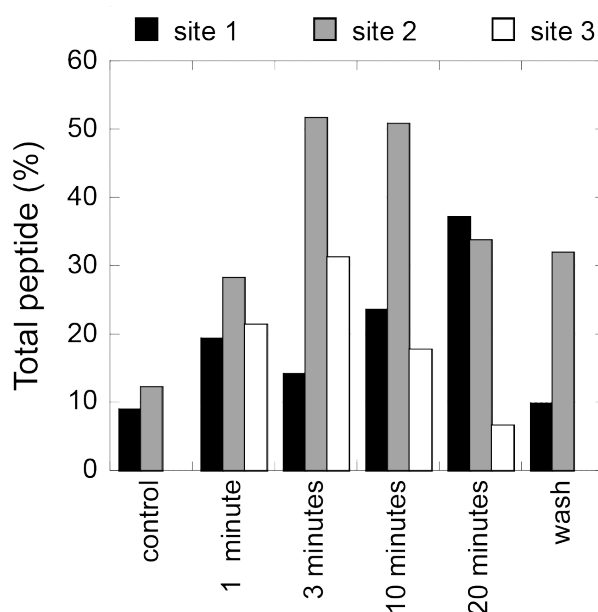
Figure 4.19.: Methylation of individual sites in peptide TEE̲QASALEE̲TAASMEE̲LTATVK.

Removal of attractant and equilibration in attractant-free buffer did not reduce methylation significantly. This could be due to a reduced accessibility of site 2 for the methylesterase CheB. Site 1 displayed 9% methylation before stimulation. After addition of attractant, methylation rised gradually up to 23% after 10 minutes. A further increase was seen after 20 minutes with 37%. After washing, methylation decreased to the prestimulus level again. We suppose that site 1 was subject to permanent stepwise methylation by CheR. Demethylation to the prestimulus level occured within 20 minutes, suggesting that CheB was able to efficiently demethylate site 1. Methylation at site 3 was not detected without stimulation. After the addition of attractant, site 3 methylation quickly rose to more than 20% after one minute and reached a peak of 31% after 3 minutes. Methylation levels reduced again to 17% after 10 minutes and 5% after 20 minutes. Removal of MeAsp completely abolished detection of methylated site 3.

4.3. Dynamic range of alanine substituted chemoreceptors

To further characterize the properties of the alanine substituted receptors, their dynamic range was determined, that is the range over which the chemoreceptor can discriminate varying attractant concentrations. The adaptation system is mainly responsible for this ability. Chemoreceptors stimulated with increasing attractant concentrations require gradually more methyl groups at the methylation sites to regain their activity. Fully saturated receptors get insensitive and thus cells cannot respond to an increased attractant concentration anymore. This point defines the upper limit of the respective dynamic range. The lower limit is determined by the steady-state activity of the receptor, represented by the EC_{50} (Chapter 4.1.3). The higher the steady-state activity is, the more attractant is needed to decrease it. Thus, receptors with a low steady-state activity also start sensing at low attractant concentrations. The dynamic ranges of several chemoreceptors carrying zero to four alanines were measured by stimulus-dependent FRET. Analysis was carried out as described in Fig.4.20. The respective responses were normalized to a full saturating response of buffer-adapted cells. Measurements looked different, depending on the ability of the respective strain to adapt to stimuli, as shown in Fig.4.20A and B.

When comparing wild-type Tar^{EEEE} and Tar carrying one alanine substitution, only minor differences could be observed (Fig.4.21). The dynamic range curves were similar in shape and differed only at the borders of their ranges, accounting for three orders of magnitude in total. Tar^{EEAE} started detecting MeAsp at marginally higher concentrations than wild-type Tar, consistent with its higher EC_{50} value (Chapter 4.1.3). A narrower dynamic range was observed when a second methylation site was substituted with an alanine residue. We investigated Tar^{AAEE}, Tar^{EAAE} and Tar^{EEAA} out of the $2{\times}A$ receptor set. For all three receptors, the dynamic range was narrower compared to wild-type, spanning a range of only two orders of magnitude. Also, the relative response to attractant concentrations at the peak of the dynamic range compared to a fully saturating response of buffer-adapted cells decreased to a maximum of 70%. Interestingly, the three $2{\times}A$ receptors were shifted relative to each other within the dynamic range covered by wild-type and $1{\times}A$ receptors. Increasing the number af alanine substitutions at the methylation sites from two to three slightly decreased the sensitivity towards low attractant concentrations, as indicated by comparison of the
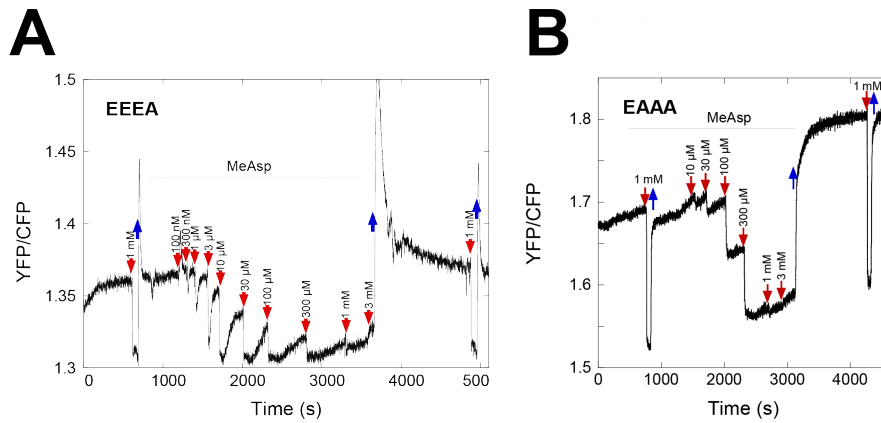
Figure 4.20.: Representative dynamic range measurements. Cells were first adapted to buffer and then stimulated with increasing concentrations of the attractant MeAsp. In contrast to dose response measurements, cells were allowed to fully adapt to the approximately three-fold increasing stimulus concentrations and the next higher MeAsp concentration was added without going back to buffer again. Red arrows indicate the addition of the respective MeAsp concentration in approximately three-fold steps. Blue arrows indicate the removal of MeAsp solutions. **(A)** Tar^{EEEA}. **(B)** Tar^{EAAA}.

dynamic ranges of Tar^{EEAA} and Tar^{EAAA}. The highest response peak for 3×A receptors was approximately 60% of a full response. We also tested Tar^{AAAA}, which was not able to adapt, but still responded to attractants. The dynamic range of this receptor was much narrower compared to the wild-type Tar^{EEEE}. Tar^{AAAA} could distinguish attractant concentrations over only one order of magnitude and the highest response peak was only about one half of a full response. In comparison, Tar^{EAAA} started detecting MeAsp at lower concentrations than Tar^{AAAA}, which was consistent with their respective EC$_{50}$ values.

Summing up, the more methylation sites were eliminated, the narrower became the dynamic ranges and the lower were the relative responses of the respective receptors. The lower limit was determined by the receptors steady-state activity, the upper limit by the saturation of methylation sites making a further discrimination of higher attractant concentration impossible. Chemoreceptors that had only a limited number of methylation sites available reached this point earlier than wild-type receptors with four available glutamate residues. Receptors with only one alanine substitution showed a wide dynamic range, suggesting that three available methylation sites were still sufficient to distinguish between increasing attractant concentrations nearly similar to the wild-type. The strongest increase in impairment was observed for the 1×A and 2×A receptors. When only two instead of three methylation sites
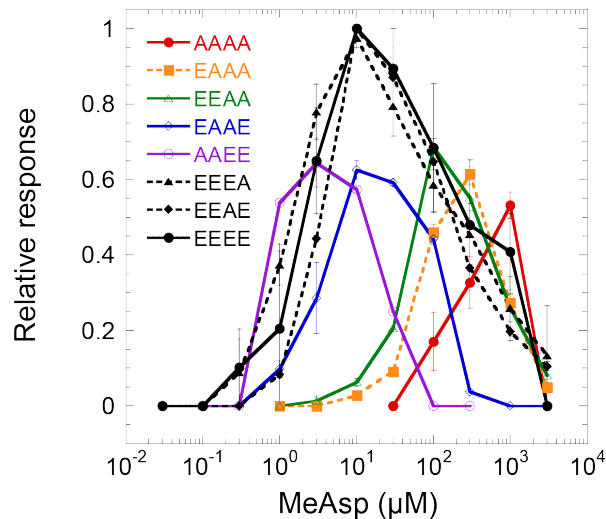
Figure 4.21.: Dynamic range of Tar mutant chemoreceptors carrying different numbers of alanines at their methylation sites. The dynamic range was determined for Tar chemoreceptors with different numbers of alanine substitutions at their methylation sites. The relative responses were determined by comparing the response to each concentration tested to a full saturating response. Error bars represent SEM of at least two experiments. Error bars are not visible for all chemoreceptors.

were available, the dynamic range was clearly narrower. Thus, two sites were not sufficient to distinguish steps of attractant similar to wild-type anymore.

Tar^{AAAA} responded to a narrow range of MeAsp concentrations although it could not adapt to them due to the substitution of all methylation sites. The low affinity of these receptors for their ligand MeAsp led to a higher threshold of the response. Thus, these receptors needed high attractant concentration to diminish their activity. Their dynamic range reached from the onsetting activity decrease due to sufficiently high MeAsp concentrations to the point where all ligand binding sites were occupied with attractant. Furthermore, we observed for most of the receptors a shift to higher ligand concentrations when increasing the number of alanine substitutions. Presumably, this was due their increased steady-state activity, requiring a higher attractant concentration to decrease their activity. An exception was seen for the three 2×A chemoreceptors tested. Here, we observed that their dynamic ranges -of similar widths- were distributed over the MeAsp concentration spectrum. Consistent with the low receptor steady-state activity of Tar^{AAEE}, indicated by the lowest EC_{50} of 1.35 μM, the dynamic range of this receptor was shifted to the lower concentrations within the spectrum. Moreover, Tar^{EAAE} whose dynamic range has an intermediate position within the concentration spectrum, has an EC_{50} of 4 μM. The dynamic range of Tar^{EEAA} was most shifted to

the right consistent with the highest EC_{50} value of 53 μM. Thus, the position-dependent placement of each receptors dynamic ranges within the concentration spectrum was clearly connected to the receptors activity. Theoretically, the upper limit of all the receptors dynamic ranges should by similar because fully saturated methylation sites -represented either by alanine or methylated glutamate residues- result in a similarly high receptor activity. We observed this amongst others for both Tar^{AAAA} and Tar^{EEEE}, with the latter one reaching the same upper limit as fully methylated Tar^{EEEE}. We were asking why 2×A did not display similar upper limits, as receptors carrying exclusively alanine or methylated glutamates were able to do so (Fig.4.21). The combination of two alanines and two glutamates did not have the same effect on receptors activity as alanines or methylated glutamates alone. The only receptor that displayed an expected upper limit consistent with our assumption was Tar^{EEAA}. The two other receptors, Tar^{EAAE} and Tar^{AAEE}, were not in agreement with the expected upper limit, indicating that the positions of alanine and glutamate residues in these receptors are critical. The differences between the receptor that displayed the expected upper limit in its dynamic range and the other two receptors was a glutamate at methylation site 2 and an alanine at methylation site 4, whereas the other receptors carried an alanine at site 2 and a glutamate at site 4, indicating that the chemical nature of these specific sites changed the impact on the receptors activity. We hypothesize that structural differences between the two cytoplasmic helices of the Tar receptor -helix 1 containing methylation sites 1 to 3 and helix 2 containing methylation site 4- could lead to a full activation of several 2×A receptors already at a relatively low attractant concentration. Structural differences might also exist between receptors with four alanines and receptors with four methylated glutamates at the methylation sites, but they might be more balanced due to the fact that all four methylation sites are replaced with the same amino acid type. One amino acid type at site 4 on helix 2 and at least two sites of helix 1 replaced with a second amino acid type might lead to structural differences between these two helices and thereby activate the receptors at lower MeAsp concentrations. This question has to be further examined by analyzing the dynamic ranges of other 2×A receptors.

4.4. Alignment of adaptation halftime and response in mixed chemoreceptor clusters

Wild-type *E. coli* cells respond and adapt to any attractant specific for one chemoreceptor type collectively due to cooperative interactions among receptors in sensory complexes. Chemoreceptors form mixed dimers which in turn are organized as trimers of dimers in clusters at the cell poles. Ligands have different affinities for their respective chemoreceptors and can be bound either directly or indirectly by periplasmic binding proteins. We wanted to investigate systematically the responses of wild-type cells to attractants specific for all chemoreceptor types by measuring dose response curves and adaptation halftime (Fig.4.22A). As expected, the adapation halftime increased when cells were stimulated with increasing attractant concentrations, because a higher receptor methylation is required to offset a stronger stimulus. Interestingly, when plotting the relative response against the adaptation halftime, a strong exponential correlation could be observed, independent of the type of attractant (Fig.4.22B). We hypothesized that this relationship between response strength and adaptation halftime might be a unique feature of chemoreceptors. However, it was not clear if this relation was mediated by a single chemoreceptor type or if allosteric interactions between chemoreceptors of different types in sensory complexes caused this effect.
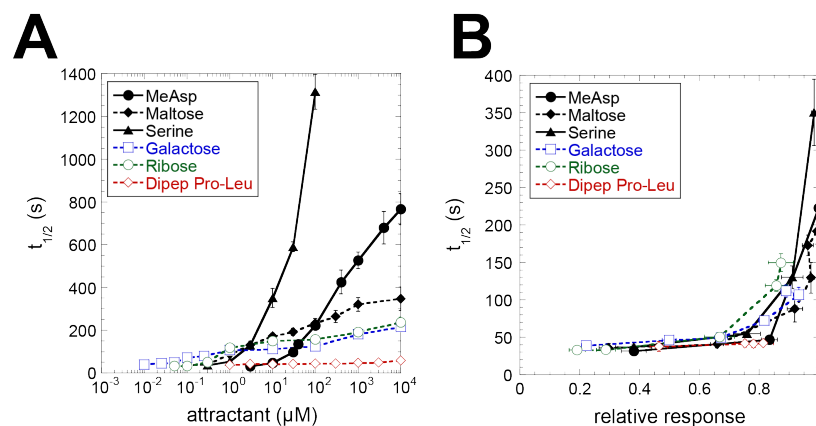
Figure 4.22.: Adaptation halftime and relative response of wild-type *E. coli* cells to different attractants. Wild-type *E. coli* cells were stimulated with the attractants MeAsp, Maltose, Serine, Galactose, Ribose and the dipeptide Pro-Leu in a dose response measurement where cells were allowed to adapt fully to all concentrations. Adaptation halftime and relative response from these measurements were calculated.**(A)** Adaptation halftime as a function of the attractant concentration.**(B)** Adaptation halftime from **A** plotted against the relative response. Data were kindly provided by Silke Neumann.

We analyzed cells that were expressing only one type of chemoreceptor, Tar or Tsr, as the only chemoreceptors stimulated with MeAsp or serine as attractants (Fig.4.23A) and found that the relation between relative response and adaptation halftime of Tar only and Tsr only cells did not align. The presence of only one receptor type abrogated the alignment of adaptation halftime. Different expression levels of Tar or Tsr receptors did not significantly change the relation between relative response and adaptation halftime, indicating that the ratio of methylesterase CheR to the chemoreceptors did not play a role.

We assumed that the presence of other receptors would restore the alignment of adaptation halftime again. Therefore, we also investigated the response of Tar and Tsr receptors in cells that were expressing all other receptors at a native level (Fig.4.23B and C) by stimulation with both serine and MeAsp. Δtar cells expressing Tar induced by 2 μM salicylate induction did not show any response to serine due to an overexpression of Tar. Presumably, Tar receptors were outnumbering Tsr receptors at such high levels that the serine response was undetectable. Cells expressing Tar at a lower induction (1 μM salicylate) in a Δtar strain responded to both attractants, serine and MeAsp and the alignment of relative response and adaptation halftime was restored (Fig.4.23B). The same was true for Δtsr cells expressing Tsr from a plasmid (Fig.4.23C). Apparently, the interactions with other chemoreceptor types helped maintaining the optimal relation of response strength and adaptation halftime. We suppose that allosteric interactions between different receptor types within a team determine this relationship in mixed clusters, which provides a yet unknown important feature in chemotaxis.
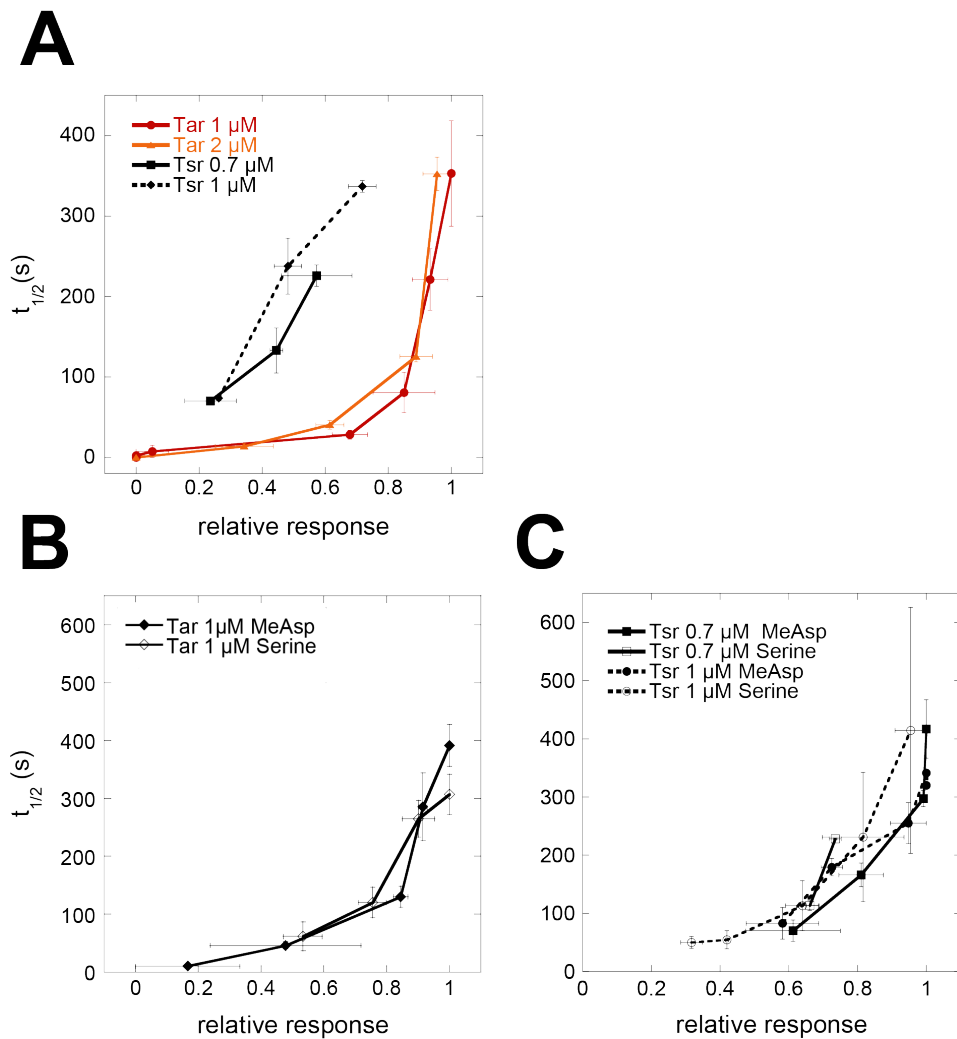
Figure 4.23.: Adaptation halftime as a function of the relative response in cells expressing Tar or Tsr either in receptorless background or in a $\triangle tar$ or $\triangle tsr$ background. Tar or Tsr chemoreceptors were expressed from plasmid pVS1086 (Tar) and pVS362 (Tsr) at the indicated salicylate inductions and stimulated with MeAsp and/or serine. **(A)** Misalignment of Tar and Tsr reponses in Tar or Tsr only cells. Tar and Tsr wild-type receptors were each expressed at two induction levels in the receptorless strain VS181. Tar was stimulated with MeAsp, Tsr was stimulated with serine. **(B)** Restoration of Tar response alignment in the presence of all other receptors. Wild-type Tar was expressed from plasmid pVS1086 at the indicated induction levels in a $\triangle tar$ strain (SN25) in the presence of all other receptors. Cells were stimulated with either serine or MeAsp. **(C)** Restoration of Tsr response alignment in the presence of all other receptors. Wild-type Tsr was expressed from plasmid pVS362 at the indicated induction levels in a $\triangle tsr$ strain (SN119) in the presence of all other receptors. Cells were stimulated with either serine or MeAsp. Error bars represent SEM of at least two experiments.

4.5. Imprecision of adaptation towards high concentrations of serine and cysteine

Precision of adaptation remains high over a wide range of attractant concentrations. However, when reaching the saturating concentration range, precision evidently decreases. The ability to distinguish between two concentrations and to adapt to them in a precise way is facilitated by receptor methylation. With increasing attractant concentrations, also occupancy of chemoreceptor methylation sites increases. At the upper limit of the dynamic range, distinction of two concentrations is hardly taking place because the receptor methylation sites are nearly saturated. Also for precise adaptation, sufficient sites for methylation need to be present. Thus, adaptation gets less precise when reaching high attractant concentrations which are correlated to saturated methylation sites of the chemoreceptors. We found a decrease in adapation precision for the wild-type *E. coli* strain SN1 when stimulated with several attractants binding to different chemoreceptors and monitoring the chemotaxis pathway activity with the stimulus-dependent FRET assay. We tested ligands specific for the chemoreceptors Tar, Tsr, Trg and Tap chemoreceptors and monitored the precision and the halftime of adaptation (Fig.4.24A). Depending on the stimulus, precision started to decrease strongly at different concentrations due to different ligand affinities. For smaller stimuli, for which adaptation halftime was less than 200 seconds, we saw a strong correlation between adaptation precision and halftime. In general, adaptation halftime increased with increasing attractant concentrations (Fig.4.24B). Particularly low adaptation precision was observed for the Tsr ligands serine and cysteine when added at higher concentrations of about 10 μM (serine) and 100 μM (cysteine), respectively (Fig.4.24A). We were asking why serine and cysteine stimulation led to such a high imprecision at much lower concentrations than for other attractants. Saturation of methylation sites could be one reason for the high imprecision. However, this imprecision was also observed for other attractants, although to a lesser extent (Fig.4.24A). Another reason could be that imprecise adaptation prevents the cells from accumulation at high concentrations of serine and cysteine that are toxic to the cells [109].
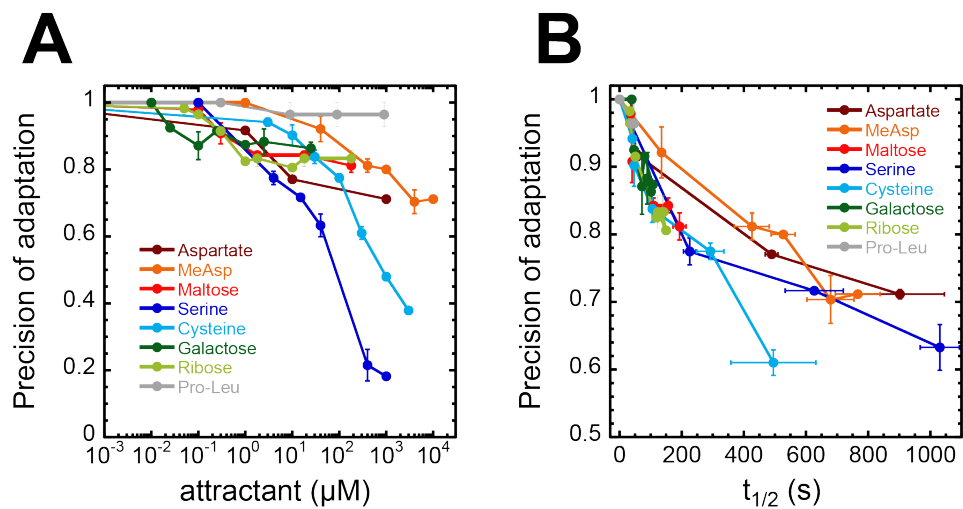
Figure 4.24.: Dependence of adaptation precision on attractant concentration and adaptation halftime. Measurements were done with the wild-type strain SN1 [LJ110 $\Delta(cheYcheZ)$] expressing CheY-YFP and CheZ-CFP from plasmid pVS88. Values were normalized to the response of buffer-adapted cells to a saturating ligand concentration. Some data were replotted from [31]. **(A)** Dependence of adaptation precision on attractant concentration. **(B)** Correlation of adaptation precision and adaptation halftime. Data kindly provided by Silke Neumann.

To further investigate this assumption, the influence of increasing serine and cysteine concentrations on the growth of *E. coli* wild-type cells was tested. For this purpose, wild-type strain MG1655 was grown in minimal medium that was supplemented with different serine or cysteine concentrations. When determining the growth rate by calculating the ratio between the actual OD_{600} of supplemented cultures compared to the one of a non-supplemented control, it was obvious that growth became worse with increasing serine or cysteine concentrations (Fig.4.25A and B).

It is known that high concentrations of both serine and cysteine severely impaired the amino acid metabolism of the cell [109]. Both serine [110, 111] and cysteine [112] inhibit the enzyme homoserine dehydrogenase I at high concentrations, which plays an important role for the synthesis of isoleucine and threonine. Therefore, we conlude that the higher imprecision towards these amino acids was evolutionary selected to prevent *E. coli* from accumulation at toxic concentrations. Other amino acids known to be chemoattractants did not influence the cell growth (Fig.4.25C).
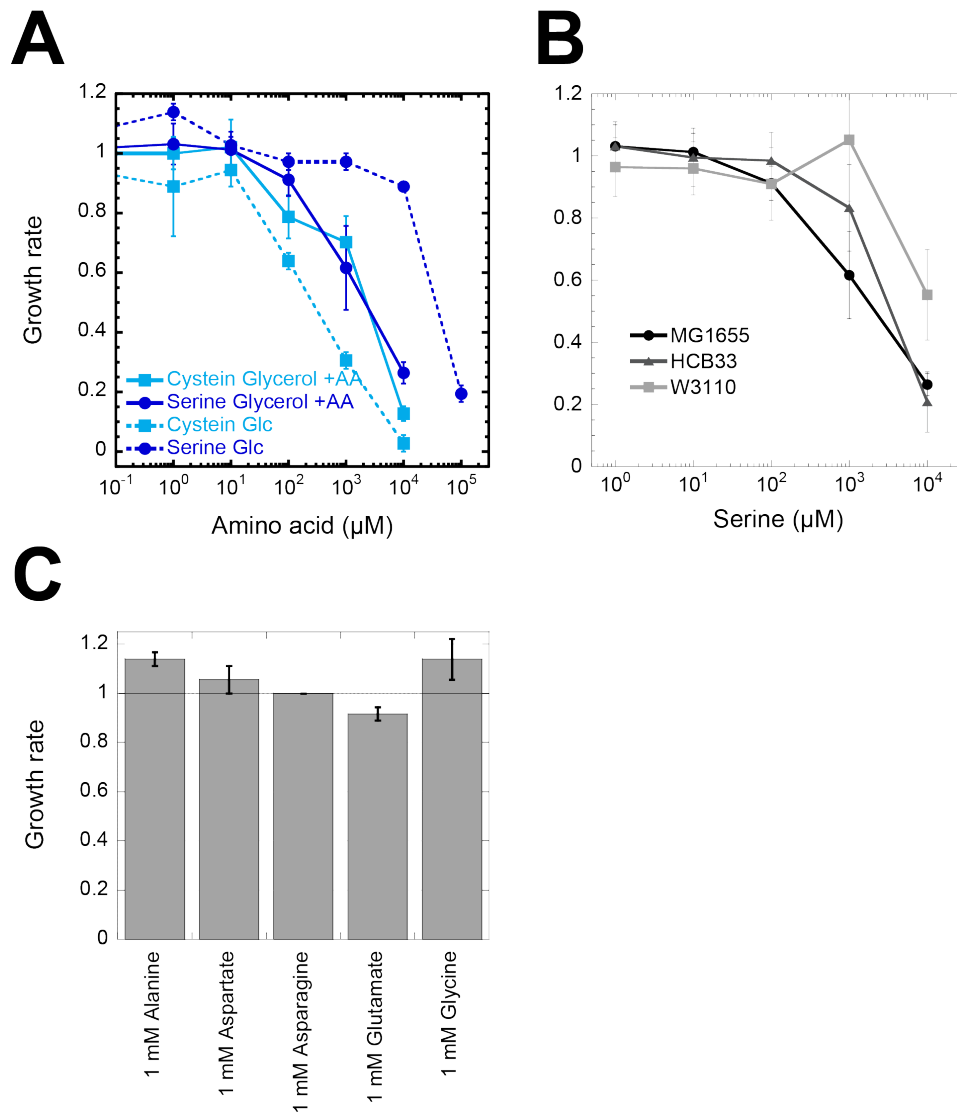
Figure 4.25.: Growth rate of wild-type *E. coli* in minimal medium 9. Cells were grown at $34\,^{\circ}\mathrm{C}$ at 275 rpm. After two hours, different concentrations of serine, cysteine or other chemoeffectors were added and cultures were shaken for additional 1.5 hours. OD_{600} was measured and growth rate was determined by comparison to a non-supplemented strain. When growing cells with glycerol as carbon source, an amino acid mix had to be added (40 μg/ml L-threonine, L-methionine, L-histidine, L-leucine). **(A)** Growth rate of wild-type MG1655 in miminal medium 9 with glycerol or glucose as carbon source and increasing concentrations of serine or cysteine as indicated. **(B)** Growth rate of the three wild-type strains MG1655, HCB33 and W3110 in minimal medium 9 with glycerol as carbon source and increasing serine concentrations. **(C)** Growth rate of wild-type MG1655 grown in minimal medium 9 with glycerol as carbon source and 1 mM of chemoeffectors alanine, aspartate, asparagine, glutamate or glycine. Error bars represent the SEM of at least two experiments.

5 | Discussion

5.1. Methylation and adaptation in chemotaxis

Chemotaxis is a sophisticated process by which cells are able to navigate in complex gradients of nutrients. Chemicals are sensed by periplasmic chemoreceptors, which transduce a signal to the flagella motors and thereby regulate the swimming behaviour of the cells. A molecular memory is established by the adaptation system, mediated by the methylation of specific glutamate residues in the chemoreceptors cytoplasmic part. Although much is known about receptor methylation [24, 27, 28, 113], the hierarchy and the benefit of four specific methylation sites for the aspartate chemoreceptor Tar remains to be elucidated. To address this question, methylation sites were rendered unavailable by substituting the native glutamate residues with alanine residues, which cannot be modified. We then systematically analyzed the effects on chemotaxis and adaptation *in vivo*. Furthermore, we determined the exact positions of transferred methyl groups upon stimulation of cells expressing the wild-type chemoreceptor.

5.1.1. Kinetics of attractant and repellent response in Tar wild-type and mutants

To get a broader understanding of the molecular processes during methylation-mediated adaptation in chemotaxis, adaptation of wild-type Tar[EEEE] and mutant Tar receptors to persistent stimulation with the attractant MeAsp was analyzed in-depth. Methylation kinetics to attractant stimuli were analyzed in cells expressing wild-type Tar chemoreceptors and both the methylation levels and the exact methylated sites were determined by immunoblot and mass spectrometrical analysis. Samples were analyzed after 1, 3, 10 and 20 minutes stimulation with 100 μM MeAsp as well as in attractant-free conditions after preincubation of 20 minutes in 100 μM MeAsp. To identify the effects of unavailability or availability of each individual methylation site on adaptation, the adaptation kinetics were determined by

Discussion

stimulus-dependent FRET in cells expressing Tar chemoreceptors with either one or three alanine substitutions.

Methylation level analysis of wild-type Tar^{EEEE} by immunoblot revealed that more than 40% of the chemoreceptors had already been methylated at steady-state in the absence of attractant. The pre-stimulus methylation levels of the two peptides in the mass spectrometrical analysis -the first peptide containing methylation sites 1 to 3 on the cytoplasmic helix 1, the second peptide containing methylation site 4 on cytoplasmic helix 2 (Fig.1.3)- added up to a value of 60 to 65% receptor methylation. As the receptor was split into two peptides in the mass spectrometrical analysis, we assume that the total number of methylated receptors is lower and similar to the value determined by immunoblot. The steady-state methylation level probably is a combination of methylation at either sites 1 through 3 and methylation at site 4 within one receptor. Stimulation with MeAsp increased the amount of methylated Tar protein mainly in the first 3 minutes, indicating that the majority of receptor methylation is completed after this time period. Only minor increases of the methylation level occured at later time points. Interestingly, the adaptation profile determined by stimulus-dependent FRET did not display beginning recovery of the kinase CheA activity after 3 minutes, possibly because a sufficiently high methylation level is required before the offsetting of the inactivation can start. Therefore, the recovery of kinase and chemoreceptor activity is delayed in comparison to the initial methylation. Although the FRET adaptation profile showed restoration, cells washed from attractant did not completely reestablish the pre-stimulus methylation levels according to the immunoblot and the mass spectrometrical analysis. The slightly increased methylation level after washing was not sufficient to keep the activity higher than at steady-state.

Mass spectrometrical analysis showed that steady-state methylation in the absence of a stimulus appeared at sites 1, 2 and 4, of which site 4 had the highest methylation level. Site 3 methylation was not found in steady-state. Methylation level of all sites increased upon stimulation with 100 μM MeAsp, with different rates specific for the individual sites. Methylation site 2 had the highest methylation rate, site 3 with the second highest rate followed by site 1 and site 4 with similarly low methylation rates. We do not have data for site 4 methylation later than 10 minutes after stimulation. Overall, the mass spectrometrical results allow a rough quantification of methylation rates for the four sites, but not of demethylation rates. The determination was done based on the time points we measured. Although we cannot exclude that methylation and demethylation processes going on in-between the obtained time points may influence our estimation, we determined, as mentioned, the highest methylation rate for site 2. The second highest methylation rate was found for site 3 with three quarters

of site 2 methylation. Site 1 and site 4 methylation rates were equal with approximately one eighth of site 2 methylation.

The mass spectrometrical analysis allowed us to determine combinations of methylated sites in the peptide comprising site 1 to 3. Twice methylated peptides occured before stimulation at an extremely low level, if at all. One minute after the addition of attractant, two peptide species were observed, with either site 1 and 3 or site 1 and 2 methylated. Thus, site 3 was methylated only upon stimulation and in combination with another site. After 3 minutes, only one twice methylated peptide species with methyl groups at site 2 and 3 was present at a high level, whereas the peptide with site 1 and 3 methylated completely vanished, pointing to a "start-up" function of the latter mentioned peptide. At later time points, the twice methylated peptide with methyl groups at site 1 and 2 stepwise dominates over the peptide with sites 2 and 3, which might be due to an initiated demethylation. A possible starting point might be methylation site 3, as its overall methylation decreased after 3 minutes of stimulation already in the presence of attractant. The highest overall methylation level of the Tar chemoreceptor was reached after 3 minutes of stimulation and did not change significantly anymore. The different peptide species found at later time points indicate that methyl groups get removed from site 3 and methylation of site 1 increases. This finding points to site 3 being the first to be demethylated. Furthermore, we observed that site 1 methylation constantly increased over time until the attractant is removed, whereas site 3 and 2 were already demethylated during stimulation. Thus, we think that site 1 methylation is important to complete the adaptation process.

Adaptation kinetics measured by stimulus-dependent FRET in receptors with one alanine substitution at each of the methylation sites enabled us to determine the rates of adaptation in the absence of one single site. The highest adaptation rate was observed for Tar^{EEAE} and was similar to wild-type. Substitutions of sites 4 and 1 displayed intermediate effects and site 2 the strongest effect on adaptation rate (Tab.5.1). Methylation site 3 seems to be dispensable for an adaptation rate similar to wild-type, although we observed an increase in site 3 methylation upon stimulation in the mass spectrometry time series. However, site 3 appears to be methylated in a dose-dependent way in response to strong stimuli, indicating that site 3 is the last to be methylated and likely the first to be demethylated in cytoplasmic helix 1.

Demethylation of site 2 and 3 was observed even in the presence of attractant. Site 3 demethylation started already after 3 minutes, whereas site 2 demethylation began after 10 minutes of stimulation. The recovery of the chemoreceptor activity might lead to an increased demethylation mediated by CheB with a higher affinity for active receptors, although the

Table 5.1.: Summary of effects of alanine substitutions on different features in Tar wild-type and mutants. Effects ranging from +++ for the wild-type Tar^{EEEE} to - for Tar^{AAAA}, except for the steady-state activity, where +++ indicates a high value and - a low value.

Feature Receptor	Chemotaxis in soft agar	Adaptation precision	Methylation rate	Demethylation rate	Dynamic range	Steady-state activity CheRB$^+$	Steady-state activity Δ*cheRB*
EEEE	+++	+++	+++	+++	+++	n.d.	-
AEEE	+++	+	++	+++	+++	n.d.	-
EAEE	++	++	++	+	+++	n.d.	-
EEAE	+	+++	+++	+	+++	n.d.	-
EEEA	+++	++	++	+++	+++	n.d.	-
AAEE	-	n.d.	n.d.	n.d.	++	-	-
AEAE	-	n.d.	n.d.	n.d.	n.d.	-	-
AEEA	+	n.d.	n.d.	n.d.	n.d.	n.d.	-
EAAE	-	n.d.	n.d.	n.d.	++	n.d.	+
EAEA	+	n.d.	n.d.	n.d.	+++	n.d.	++
EEAA	+	+	-	-	++	+	+
EAAA	-	+	-	-	+	+	+
AEAA	-	-	-	-	n.d.	+	++
AAEA	-	+	-	-	n.d.	+	++
AAAE	-	-	-	-	n.d.	++	+
AAAA	-	n.d.	n.d.	n.d.	-	+++	+++

n.d.   not determined

stimulus is still present. We suggest that CheB first demethylates site 3, followed by site 2, and site 1 is the last to be demethylated in the cytoplasmic helix 1. After removing the attractant, site 1 and site 3 recovered their pre-stimulus methylation level within 20 minutes, whereas site 2 demethylation was stalled at the same level as after 20 minutes of stimulation. We do not have data for site 4 demethylation. So far, a connection of the demethylation rates of all four methylation sites within the same receptor is not possible due to the separate analysis of the two peptides comprising either site 1 to 3 or site 4. We were not able to quantify the respective demethylation rates, particularly because demethylation started when the attractant was still present. We need to analyze more time points after the removal of attractant.

The demethylation rate was also determined by stimulus-dependent FRET for $1\times$A receptors and for wild-type Tar receptors. Interestingly, the rate was nearly ten times lower for Tar^{EAEE} and Tar^{EEAE} than for wild-type receptors. The other two $1\times$A receptors, Tar^{AEEE} and Tar^{EEEA}, displayed a demethylation rate similar to wild-type, indicating that either the accessibility of methylated glutamates by CheB or the demethylation itself was disordered in receptors with an alanine residue at methylation site 2 or 3 (Tab.5.1). Because we suggested that site 3 is the first and site 2 the second site to be demethylated, the start of demethylation might be perturbed when exactly these sites were substituted with alanine residues. In contrast, the persistent methyl group at site 2 of wild-type Tar^{EEEE} after the removal of attractant did not disturb the demethylation of the other sites.

Methylation kinetics of chemoreceptors were previously determined by Terwilliger and coworkers [114]. They found the highest methylation rate constant for methylation site 2. Site 3 had the second highest methylation rate constant with three quarters of site 2 rate. Site 1 methylation rate constant was rather low with one quarter of site 2 rate, and the lowest methylation rate constant was determined for site 4 with approximately one eighth of site 2 rate. The previous determination of methylation rates is in agreement with our data, with the exception of the value for site 3 and under consideration of the limited number of time points. Moreover, demethylation rate constants for each of the four methylation sites have been determined by Terwilliger and colleagues [114]. They measured the highest rate for site 3. Equal intermediate demethylation rates were determined for site 1 and 2, about one half of site 3 rate. The lowest demethylation rate constant was observed for site 4 with 30% of site 3 rate. Thus, our data are in agreement with previous findings, although we do not know about site 4 demethylation. Also, we observed a stalling of site 2 demethylation, which was not seen by Terwilliger et al.

However, Terwilliger and coworkers performed their analysis in a different way than we did.

For determination of the methylation rates, cells expressing wild-type Tar chemoreceptors were cultivated in medium containing ^{3}H-methionine as methyl group donor. Cells were stimulated with 1 mM aspartate and samples were taken at various time points, whereas we used only 100 μM of the structural analog MeAsp for stimulation. After protein purification and protease digestion, the four methylation sites were found on four separate small peptides that were analyzed for their tritiated methyl groups on an HPLC by counting the radioactivity in the fractions with different retention times. In our experiments, the first three methylation sites were found together on one peptide after trypsin digestion, which allowed conclusions about combined methylation at these sites in one receptor. The demethylation rates were determined by analysis of samples taken at various time points after removing the stimulus and the ^{3}H-methionine on an HPLC for their reduction of radioactivity, reflecting the removal of methyl groups.

Although we used a different method, our results for the methylation rates are similar to the previous study. Moreover, we could get a deeper insight into the dynamics of receptor methylation because we were able to detect combinations of methylation sites 1 to 3, which are found together on one peptide.

5.1.2. Precision of adaptation in Tar wild-type and mutants

Detailed analysis of adaptation kinetics in cells expressing Tar receptors where either one or three sites were substituted with alanine residues, revealed which methylation sites do not have a significant contribution and which sites were indispensable for the performance of proper adaptation similar to wild-type Tar. We found the strongest effect of one alanine substitution for methylation site 1, followed by site 2 and 4 with intermediate effects and finally site 3 with the weakest effect of substitution (Tab.5.1). Chemoreceptors with one alanine substitution at site 3 adapted almost as precisely as wild-type receptors, thus, proposing that site 3 is dispensable for precise adaptation. Additionally, the highest ability to preserve adaptation precision in 3×A receptors was observed for site 1 and 4 with similar values, followed by site 2, and finally site 3 with the lowest precision. Taken together, site 1 is most important for precise adaptation and site 3 has the lowest contribution to it.

Notably, 1×A Tar receptors were stimulated with a saturating MeAsp concentration of 10 μM, whereas 3×A receptors were stimulated with a subsaturating MeAsp concentration correlating to their respective steady-state activity. Again, we found that methylation site 3 had the lowest effect, indicating that this specific site might be less involved in certain features of chemotaxis such as the precision of adaptation and methylation rate.

5.1.3. Steady-state activity of chemoreceptors

Chemoreceptor and kinase CheA activity in steady-state were determined by measuring dose response curves using stimulus-dependent FRET. The activity is represented by the EC_{50} value, which is higher the more methylation sites are blocked. Alanine substitutions of the methylation sites presumably cause some conformational changes of the chemoreceptors due to the removal of the charge

We determined an order that indicates the degree of conformational change caused by substitutions of the respective methylation site, with high EC_{50} values corresponding to strong conformational changes. Site 3 is most important for maintaining lower steady-state activities similar to wild-type, because the Tar receptor with one glutamate available at site 3 displayed the lowest EC_{50} among 3×A receptors, and the Tar receptors with one alanine substitution at site 3 had the highest EC_{50} of all 1×A receptors. Site 1 showed the second-highest importance for the maintainance of a low steady-state activity, followed by site 2 and 4 which showed equallyl high activities and thus the strongest change in conformation when being the only available site (Tab.5.1). Low EC_{50} values correlate with high chemotactic spreading on soft agar plates and an increased ability to be methylated, as shown on the immunoblot (Fig.4.6). Accordingly, wild-type Tar^{EEEE}, all 1×A Tar and several 2×A Tar receptors, e.g. Tar^{AEEA} and Tar^{EAEA} -all having a comparatively low EC_{50}- displayed a higher mobility on an immunoblot after stimulation, indicating an increased methylation.

EC_{50} values were determined previously in receptors with Q-substituted methylation sites *in vitro* [115] and *in vivo*, performed in a $\Delta cheRB$ strain to prevent CheB-mediated deamidation of glutamine residues (Tab.4.2, data kindly provided by David Kentner). When comparing the EC_{50} values from A- and Q-substituted receptors in a $\Delta cheRB$ background measured *in vivo*, we observed correlations relating to the number of sites that are substituted. The more native methylation sites were replaced with A or Q residues, the higher was the steady-state activity. EC_{50}. However, we could not observe correlations of EC_{50} values in receptors with the same methylation sites replaced with either alanine or glutamine residues, indicating that the two amino acids do not have the same effects on the chemoreceptor activity. EC_{50} values could be determined for all receptors with two glutamine substitutions, whereas only values for three out of six 2×A receptors could be measured. We therefore suggest that glutamine residues at the methylation sites activate the receptors to a higher extent and that the resulting conformational change is stronger than for alanines. Glutamine resembles the methylated glutamate more in size than alanine does and is polar, whereas alanine is nonpolar. Although the neutral charge of the two amino acids is the foremost determinant

for the activity of the chemoreceptors, the size difference and the polarity are responsible for the fine-tuning of the receptor conformation.

5.1.4. Dynamic range of Tar wild-type and mutants

The dynamic range is defined as the range over which chemoreceptors can discriminate different attractant concentrations. It generally got narrower the more methylation sites were replaced with alanine residues. The dynamic ranges of receptors with one alanine substitution were not changed and were similar to wild-type. The single alanine substitution might have the same effect as (and occur instead of) the steady-state methylation level in wild-type receptors. The clearly narrower dynamic range in 2×A receptors is due to their inability to distinguish the same range of concentrations as wild-type with only two glutamates available for methylation. The lower limits of the dynamic ranges differed for the three analyzed 2×A receptors, but reflect the respective receptors steady-state activity indicated by the EC_{50} value. The 2×A receptors substantiated the assumption that alanine residues do not have the same effects as methylated glutamates, because the upper limit of the three 2×A dynamic ranges measured were different. Receptors with either four alanines or four methylated glutamates displayed equal upper limits of their dynamic ranges and we would have expected that the upper limits of all dynamic ranges measured were similarly high, because all methylation sites are either substituted or methylated at such high attractant concentrations. The difference of receptor Tar^{EEAA} dynamic range, which has a similar upper limit as Tar^{EEEE} and Tar^{AAAA}, and the two other 2×A receptors that were investigated, Tar^{EAAE} and Tar^{AAEE}, was seen at two positions. The receptor with an upper limit in accordance to wild-type carried a glutamate at methylation site 2 and an alanine at methylation site 4, whereas the two other receptors carried an alanine at methylation site 2 and a glutamate at methylation site 4. Thus we think that one or both of these two residues at methylation sites 2 and 4 keeps the upper limit of the receptors dynamic range at a similar concentration as in Tar^{EEEE} and Tar^{AAAA}. Tar^{EEEE} might represent one conformational change whereas Tar^{AAAA} represents the other. We hypothesize that conformational differences between the two cytoplasmic helices containing either methylation sites 1 to 3 or methylation site 4 might by changed in a way that activates receptors to a maximum already at lower concentrations.

5.1.5. Chemotaxis in gradients

Chemotaxis in an attractant gradient on soft agar works differently than in liquid medium because the agar polysaccharide forms a network with pores of different sizes.

Tar chemoreceptor mutants were tested for their ability to sense attractant in self-established gradients of nutrients and in applied gradients of the attractant MeAsp. All chemoreceptors with one alanine substitution were able to sense and follow attractant gradients. Comparisons of the $1\times$A receptors spreading with wild-type receptor Tar^{EEEE} elucidated the significance of the respective blocked site for the performance of proper chemotaxis. Methylation site 3 displayed the highest significance for sensing and following gradients, followed by site 2, whereas site 1 and site 4 showed the lowest significance (Tab.5.1). When two sites were unavailable for methylation, many receptors lost their ability to sense gradients. Cells expressing receptors that cannot sense gradients spread only in an undirected way through the agar. Only when two methylation sites that we assigned as less significant were replaced by alanines and thus unavailable, cells expressing the respective receptor could still navigate within a gradient with the help of the two remaining glutamates. Particularly, receptors with alanine substitutions of either site 1 and 4 or site 2 and 4 maintained their sensing properties. This finding emphasized again that the order of significance we determined is reproducible and that not only the numbers, but also the positions of alanine substitutions are crucial.

Accordingly, receptors with three alanine substitutions at the methylation sites failed to sense attractant gradients. A single glutamate residue available for methylation is not enough to make spatiotemporal comparisons over a wide concentration range, probably due to the high steady-state activity of these receptors or due to their narrow dynamic range which does not comprise the concentration range of the gradient. Furthermore, a good gradient detection comes along with low EC_{50} values and thus a low steady-state activity of the respective receptors.

5.1.6. Interpretation of CheR and CheB binding dynamics with the methylation sites of the Tar chemoreceptor

Following the models of Shapiro and colleagues [104] and of Perez and colleagues [105] for CheR interaction with the methylation sites, we aimed to describe the interaction of CheR and CheB with the Tar methylation sites.

Methylation sites 1, 2 and 4 are methylated by CheR in steady-state without the presence of attractants, with site 4 having the highest methylation level, followed by site 2 and site 1. A very low (to undetectable) amount of chemoreceptors seems to be methylated at two sites in the cytoplasmic helix 1 (containing methylation sites 1 to 3) in steady-state, whereas the major portion of helix 1 is methylated only once in steady-state. Interestingly, only site 1 or 2 are methylated, whereas methylation never occurs at site 3 alone, indicating that

site 3 might be subjected to demethylation as first site which is substantiated by the high adaptation precision maintained by Tar^{EEAE}, similar to the wild-type.

Upon stimulation with an attractant, the overall methylation of all four sites increases. Methylation increase of site 1, 2 or 4 can occur only in their respective helix. Site 3 methylation exclusively occurs in connection with either site 1 or site 2 methylation, pointing to a dose-dependent modification of site 3 only at high attractant concentrations. Triple methylation of all sites in helix 1 was never observed. Possibly, methylation of all three sites might as well occur only in response to higher attractant concentrations than 100 μM MeAsp. At the very onset of stimulation, mainly double methylation of site 1 and 3 together, but also of site 2 and 3 together occurs within cytoplasmic helix 1. After 3 minutes, a large amount of double methylated helix 1 at site 2 and 3 dominates, which is decreasing at later time points, whereas peptides with site 1 and 2 methylation appear and dominate after 20 minutes of stimulation.

Demethylation mediated by CheB already takes place in the presence of attractant, probably in a dose-dependent manner, due to the recovery of kinase and chemoreceptor activity and the resulting affinity increase of the enzyme for its substrate. The first site to be demethylated in the presence of MeAsp is site 3. Following, site 2 is demethylated by approximately 30% of its highest methylation level. Interestingly, demethylation of site 2 stops at that level and does not proceed even after the attractant is removed. A reason for this behaviour might be the residual attractant after washing. We consider the amount to be around 0.01 to 0.1 μM MeAsp, which is likely in a range to keep the receptor stimulated. This would also point to site 2 being the first one to be methylated by CheR. Site 1 demethylation occurs only after the removal of attractant, indicating that this site is the last to be subjected to demethylation by CheR in helix 1. After the removal of attractant and re-incubation in attractant-free buffer, site 1 and site 3 recovered their pre-stimulus methylation level. Only site 2 keeps its highly methylated state, as described.

Our results suggest that site 2 is the first site to be methylated, followed by site 3 and site 1 and 4 being the last ones to be methylated, which is confimed by the demethylation kinetics of Tar^{EAEE} and Tar^{EEAE} which is ten times slower in comparison to the wild-type. In contrast, the previously described models of CheR interaction with the methylation sites propose that site 3 is the first site to be methylated, followed by site 2, 1 and 4 in exactly this order [104, 105]. These models stated that the interaction with CheR does not only occur at the Tar methylation site subjected to methylation, but also at a site of a heptad C-terminal. The second contact is stronger if the respective residue has a neutral charge, as both models have shown by mutagenic studies of the chemoreceptor methylation sites and the respective

contact sites in CheR. Therefore, site 3 would be the first site to be methylated, because the amino acid residue a heptad C-terminal is a glutamine. After methylation of site 3, the enzyme would "glide" to site 2 and 1, as the second contact site would then be the previously methylated -and thereby neutralized- methylation site. The models suggested that site 3 is the first to be methylated, because the second contact site of CheR is a neutral glutamine residue a heptad C-terminal of site 3. After methylation of site 3, the enzyme would "glide" to site 2 and 1, as the second contact site of CheR would then be the previously methylated -and thereby neutralized- methylation site. Experiments for both assays were done *in vitro* with membranes containing the Tar receptor mutated at different site and either wild-type or mutated CheR. The methylation rates were determined on an HPLC or by liquid scintillation spectrometry after incubation with a tritiated methyldonor and subsequent protease digestion of the Tar receptor resulting in four smal peptides containing one methylation site each. Interestingly, methylation rates determined for the wild-type Tar[EEEE] in one of the studies [104] was not in agreement with the previous study by Terwilliger and colleagues [114].

We think that our model allows a better description of the interactions of CheR and the chemoreceptor methylation sites due to the *in vivo* conditions, the concomitant analysis of three out of the four methylation sites and the more sensitive techniques that we used. Moreover, we were also able to characterize the interaction of CheB with the methylation sites.

Summarizing our data, we found that specific sites play different roles in chemotaxis and adaptation. Methylation site 1 is most important for precise adaptation and for the methylation rate, whereas it plays a minor role for chemotaxis and the demethylation rate. Site 2 has a major contribution to the methylation and demethylation rates, but is dispensable for adaptation precision, chemotaxis and steady-state activity. Site 3 plays a major role for chemotaxis, demethylation rate and retention of steady-state activity and is less important for adaptation precision and methylation rate. Methylation site 4 is important for the methylation rate, whereas it is less significant for the demethylation rate, adaptation precision, chemotaxis and steady-state activity (Fig.5.1).

Analysis of the kinetics of methylation of single sites upon stimulation by mass spectrometry revealed that site 2 displays the highest methylation rate, followed by site 3, site 1 and finally by site 4. Furthermore, demethylation of site 2 was disturbed which is differing from the previous work. Here, we suggest an order in which specific sites are preferentially methylated and propose a model for CheR and CheB interaction with the methylation region of the aspartate chemoreceptor Tar.
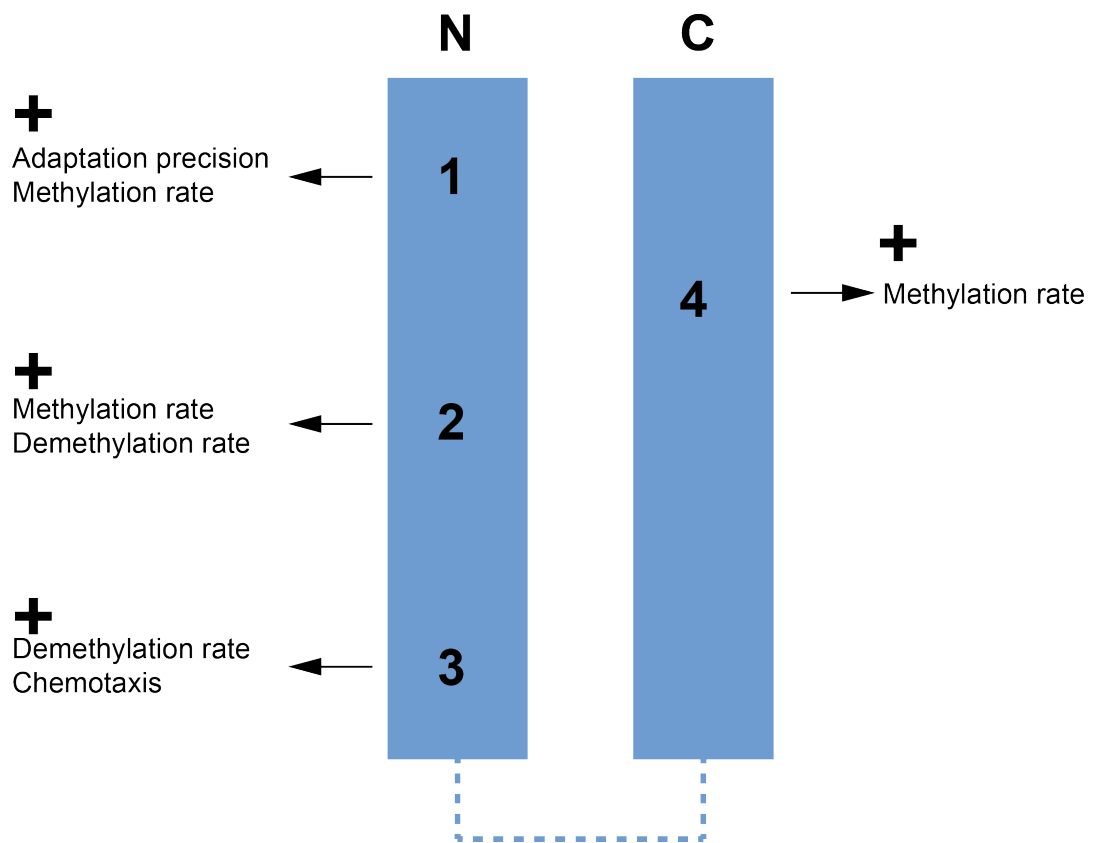
Figure 5.1.: Contribution of specific methylation sites to chemotaxis features. Cytoplasmic helices of the Tar chemoreceptor are shown schematically. Methylation sites are indicated by numbers. Positive effects of specific methylation sites on chemotaxis features are indicated by +.

Bibliography

[1] M. D. Manson, P. Tedesco, H. C. Berg, F. M. Harold, and C. Van der Drift. A protonmotive force drives bacterial flagella. *Proc Natl Acad Sci U S A*, 74(7):3060–3064, Jul 1977.

[2] S. Kojima, K. Yamamoto, I. Kawagishi, and M. Homma. The polar flagellar motor of vibrio cholerae is driven by an na+ motive force. *J Bacteriol*, 181(6):1927–1930, Mar 1999.

[3] P. Cluzel, M. Surette, and S. Leibler. An ultrasensitive bacterial motor revealed by monitoring signaling proteins in single cells. *Science*, 287(5458):1652–1655, Mar 2000.

[4] H. C. Berg and D. A. Brown. Chemotaxis in escherichia coli analysed by three-dimensional tracking. *Nature*, 239(5374):500–504, Oct 1972.

[5] R. M. Macnab and DE Koshland, Jr. The gradient-sensing mechanism in bacterial chemotaxis. *Proc Natl Acad Sci U S A*, 69(9):2509–2512, Sep 1972.

[6] Ekaterina Korobkova, Thierry Emonet, Jose M G. Vilar, Thomas S. Shimizu, and Philippe Cluzel. From molecular noise to behavioural variability in a single bacterium. *Nature*, 428(6982):574–578, Apr 2004.

[7] L. Turner, W. S. Ryu, and H. C. Berg. Real-time imaging of fluorescent flagellar filaments. *J Bacteriol*, 182(10):2793–2801, May 2000.

[8] A. M. Reynolds and C. J. Rhodes. The lÃľvy flight paradigm: random search patterns and mechanisms. *Ecology*, 90(4):877–887, Apr 2009.

[9] G. W. Ordal. Bacterial chemotaxis: biochemistry of behavior in a single cell. *Crit Rev Microbiol*, 12(2):95–130, 1985.

[10] R. B. Bourret, K. A. Borkovich, and M. I. Simon. Signal transduction pathways involving protein phosphorylation in prokaryotes. *Annu Rev Biochem*, 60:401–441, 1991.

[11] J. A. Hoch and K. I. Varughese. Keeping signals straight in phosphorelay signal transduction. *J Bacteriol*, 183(17):4941–4949, Sep 2001.

[12] J. S. Parkinson and E. C. Kofoid. Communication modules in bacterial signaling proteins. *Annu Rev Genet*, 26:71–112, 1992.

[13] H. Itou and I. Tanaka. The ompr-family of proteins: insight into the tertiary structure and functions of two-component regulator proteins. *J Biochem*, 129(3):343–350, Mar 2001.

[14] M. N. Levit, Y. Liu, and J. B. Stock. Stimulus response coupling in bacterial chemotaxis: receptor dimers in signalling arrays. *Mol Microbiol*, 30(3):459–466, Nov 1998.

[15] R. C. Stewart. Kinetic characterization of phosphotransfer between chea and chey in the bacterial chemotaxis signal transduction pathway. *Biochemistry*, 36(8):2030–2040, Feb 1997.

[16] Victor Sourjik and Howard C. Berg. Receptor sensitivity in bacterial chemotaxis. *Proc Natl Acad Sci U S A*, 99(1):123–127, Jan 2002.

[17] M. Welch, K. Oosawa, S. Aizawa, and M. Eisenbach. Phosphorylation-dependent binding of a signal molecule to the flagellar switch of bacteria. *Proc Natl Acad Sci U S A*, 90(19):8787–8791, Oct 1993.

[18] M. Eisenbach and S. R. Caplan. Bacterial chemotaxis: unsolved mystery of the flagellar switch. *Curr Biol*, 8(13):R444–R446, Jun 1998.

[19] Howard C. Berg. The rotary motor of bacterial flagella. *Annu Rev Biochem*, 72:19–54, 2003.

[20] David Kentner and Victor Sourjik. Dynamic map of protein interactions in the escherichia coli chemotaxis pathway. *Mol Syst Biol*, 5:238, 2009.

[21] Ady Vaknin and Howard C. Berg. Single-cell fret imaging of phosphatase activity in the escherichia coli chemotaxis system. *Proc Natl Acad Sci U S A*, 101(49):17072–17077, Dec 2004.

[22] M. Silverman and M. Simon. Operon controlling motility and chemotoxis in e. coli. *Nature*, 264(5586):577–580, Dec 1976.

[23] A. L. DeFranco and DE Koshland, Jr. Molecular cloning of chemotaxis genes and over-production of gene products in the bacterial sensing system. *J Bacteriol*, 147(2):390–400, Aug 1981.

[24] D. Sherris and J. S. Parkinson. Posttranslational processing of methyl-accepting chemotaxis proteins in escherichia coli. *Proc Natl Acad Sci U S A*, 78(10):6051–6055, Oct 1981.

[25] W. R. Springer and DE Koshland, Jr. Identification of a protein methyltransferase as the cher gene product in the bacterial sensing system. *Proc Natl Acad Sci U S A*, 74(2):533–537, Feb 1977.

[26] J. B. Stock and DE Koshland, Jr. A protein methylesterase involved in bacterial sensing. *Proc Natl Acad Sci U S A*, 75(8):3659–3663, Aug 1978.

[27] M. S. Springer, M. F. Goy, and J. Adler. Protein methylation in behavioural control mechanisms and in signal transduction. *Nature*, 280(5720):279–284, Jul 1979.

[28] R. M. Weis and DE Koshland, Jr. Reversible receptor methylation is essential for normal chemotaxis of escherichia coli in gradients of aspartic acid. *Proc Natl Acad Sci U S A*, 85(1):83–87, Jan 1988.

[29] B. H. Morimoto and DE Koshland, Jr. Short-term and long-term memory in single cells. *FASEB J*, 5(7):2061–2067, Apr 1991.

[30] M. R. Kehry and F. W. Dahlquist. Adaptation in bacterial chemotaxis: Cheb-dependent modification permits additional methylations of sensory transducer proteins. *Cell*, 29(3):761–772, Jul 1982.

[31] Silke Neumann, Clinton H. Hansen, Ned S. Wingreen, and Victor Sourjik. Differences in signalling by directly and indirectly binding ligands in bacterial chemotaxis. *EMBO J*, 29(20):3484–3495, Oct 2010.

[32] Yiling Yang and Victor Sourjik. Opposite responses by different chemoreceptors set a tunable preference point in escherichia coli ph taxis. *Mol Microbiol*, 86(6):1482–1489, Dec 2012.

[33] Olga Oleksiuk, Vladimir Jakovljevic, Nikita Vladimirov, Ricardo Carvalho, Eli Paster, William S. Ryu, Yigal Meir, Ned S. Wingreen, Markus Kollmann, and Victor Sourjik. Thermal robustness of signaling in bacterial chemotaxis. *Cell*, 145(2):312–321, Apr 2011.

[34] C. Li, A. J. Boileau, C. Kung, and J. Adler. Osmotaxis in escherichia coli. *Proc Natl Acad Sci U S A*, 85(24):9451–9455, Dec 1988.

[35] Christopher V. Rao and George W. Ordal. The molecular basis of excitation and adaptation during chemotactic sensory transduction in bacteria. *Contrib Microbiol*, 16:33–64, 2009.

[36] S. I. Bibikov, R. Biran, K. E. Rudd, and J. S. Parkinson. A signal transducer for aerotaxis in escherichia coli. *J Bacteriol*, 179(12):4075–4079, Jun 1997.

[37] Sergei I. Bibikov, Andrew C. Miller, Khoosheh K. Gosink, and John S. Parkinson. Methylation-independent aerotaxis mediated by the escherichia coli aer protein. *J Bacteriol*, 186(12):3730–3737, Jun 2004.

[38] S. I. Bibikov, L. A. Barnes, Y. Gitin, and J. S. Parkinson. Domain organization and flavin adenine dinucleotide-binding determinants in the aerotaxis signal transducer aer of escherichia coli. *Proc Natl Acad Sci U S A*, 97(11):5830–5835, May 2000.

[39] A. Repik, A. Rebbapragada, M. S. Johnson, J. O. Haznedar, I. B. Zhulin, and B. L. Taylor. Pas domain residues involved in signal transduction by the aer redox sensor of escherichia coli. *Mol Microbiol*, 36(4):806–816, May 2000.

[40] Barry L. Taylor. Aer on the inside looking out: paradigm for a pas-hamp role in sensing oxygen, redox and energy. *Mol Microbiol*, 65(6):1415–1424, Sep 2007.

[41] L. Aravind and C. P. Ponting. The cytoplasmic helical linker domain of receptor histidine kinase and methyl-accepting proteins is common to many prokaryotic signalling proteins. *FEMS Microbiol Lett*, 176(1):111–116, Jul 1999.

[42] John S. Parkinson. Signaling mechanisms of hamp domains in chemoreceptors and sensor kinases. *Annu Rev Microbiol*, 64:101–122, 2010.

[43] Stanislaw Dunin-Horkawicz and Andrei N. Lupas. Comprehensive analysis of hamp domains: implications for transmembrane signal transduction. *J Mol Biol*, 397(5):1156–1174, Apr 2010.

[44] M. R. Kehry and F. W. Dahlquist. The methyl-accepting chemotaxis proteins of escherichia coli. identification of the multiple methylation sites on methyl-accepting chemotaxis protein i. *J Biol Chem*, 257(17):10378–10386, Sep 1982.

[45] T. C. Terwilliger and DE Koshland, Jr. Sites of methyl esterification and deamination on the aspartate receptor involved in chemotaxis. *J Biol Chem*, 259(12):7719–7725, Jun 1984.

[46] D. M. Nowlin, J. Bollinger, and G. L. Hazelbauer. Sites of covalent modification in trg, a sensory transducer of escherichia coli. *J Biol Chem*, 262(13):6039–6045, May 1987.

[47] A. Krikos, N. Mutoh, A. Boyd, and M. I. Simon. Sensory transducers of e. coli are composed of discrete structural and functional domains. *Cell*, 33(2):615–622, Jun 1983.

[48] M. R. Kehry, M. W. Bond, M. W. Hunkapiller, and F. W. Dahlquist. Enzymatic deamidation of methyl-accepting chemotaxis proteins in escherichia coli catalyzed by the cheb gene product. *Proc Natl Acad Sci U S A*, 80(12):3599–3603, Jun 1983.

[49] A. N. Barnakov, L. A. Barnakova, and G. L. Hazelbauer. Efficient adaptational demethylation of chemoreceptors requires the same enzyme-docking site as efficient methylation. *Proc Natl Acad Sci U S A*, 96(19):10667–10672, Sep 1999.

[50] J. Wu, J. Li, G. Li, D. G. Long, and R. M. Weis. The receptor binding site for the methyltransferase of bacterial chemotaxis is distinct from the sites of methylation. *Biochemistry*, 35(15):4984–4993, Apr 1996.

[51] X. Yi and R. M. Weis. The receptor docking segment and s-adenosyl-l-homocysteine bind independently to the methyltransferase of bacterial chemotaxis. *Biochim Biophys Acta*, 1596(1):28–35, Apr 2002.

[52] Mingshan Li and Gerald L. Hazelbauer. Cellular stoichiometry of the components of the chemotaxis signaling complex. *J Bacteriol*, 186(12):3687–3694, Jun 2004.

[53] J. R. Maddock, M. R. Alley, and L. Shapiro. Polarized cells, polar actions. *J Bacteriol*, 175(22):7125–7129, Nov 1993.

[54] K. K. Kim, H. Yokota, and S. H. Kim. Four-helical-bundle structure of the cytoplasmic domain of a serine chemotaxis receptor. *Nature*, 400(6746):787–792, Aug 1999.

[55] Robert M. Weis. Inch by inch, row by row. *Nat Struct Mol Biol*, 13(5):382–384, May 2006.

[56] Daniel J. Fowler, Robert M. Weis, and Lynmarie K. Thompson. Kinase-active signaling complexes of bacterial chemoreceptors do not contain proposed receptor-receptor contacts observed in crystal structures. *Biochemistry*, 49(7):1425–1434, Feb 2010.

[57] T. S. Shimizu, N. Le Novere, M. D. Levin, A. J. Beavil, B. J. Sutton, and D. Bray. Molecular model of a lattice of signalling proteins involved in bacterial chemotaxis. *Nat Cell Biol*, 2(11):792–796, Nov 2000.

[58] Mingshan Li and Gerald L. Hazelbauer. Core unit of chemotaxis signaling complexes. *Proc Natl Acad Sci U S A*, 108(23):9390–9395, Jun 2011.

[59] V. Sourjik and H. C. Berg. Localization of components of the chemotaxis machinery of escherichia coli using fluorescent protein fusions. *Mol Microbiol*, 37(4):740–751, Aug 2000.

[60] David Kentner, Sebastian Thiem, Markus Hildenbeutel, and Victor Sourjik. Determinants of chemoreceptor cluster formation in escherichia coli. *Mol Microbiol*, 61(2):407–417, Jul 2006.

[61] David J. Montefusco, Anthony L. Shrout, Tatiana Y. Besschetnova, and Robert M. Weis. Formation and activity of template-assembled receptor signaling complexes. *Langmuir*, 23(6):3280–3289, Mar 2007.

[62] Anas Chalah and Robert M. Weis. Site-specific and synergistic stimulation of methylation on the bacterial chemotaxis receptor tsr by serine and chew. *BMC Microbiol*, 5:12, 2005.

[63] G. Li and R. M. Weis. Covalent modification regulates ligand binding to receptor complexes in the chemosensory system of escherichia coli. *Cell*, 100(3):357–365, Feb 2000.

[64] Tatiana Y. Besschetnova, David J. Montefusco, Abdalin E. Asinas, Anthony L. Shrout, Frances M. Antommattei, and Robert M. Weis. Receptor density balances signal stimulation and attenuation in membrane-assembled complexes of bacterial chemotaxis signaling proteins. *Proc Natl Acad Sci U S A*, 105(34):12289–12294, Aug 2008.

[65] Laila Kott, Emory H. Braswell, Anthony L. Shrout, and Robert M. Weis. Distributed subunit interactions in chea contribute to dimer stability: a sedimentation equilibrium study. *Biochim Biophys Acta*, 1696(1):131–140, Jan 2004.

[66] Victor Sourjik and Howard C. Berg. Functional interactions between receptors in bacterial chemotaxis. *Nature*, 428(6981):437–441, Mar 2004.

[67] D. Bray, M. D. Levin, and C. J. Morton-Firth. Receptor clustering as a cellular mechanism to control sensitivity. *Nature*, 393(6680):85–88, May 1998.

[68] Dennis Bray and Thomas Duke. Conformational spread: the propagation of allosteric states in large multiprotein complexes. *Annu Rev Biophys Biomol Struct*, 33:53–73, 2004.

[69] Peter Ames, Claudia A. Studdert, Rebecca H. Reiser, and John S. Parkinson. Collaborative signaling by mixed chemoreceptor teams in escherichia coli. *Proc Natl Acad Sci U S A*, 99(10):7060–7065, May 2002.

[70] John S. Parkinson, Peter Ames, and Claudia A. Studdert. Collaborative signaling by bacterial chemoreceptors. *Curr Opin Microbiol*, 8(2):116–121, Apr 2005.

[71] Fan Bai, Richard W. Branch, Dan V Nicolau, Jr, Teuta Pilizota, Bradley C. Steel, Philip K. Maini, and Richard M. Berry. Conformational spread as a mechanism for cooperativity in the bacterial flagellar switch. *Science*, 327(5966):685–689, Feb 2010.

[72] T. A. Duke, N. Le Novere, and D. Bray. Conformational spread in a ring of proteins: a stochastic approach to allostery. *J Mol Biol*, 308(3):541–553, May 2001.

[73] Thomas Simon Shimizu and Dennis Bray. Modelling the bacterial chemotaxis receptor complex. *Novartis Found Symp*, 247:162–77; discussion 177–81, 198–206, 244–52, 2002.

[74] Bernardo A. Mello and Yuhai Tu. An allosteric model for heterogeneous receptor complexes: understanding bacterial chemotaxis responses to multiple stimuli. *Proc Natl Acad Sci U S A*, 102(48):17354–17359, Nov 2005.

[75] Juan E. Keymer, Robert G. Endres, Monica Skoge, Yigal Meir, and Ned S. Wingreen. Chemosensing in escherichia coli: two regimes of two-state receptors. *Proc Natl Acad Sci U S A*, 103(6):1786–1791, Feb 2006.

111

[76] N. Barkai and S. Leibler. Robustness in simple biochemical networks. *Nature*, 387(6636):913–917, Jun 1997.

[77] Jason E. Gestwicki and Laura L. Kiessling. Inter-receptor communication through arrays of bacterial chemoreceptors. *Nature*, 415(6867):81–84, Jan 2002.

[78] Run-Zhi Lai, Josiah M B. Manson, Arjan F. Bormans, Roger R. Draheim, Ngoc T. Nguyen, and Michael D. Manson. Cooperative signaling among bacterial chemoreceptors. *Biochemistry*, 44(43):14298–14307, Nov 2005.

[79] Abdalin E. Asinas and Robert M. Weis. Competitive and cooperative interactions in receptor signaling complexes. *J Biol Chem*, 281(41):30512–30523, Oct 2006.

[80] J. MONOD, J. WYMAN, and J. P. CHANGEUX. On the nature of allosteric transitions: A plausible model. *J Mol Biol*, 12:88–118, May 1965.

[81] T. A. Duke and D. Bray. Heightened sensitivity of a lattice of membrane receptors. *Proc Natl Acad Sci U S A*, 96(18):10104–10108, Aug 1999.

[82] R. M. Weis, S. Chasalow, and DE Koshland, Jr. The role of methylation in chemotaxis. an explanation of outstanding anomalies. *J Biol Chem*, 265(12):6817–6826, Apr 1990.

[83] J. Saragosti, V. Calvez, N. Bournaveas, B. Perthame, A. Buguin, and P. Silberzan. Directional persistence of chemotactic bacteria in a traveling concentration wave. *Proc Natl Acad Sci U S A*, 108(39):16235–16240, Sep 2011.

[84] Victor Sourjik and Ned S. Wingreen. Responding to chemical gradients: bacterial chemotaxis. *Curr Opin Cell Biol*, 24(2):262–268, Apr 2012.

[85] M. S. Rice and F. W. Dahlquist. Sites of deamidation and methylation in tsr, a bacterial chemotaxis sensory transducer. *J Biol Chem*, 266(15):9746–9753, May 1991.

[86] J. B. Stock and DE Koshland, Jr. Changing reactivity of receptor carboxyl groups during bacterial sensing. *J Biol Chem*, 256(21):10826–10833, Nov 1981.

[87] T. C. Terwilliger, J. Y. Wang, and DE Koshland, Jr. Surface structure recognized for covalent modification of the aspartate receptor in chemotaxis. *Proc Natl Acad Sci U S A*, 83(18):6707–6710, Sep 1986.

[88] Usha K. Muppirala, Susan Desensi, Terry P. Lybrand, Gerald L. Hazelbauer, and Zhi-jun Li. Molecular modeling of flexible arm-mediated interactions between bacterial chemoreceptors and their modification enzyme. *Protein Sci*, 18(8):1702–1714, Aug 2009.

[89] H. Le Moual, T. Quang, and DE Koshland, Jr. Methylation of the escherichia coli chemotaxis receptors: intra- and interdimer mechanisms. *Biochemistry*, 36(43):13441–13448, Oct 1997.

[90] Mingshan Li and Gerald L. Hazelbauer. Adaptational assistance in clusters of bacterial chemoreceptors. *Mol Microbiol*, 56(6):1617–1626, Jun 2005.

[91] Frances M. Antommattei, Jennifer B. Munzner, and Robert M. Weis. Ligand-specific activation of escherichia coli chemoreceptor transmethylation. *J Bacteriol*, 186(22):7556–7563, Nov 2004.

[92] S. Djordjevic and A. M. Stock. Crystal structure of the chemotaxis receptor methyltransferase cher suggests a conserved structural motif for binding s-adenosylmethionine. *Structure*, 5(4):545–558, Apr 1997.

[93] S. Djordjevic and A. M. Stock. Structural analysis of bacterial chemotaxis proteins: components of a dynamic signaling system. *J Struct Biol*, 124(2-3):189–200, Dec 1998.

[94] A. N. Barnakov, L. A. Barnakova, and G. L. Hazelbauer. Location of the receptor-interaction site on cheb, the methylesterase response regulator of bacterial chemotaxis. *J Biol Chem*, 276(35):32984–32989, Aug 2001.

[95] Satomi Banno, Daisuke Shiomi, Michio Homma, and Ikuro Kawagishi. Targeting of the chemotaxis methylesterase/deamidase cheb to the polar receptor-kinase cluster in an escherichia coli cell. *Mol Microbiol*, 53(4):1051–1063, Aug 2004.

[96] S. A. Chervitz and J. J. Falke. Molecular mechanism of transmembrane signaling by the aspartate receptor: a model. *Proc Natl Acad Sci U S A*, 93(6):2545–2550, Mar 1996.

[97] S. A. Chervitz and J. J. Falke. Lock on/off disulfides identify the transmembrane signaling helix of the aspartate receptor. *J Biol Chem*, 270(41):24043–24053, Oct 1995.

[98] A. G. Hughson and G. L. Hazelbauer. Detecting the conformational change of transmembrane signaling in a bacterial chemoreceptor by measuring effects on disulfide cross-linking in vivo. *Proc Natl Acad Sci U S A*, 93(21):11546–11551, Oct 1996.

[99] J. J. Falke and G. L. Hazelbauer. Transmembrane signaling in bacterial chemoreceptors. *Trends Biochem Sci*, 26(4):257–265, Apr 2001.

[100] K. M. Ottemann, W. Xiao, Y. K. Shin, and DE Koshland, Jr. A piston model for transmembrane signaling of the aspartate receptor. *Science*, 285(5434):1751–1754, Sep 1999.

[101] H. Le Moual, T. Quang, and DE Koshland, Jr. Conformational changes in the cytoplasmic domain of the escherichia coli aspartate receptor upon adaptive methylation. *Biochemistry*, 37(42):14852–14859, Oct 1998.

[102] E. A. Wang, K. L. Mowry, D. O. Clegg, and DE Koshland, Jr. Tandem duplication and multiple functions of a receptor gene in bacterial chemotaxis. *J Biol Chem*, 257(9):4673–4676, May 1982.

[103] M. J. Shapiro and DE Koshland, Jr. Mutagenic studies of the interaction between the aspartate receptor and methyltransferase from escherichia coli. *J Biol Chem*, 269(15):11054–11059, Apr 1994.

[104] M. J. Shapiro, D. Panomitros, and DE Koshland, Jr. Interactions between the methylation sites of the escherichia coli aspartate receptor mediated by the methyltransferase. *J Biol Chem*, 270(2):751–755, Jan 1995.

[105] Eduardo Perez, Ann H. West, Ann M. Stock, and Snezana Djordjevic. Discrimination between different methylation states of chemotaxis receptor tar by receptor methyltransferase cher. *Biochemistry*, 43(4):953–961, Feb 2004.

[106] Daisuke Shiomi, Michio Homma, and Ikuro Kawagishi. Intragenic suppressors of a mutation in the aspartate chemoreceptor gene that abolishes binding of the receptor to methyltransferase. *Microbiology*, 148(Pt 10):3265–3275, Oct 2002.

[107] Victor Sourjik, Ady Vaknin, Thomas S. Shimizu, and Howard C. Berg. In vivo measurement by fret of pathway activity in bacterial chemotaxis. *Methods Enzymol*, 423:365–391, 2007.

[108] Jacek R. Wisniewski, E. S., Alexandre Zougman, Nagarjuna Nagaraj, and Matthias Mann. Universal sample preparation method for proteome analysis. *Nat Methods*, 6(5):359–362, May 2009.

[109] H. Amos and G. N. Cohen. Amino acid utilization in bacterial growth. ii. a study of threonine-isoleucine relationships in mutants of escherichia coli. *Biochem J*, 57(2):338–343, Jun 1954.

[110] H. Hama, Y. Sumita, Y. Kakutani, M. Tsuda, and T. Tsuchiya. Target of serine inhibition in escherichia coli. *Biochem Biophys Res Commun*, 168(3):1211–1216, May 1990.

[111] H. Hama, T. Kayahara, M. Tsuda, and T. Tsuchiya. Inhibition of homoserine dehydrogenase i by l-serine in escherichia coli. *J Biochem*, 109(4):604–608, Apr 1991.

[112] C. L. Harris. Cysteine and growth inhibition of escherichia coli: threonine deaminase as the target enzyme. *J Bacteriol*, 145(2):1031–1035, Feb 1981.

[113] Ganhui Lan, Sonja Schulmeister, Victor Sourjik, and Yuhai Tu. Adapt locally and act globally: strategy to maintain high chemoreceptor sensitivity in complex environments. *Mol Syst Biol*, 7:475, Mar 2011.

[114] T. C. Terwilliger, J. Y. Wang, and DE Koshland, Jr. Kinetics of receptor modification. the multiply methylated aspartate receptors involved in bacterial chemotaxis. *J Biol Chem*, 261(23):10814–10820, Aug 1986.

[115] Joshua A. Bornhorst and Joseph J. Falke. Quantitative analysis of aspartate receptor signaling complex reveals that the homogeneous two-state model is inadequate: development of a heterogeneous two-state model. *J Mol Biol*, 326(5):1597–1614, Mar 2003.